EFFECTS OF *Ficus deltoidea* LEAF EXTRACTS ON RAT UTERINE TISSUE CONTRACTILITY AND PROTEOME

KHANIZA HASLIZA ABDUL KHALIL

FACULTY OF SCIENCE
UNIVERSITY OF MALAYA
KUALA LUMPUR

2019

EFFECTS OF *Ficus deltoidea* LEAF EXTRACTS ON RAT UTERINE TISSUE CONTRACTILITY AND PROTEOME

KHANIZA HASLIZA ABDUL KHALIL

DISSERTATION SUBMITTED IN FULFILMENT OF THE REQUIREMENTS FOR THE DEGREE OF DOCTOR OF PHILOSOPHY

INSTITUTE OF BIOLOGICAL SCIENCES
FACULTY OF SCIENCE
UNIVERSITY OF MALAYA
KUALA LUMPUR

2019

UNIVERSITY OF MALAYA

ORIGINAL LITERARY WORK DECLARATION

Name of Candidate: **KHANIZA HASLIZA ABDUL KHALIL**
Matric No: **SHC110052**
Name of Degree: **DOCTOR OF PHILOSOPHY**
Title of Project Paper/Research Report/Dissertation/Thesis ("this Work"):
EFFECTS OF *Ficus deltoidea* LEAF EXTRACTS ON RAT UTERINE TISSUE CONTRACTILITY AND PROTEOME
Field of Study: **BIOCHEMISTRY**

I do solemnly and sincerely declare that:

(1) I am the sole author/writer of this Work;
(2) This Work is original;
(3) Any use of any work in which copyright exists was done by way of fair dealing and for permitted purposes and any excerpt or extract from, or reference to or reproduction of any copyright work has been disclosed expressly and sufficiently and the title of the Work and its authorship have been acknowledged in this Work;
(4) I do not have any actual knowledge nor do I ought reasonably to know that the making of this work constitutes an infringement of any copyright work;
(5) I hereby assign all and every rights in the copyright to this Work to the University of Malaya ("UM"), who henceforth shall be owner of the copyright in this Work and that any reproduction or use in any form or by any means whatsoever is prohibited without the written consent of UM having been first had and obtained;
(6) I am fully aware that if in the course of making this Work I have infringed any copyright whether intentionally or otherwise, I may be subject to legal action or any other action as may be determined by UM.

Candidate's Signature   Date:

Subscribed and solemnly declared before,

Witness's Signature   Date:

Name:

Designation:

EFFECTS OF *Ficus deltoidea* LEAF EXTRACTS ON RAT UTERINE TISSUE CONTRACTILITY AND PROTEOME

ABSTRACT

Ficus deltoidea, a plant known for its uterotonic effect, is a herb used by women to improve their wellbeing. The aim of this study was to investigate the molecular mechanisms underlying the uterotonic property of crude extract (CE) and water fractionated (WF) leaf extracts of *F. deltoidea*. Female nulliparous ICR mice and WKY rats were administered with CE and WF, with the former animals subjected to an embryo implantation study. All animals were measured for their levels of steroid hormones, whilst resected uterine segments of the WKY rats were subjected to a contractility study and analyzed for the expression of the M2 muscarinic acetylcholine receptor (mAChR). The embryo implantation study demonstrated failure of conception of mice administered with WF at 100 mg/kg body weight although the animals did not show any signs of toxicity. Isolated uterine segments of WKY rats administered with the same dose of CE and WF demonstrated increased contractility, which appeared to be associated with higher levels of serum progesterone and uterine tissue expression of M2 mAChR. *F. deltoidea* has the ability to increase uterine contractility by alteration of serum progesterone and uterine tissue M2 mAChR expression.

In a follow-up proteomics analysis of uterine proteins of rats treated with WF100, a total of 833 proteins was initially detected by LC-MS/MS, with 380 of these proteins commonly detected in all groups of rat uterine tissue samples. A total of 100 proteins were later found to be differentially regulated in rats treated with WF100, with the majority of these proteins showing reduction in their expression levels. When analyzed using STRING, the rat uterine proteins that appeared up-regulated by WF100 displayed six protein-protein interaction networks involving 16 proteins. Whilst many of the protein-protein interaction networks are generally associated with general proteins with

structural and regulatory functions, the study also highlighted a network involving Ras-related C3 botulinum toxin substrate 1 with alpha-actinin-4, which was also shown to interact with transgelin, an actin-crosslinking/gelling protein that may have induced smooth muscle contraction that lead to the abortifacient effects on the rats. When similar STRING analysis was performed on uterine proteins of interest that were down-regulated by WF100, two protein-protein interaction networks were generated involving a total of 56 proteins. One of the networks displayed showed interactions with prostaglandin E synthase 3, which is involved in biosynthesis of this specific type of eicosanoid that inhibits smooth muscle contraction. Hence, this enzyme appeared to have been down-regulated so as to induce uterine muscle contraction, inhibit embryo implantation and allow abortion.

Keywords: *Ficus deltoidea*; M2 muscarinic acetylcholine receptors; progesterone; uterine contractility

KESAN EKSTRAK DAUN *Ficus deltoidea* TERHADAP KONTRAKSI DAN PROTEOME TISU UTERUS TIKUS

ABSTRAK

Ficus deltoidea adalah tumbuhan yang dipercayai mempunyai kesan terhadap organ uterus dan kaum wanita mengamalkan pengambilan herba ini untuk meningkatkan kesejahteraan. Kajian ini telah dijalankan untuk mengetahui mekanisme di sebalik kemujaraban ekstrak mentah (CE) dan fraksi akueus (WF) daun *F. deltoidea*. CE dan WF telah diberikan kepada mencit ICR dan tikus WKY. Susulan daripada itu, kadar implan embrio ke atas mencit-mencit diselidiki. Analisa perubahan hormon steroid turut dijalankan ke atas kedua-dua kumpulan haiwan kajian. Seterusnya adalah kajian kontraksi segmen uterus dan ekspresi reseptor muscarinic acetylcholine (mAchR) M2 ke atas tikus-tikus. Hasil kajian mendapati bahawa mencit-mencit yang diberikan WF sebanyak 100 mg/kg berat badan mengalami tiada implan embrio walaupun tidak menunjukkan sebarang ciri kesan ketoksikan. Peningkatan kontraksi segmen uterus tikus yang diberikan dos CE dan WF yang sama, berkemungkinan ada hubungkait dengan peningkatan tahap progesteron serum dan peningkatan expresi mAChR M2 uterus. *F. deltoidea* berupaya meningkatkan kontraksi uterus melalui perubahan progesteron serum serta expresi M2 mAChR tisu uterus.

Melalui analisis proteomik, LC-MS/MS mengesan sebanyak 833 protein dalam sample tisu uterus tikus yang telah diberikan WF100 dengan 380 daripadanya ditemui dalam kesemua kumpulan sampel tisu uterus tikus. Sejumlah 100 protein adalah dikawal selia secara berbeza susulan menerima WF100 dengan kebanyakannya menunjukkan pengurangan tahap ekspresi. Analisa STRING ke atas protein tisu uterus tikus yang mengalami peningkatan tahap ekspresi memaparkan enam rangkaian interaksi protein-protein yang melibatkan 16 protein. Walaupun kebanyakan interaksi protein-protein tersebut secara amnya berkait dengan fungsi struktur dan kawal selia, namun turut

diserlahkan adalah satu rangkaian yang melibatkan 'Ras-related C3 botulinum toxin substrate 1' dan 'alpha-actinin-4' yang juga berinteraksi dengan transgelin, iaitu satu protein penghubung-silang yang mungkin menyebabkan peningkatan kontraksi otot licin serta seterusnya menyumbang kepada kesan 'abortifacient' di kalangan tikus. Apabila analisa STRING yang serupa dilakukan ke atas protein tisu uterus tikus yang mengalami penurunan tahap ekspresi, dua rangkaian interaksi protein-protein melibatkan sejumlah 56 protein telah dipaparkan. Salah satu rangkaian tersebut memaparkan interaksi dengan 'prostaglandin E synthase 3' yang diketahui terlibat dalam biosintesis 'eicosanoid' jenis tertentu dan menghalang konstraksi otot licin. Maka, dapatan penurunan kawal selia enzim ini adalah bagi membolehkan berlakunya peningkatan kontraksi otot uterus, menghindar implan embrio serta membenarkan pengguguran.

Kata kunci: *Ficus deltoidea*; reseptor muscarinic acetylcholine M2; progesteron; kontraksi uterus

ACKNOWLEDGEMENTS

TABLE OF CONTENTS

LIST OF FIGURES

LIST OF TABLES

LIST OF SYMBOLS AND ABBREVIATIONS

°C   :   Celcius

pI   :   isoelectric points

M_r :   relative molecular mass

AChE   :   acetylcholinesterase

PLC   :   activate phospholipase C

ACTH   :   adrenocorticotropic hormone

ACE   :   angiotensin-converting enzyme

CaM   :   calmodulin

DAG   :   diacylglycerol

E2   :   estradiol

E3   :   estriol

E1   :   estrone

FSH   :   Follicle Stimulating Hormone

GnRH   :   Gonadotrophic-releasing Hormone

GPCR   :   G-protein coupled receptors

IP3   :   inositol-1,4,5-triphosphate

LH   :   Luteinizing Hormone

mAChR   :   muscarinic receptor

MLCK   :   myosin light chain kinase

PIP   :   phosphatidylinositol biphosphate

PKC   :   protein kinase

MLC   :   regulatory light chain of myosin

SR   :   sarcoplasmic reticulum

VGCC   :   voltage gated calcium channels

LIST OF APPENDICES

CHAPTER 1: INTRODUCTION

The flora of Malaysia has long been known for its richness in medicinal plant species. This stems from the culture of consuming herbs as a preventive measure and/or treatment of ailments (Mat-Salleh & Latif, 2002). These herbs are consumed fresh or in prepared forms of a concoction, powder or an extract from one plant or a combination of several plants.

Among herbal remedies, *Ficus deltoidea* has gained much popularity as a phytomedicine due to its promising potential. For over many generations, local Malay women of all reproductive ages frequently consume *F. deltoidea*. Dried leaves of 5 to 10 pieces immersed in a cup of hot water simply can be consumed throughout the day (Hassan & Mahmood, 2006). In the commercial preparation, dried leaves packed in sachet is recommended to be infused in 1 liter of hot water.

F. deltoidea has been claimed to heal the uterus and birth canal after parturition, restore the strength of a mother during confinement and delay subsequent pregnancy (Andersen et al., 2003). Uterus is a part of the female reproductive organ that responds to changes in steroid hormones. This muscular organ expands to hold the fetus during pregnancy, and contracts forcefully during childbirth (Kimura et al., 1999). Hence, contraction of the uterus during post-parturition is indeed crucial in order for it to shrink to its original pre-pregnancy size. *F. deltoidea* has been previously shown to induce uterine contractility, which involved extracellular calcium channeling and multiple receptors signaling (Nikolajsen et al., 2011).

While investigation on herbal medicine continues to progress in search for an effective therapeutic alternative for various treatment, the purpose of this study is to investigate the

effects of consuming *F. deltoidea* on rat uterine tissue contractility, reveal the underlying molecular mechanisms that supports its usage and suggest its future research perspective.

1.1   Research Objectives

The present study was aimed to assess the uterotonic property of crude extract and water fractionated leaf extracts of *F. deltoidea* in laboratory animals, and to investigate the underlying mechanisms involved with respect to their influence on the embryo implantation, levels of steroid hormones and uterine tissue expression of the M2 muscarinic acetylcholine receptors specifically as well as the expression of other uterine tissue proteins in general.

The specific objectives of this study were:

1. to investigate the uterotonic property of crude extract and water fractions *F. deltoidea* leaf extracts.

2. to identify proteins of altered abundance involved in uterus contractility via proteomics analysis using MALDI-ToF and LC-MS/MS Q-ToF.

3. to inspect functional annotation and analyze protein-protein interactions of identified rat uterine proteins.

CHAPTER 2: LITERATURE REVIEW

2.1 Female reproductive system

The human female reproductive system is located in the midline of pelvic region and consists of the ovaries, uterus and vagina. Uterus is a hollow, thick-walled muscular organ about the size and shape of an inverted pear. In the pelvis, the uterus is situated anterior to rectum and posterosuperior to bladder. Functions of the uterus includes to receive, retain and nourish fertilized eggs until parturition. Three basic layers of the uterine walls are perimetrium (outer serous membrane), myometrium (smooth muscle) and endometrium (inner mucosal lining). Cervix is a narrow fibrous ring at the opening of the uterus with an inferior tip that projects into vagina. The vagina serves as the birth canal and facilitates sexual intercourse.

Ovaries situated on each side of the upper pelvic cavity are the female gonads. They are almond-shaped and paired. Each ovary is made of a fibrous capsule called tunica albuginea that surrounds the outer cortex. Inner medulla of ovary consists of loose connective tissue, blood vessels and nerves. Follicles develop within the ovary and each month one oocyte is produced. The fallopian tube extends from the uterus to the ovaries. Oocyte enters the uterus into fallopian tubes through the oviducts. Oviducts are not attached to the ovaries, but have fingerlike projections called fimbria that lie over the ovaries. Fertilization normally occurs in the oviduct, and then the developing embryo is slowly propelled to the uterus by tubular muscle contraction and ciliary movement.

The female reproductive system undergoes the same cyclic changes each month at an average of 28 days. Ovaries undergo the same series of events each month controlled by a complex interaction between hormones and organs at level of brain, ovaries and uterus. Follicular phase is approximately the 1st to 14th days. Follicular phase is the time when the anterior pituitary produces the Follicle Stimulating Hormone (FSH). FSH promotes

the development of follicles which secretes estrogen and some progesterone. Highest estrogen level causes hypothalamus to secrete a large amount of Gonadotrophic-releasing Hormone (GnRH). Then a surge in Luteinizing Hormone (LH) production by anterior pituitary is followed by ovulation at around the 14th day. The egg(s) from follicle released into the abdominal cavity, is then picked up by fimbria of fallopian tube. During the subsequent luteal phase/postovulatory phase of the ovarian cycle, LH promotes the development of corpus luteum, which developed from exploded follicle. Corpus luteum produces progesterone and estrogen. Progesterone stimulates the uterus to be ready for fertilized eggs. If there is no fertilization and pregnancy, the corpus luteum degenerates into corpus albicans (Johnson, 2018).

In the reproductive system of female rodents, the main structures are the uterus, ovaries, vagina and mammary glands. The uterus consists of the right and left horns referred as bicornuate uterus. Ovaries are paired and releases eggs into the oviducts. In the presence of sperms, if fertilization occurs, it is then followed by implantation in one of the uterine horns. The uterus supports growth and development of the embryos until birth. Vagina forms where the two uterine horns come together. Other than acceptance of sperms during mating, it also serves as a birth canal. In rodents, several fetuses can develop simultaneously. Typically. the average gestation period in mice is between 18 to 20 days whereas in rats it is between 21 to 24 days (Suckow et al., 2005; Sharp & Villano, 2012).

2.1.1 Uterus contraction

Reproductive roles such as menstruation, transport of sperms, implantation of embryo, pregnancy and parturition require contractions of the uterus. Irregular uterus contraction could contribute to improper implantation of embryo and preterm labour. Recently, the

physiology and mechanisms modulating contraction in non-pregnant uterus has been of interest (Meirzon et al., 2011; Şimşek et al., 2014). The pregnant uterus is quiescent most of the duration allowing growth of fetus and then transforms to forceful contractions toward the end of pregnancy to expel the fetus and placenta.

On the other hand, the non-pregnant uterus is not quite quiescent, producing contractions to facilitate movement of sperms into the fallopian tubes and shedding of the endometrium during menstruation. The uterine contractile patterns in pregnant and non-pregnant state is apparently different with the latter producing 'wave-like activity' (Van Gestel et al., 2003). The contraction of uterine smooth muscle is phasic with varying amplitude, duration and frequency. Between each cycle is a short intermittent relaxation period. The amplitude, duration and frequency of contractions are affected by several factors and agonists (Wray, 2007).

Uterus contraction is generated by shortening of myometrial cells. For this to occur, it mainly depends on calcium as the key regulator. The transient increase in intracellular calcium concentration initiates cycles of myometrium contraction and relaxation. Alteration to calcium ion concentration would affect the strength of uterus contraction (Sanborn, 2001).

2.1.2   Intracellular calcium store in myometrium

Uterus contraction is generated by shortening of myometrial cells. For this to occur, it mainly depends on regulation of intracellular calcium. Intracellular calcium is stored in organelles known as sarcoplasmic reticulum (SR) which is located close to the surface of myometrium membrane or towards center of the cells. SR functions to actively take

up cytosolic calcium against calcium gradient and store it until required. The release of calcium ions (Ca^{2+}) from the SR thus increases cytoplasmic calcium.

Contraction of the myometrium mostly depends on generation of action potential, a transient rise in intracellular calcium, presence of contractile elements along with a conducting system between the uterine myocytes (Wrayzx et al., 2003). Uterine action potential is characterized by cycles of depolarization and repolarization that occurs within the myocytes (Matthew et al., 2004). The excitability of myometrial cells depends on movement of sodium (Na^+), calcium (Ca^{2+}) and chloride (Cl^-) ions into cytoplasm and movement of potassium (K^+) ions into extracellular fluid. K^+ is concentrated inside the myometrium cytoplasm whilst, Na^+, Ca^{2+} and Cl^- are concentrated outside the myometrium. With the plasma membrane being more permeable to K^+ an electrochemical potential is produced (Jain et al., 2000).

Excitation-contraction coupling in myometrium can occur via two main mechanisms which is electrochemical coupling and pharmacomechanical coupling. The increase in Ca^{2+} is primarily due to electrochemical coupling which is the depolarization of plasma membrane. Depolarization of the plasma membrane opens the voltage gated calcium channels (VGCC) and subsequently Ca^{2+} influx into the cell. Ca^{2+} binds to calmodulin (CaM) forms calcium-CaM complex that activates the myosin light chain kinase (MLCK). MLCK phosphorylates serine 19 on the regulatory light chain of myosin (MLC). This enables acto-myosin crossbridge cycling and interaction, hydrolysis of Mg-ATP and production of contraction (Taggart, 2001). For relaxation to occur, myosin light chain phosphatase (MLCP) must dephosphorylate the phosphorylated myosin.

In the pharmacomechanical coupling, it is receptor-agonist binding that increases Ca^{2+} although changes in membrane potential possibly occur. Agonists such as prostaglandins or oxytocin binds their specific receptors on plasma membrane. They cause small G-

proteins to bind to GTP and thus activate phospholipase C (PLC). Activated PLC cleaves to phosphatidylinositol biphosphate (PIP) at the plasma membrane producing inositol-1,4,5-triphosphate (IP3) and diacylglycerol (DAG). IP3 a second messenger derived from PI. It binds to its specific receptors on the surface of SR, thus increases Ca^{2+}. DAG activates protein kinase (PKC) (Alotaibi, 2014).

2.1.3 Muscarinic receptors

Muscarinic receptors (mAChRs) are found distributed widely in the plasma membranes of mammalian cells (transmembrane proteins) and certain neurons. They belong to the family of G-protein coupled receptors (GPCRs), a guanine nucleotide-binding protein that interact with G proteins and regulates second messengers and ion channels. GPCRs consist of one alpha, beta and gamma subunits (Lanzafame et al., 2003).

mAChRs plays vital role during the event of muscle contraction. In smooth muscle, mAChRs could be divided into five subtypes M1, M2, M3, M4 and M5 depending on the targeted organ or tissue. In different tissues, a varying mixed population of mAChRs subtypes are present, and interact both neuron and non-neuronal cells in regulation of autonomic response, often producing a combined effect. Hormonal changes and agonists may modify the activity of these receptors (Kamishima et al., 2000).

In many smooth muscle tissues, both M2 and M3 receptors are usually the types involved in the contractile function. In rat uterus, the M2 and M3 subtypes have been identified (Varol et al., 1989; Pennefather et al., 1994; Munns & Pennefather, 1998; Choppin et al., 1999). M2 mAChRs may interact synergistically with M3 in controlling smooth muscle contraction. Possible interaction s between M2 and M3 receptors could

also occur by other mechanism such as activation of store-operating calcium channels (van Koppen et al., 2001), activation of RhoA which enhances smooth muscle contraction by calcium sensitization or activation of cation channels which increases calcium ion (Sakamoto et al., 2006; Kruse et al., 2013).

All muscarinic receptors appear to be part of the G-protein family with seven segments arranged in serpentine fashion across membrane. An important result of muscarinic binding is activation of the inositol triphosphate (IP3) and diacylglycerol (DAG) cascade. Some evidence implicates DAG in the opening of the smooth muscle calcium channels. IP3 evokes the release of calcium from the endoplasmic and sarcoplasmic reticulum. Muscarinic agonist also increases cellular concentration of cyclic GMP. Activation of muscarinic receptors also increase potassium flux across cell membrane. An effect mediated by direct binding of activated G-protein to the channels (Pennefather et.al., 1994).

Acetylcholine, a known muscarinic agonist can induce spontaneous contraction of the uterine tissue to its maximum. The agonist effect that increases uterine contractile activity with the escalating acetylcholine dosage is due to its direct interaction with specific muscarinic receptors in the uterine smooth muscle (Bafor et al., 2009). Atropine which is a non-specific muscarinic competitive antagonist can reduce the maximal contractile responses to acetylcholine in a concentration-dependent way.

The increase in frequency of contraction may cause the open state probability of voltage-dependent calcium channels in the smooth muscle. This allows an influx of extracellular calcium that enhance contractions. Calcium influx from the extracellular space into the cytosol is important in regulating myometrial contractility (Bafor et al., 2009; Kawarabayashi, 1994). Increase in frequency could also be the results of the activation of receptor-operated calcium channels that possibly interfere with the voltage-

gated potassium channels (Vane & Williams, 1973). This has been proposed as a major contributing factor to basal myometrium contractility. Horowitz et al. (1996) described that a solution high in K^+ produces depolarization of the membranes resulting in the contraction similar to the reference L-type Ca^{2+} channel blocker.

2.1.4 Steroid hormones

Estrogens, progesterone and testosterone are hormones produced in the ovaries. The interaction of these hormones regulates the function of the female reproductive organ. Estrogens, the primary female hormones are essential for the normal development and functioning of the female reproductive organs, and also responsible for the secondary sex characteristics in females. Estrogens build up and maintain the uterine endometrium where else progesterone prepares the uterus for an egg to implant. Testosterone plays a role in stimulating sexual desire and muscle mass development.

In non-pregnant woman, the three major active estrogens are estrone (E1), estradiol (E2) and estriol (E3). E2 is produced primarily in ovaries, and in small amounts in the adrenal glands and fat tissues, whilst E1 is produced from peripheral aromatization of androstenedione. E2 and E1 are convertible to one another by hydroxylation and conjugation. E2 is 1.25 to 5 times the potency of E1. In premenopausal women, E2 circulates at 1.5 to 4 times the concentration of E1. The concentration of E2 in men and postmenopausal woman are much lower than non-pregnant women (Jensen, 1990).

Cholesterol is the most common steroid in animals and the precursor for all other animal steroids. It is one of the principal components of animal cell plasma membranes, and smaller amounts of cholesterol are found in the membranes of intracellular organelles. Steroid hormones, which are crucial signal molecules in mammals, are generally

synthesized from cholesterol. The common molecular structure of steroid hormones is based on a common structure of three 6-membered rings and one 5-membered ring fused together.

In animals, five families of steroid hormones derived from cholesterol includes the androgens, estrogens, progestins, glucocorticoids and mineralocorticoids. Male sex steroid hormones are called androgens, whilst the female hormones, estrogens. Androgens such as testosterone and estrogens such as estradiol mediate the development of sexual characteristics and sexual function in males and females, respectively. On the other hand, the progestins, such as progesterone, participate in control of the menstrual cycle and pregnancy. These steroid hormones are mainly synthesized in the gonads, whilst two other steroid hormones, i.e., glucocorticoids and mineralocorticoids are mainly synthesized in the adrenal cortex. Whilst glucocorticoids, mainly cortisol, participate in the control of carbohydrate, protein and lipid metabolism, the mineralocorticoids such as aldosterone regulate salt (Na^+, K^+ and Cl^-) balances in tissues.

The synthesis of steroid hormone begins with the desmolase reaction. Desmolase is found in the mitochondria of the adrenal glands and gonads. It is a multienzyme complex consisting of two hydroxylases and utilizing cytochrome P-450. Desmolase converts cholesterol to pregnenolone. In the adrenal cortex, the biosynthesis of pregnenolone is activated by adrenocorticotropic hormone (ACTH), which is secreted by anterior pituitary gland. Pregnenolone is then transported from the mitochondria into the endoplasmic reticulum and undergo a hydroxyl oxidation and migration of the double bond to yield progesterone, which is the precursor for synthesis of glucocorticoids and mineralocorticoids. These initial steroidogenic reactions to produce pregnenolone and progesterone occur in the same manner in the gonads. However, instead of producing glucocorticoids and mineralocorticoids, the progesterone that is synthesized in the gonads

may itself play a specific function. For example, the corpus luteum, a hormone-secreting structure that develops in an ovary, produces and secretes progesterone during the latter half of the menstrual cycle and prepares the lining of the uterus for embryo implantation. If implantation occurs, progesterone secretion continues to ensure the successful maintenance of pregnancy.

Alternatively, gonadal progesterone can also be used to synthesize testosterone that can then be converted to produce estrogens via the action of aromatase. In males, testosterone which is necessary for sperm maturation, is mainly synthesized in the testes. The hormone is produced in smaller amounts in females and primarily synthesized in the ovary as a precursor for estrogens, particularly ß-estradiol. Defects in the synthesis or action of testosterone can impair the development of the male phenotype during embryogenesis and cause the disorders of human sexuality termed male pseudo-hermaphroditism.

Steroid hormones exert their effects in two ways:

1.   By entering the cells, migrating to the nucleus and act as transcription regulators, altering gene expression. The effects of steroid hormones usually involve synthesis of new proteins and occurs on time scales of hours.

2.   By binding to plasma membrane receptors or by cell membrane, directly regulating ligand-gated ion channels and perhaps other process. These processes usually take place very rapidly, on time scales of seconds and minutes.

2.2   *Ficus deltoidea*

F. deltoidea is one of the popularly used plants among the Malay community due to its curative properties. It has long been used to heal numerous ailments. At present, this plant is gaining much international recognition for its medicinal benefits. In various parts of the world, *F. deltoidea* is often cultivated as herbal plants, ornamental plants or grown as house plants in cooler regions. In nature, *F. deltoidea* is more regularly found as a cascading shrub of about 5 to 7 meters in height and 1 to 3 meters in width. In dense tropical rain forests, it can grow as epiphytes on larger trees. *F. deltoidea* plants produce aerial roots in warm and humid conditions (Brickell & Zuk, 1997; Starr et al., 2003).

Leaves of *F. deltoidea* are dark green on the above with rust red to olive brown beneath. Characteristic golden spots are seen on the upper surface and on the bottom surface are presence of black spots at the joint of the veins. The leaves are thick, leathery and almost succulent with varying in sizes between 4 to 8 cm in length depending on species. Shape of the leaves vary among genus with the spatulate-shaped being most regularly cultivated (as shown in Figure 2.1). At the end of the spatulate-shaped leaves is a shallow notch. Other shapes of leaves include elliptical or lanceolate to obovate. Female plants have larger, rounder leaves whilst male plant leaves are smaller and longer than wide (Berg, 2003; Hassan & Mahmood, 2006; Mat et al., 2012).

The plant foliage appears attractive with slender trunks that usually slants with zigzagging branches (Figure 2.2). Stems and branches are smooth whitish grey. New plants can be propagated from seeds and cuttings. Spherical figs of about 1.5 cm in diameter with minute seeds are produced in pairs that ripens from dull yellow to orange red (Riffle 1998; Starr et al., 2003). Injuries to the trunks and branches causes excretion of latex-like sap. *F. deltoidea* is native to Southeast Asia, which includes Malaysia, Indonesia, Thailand and Philippines (Starr et al., 2003; Mat et al., 2012). In Malaysia,
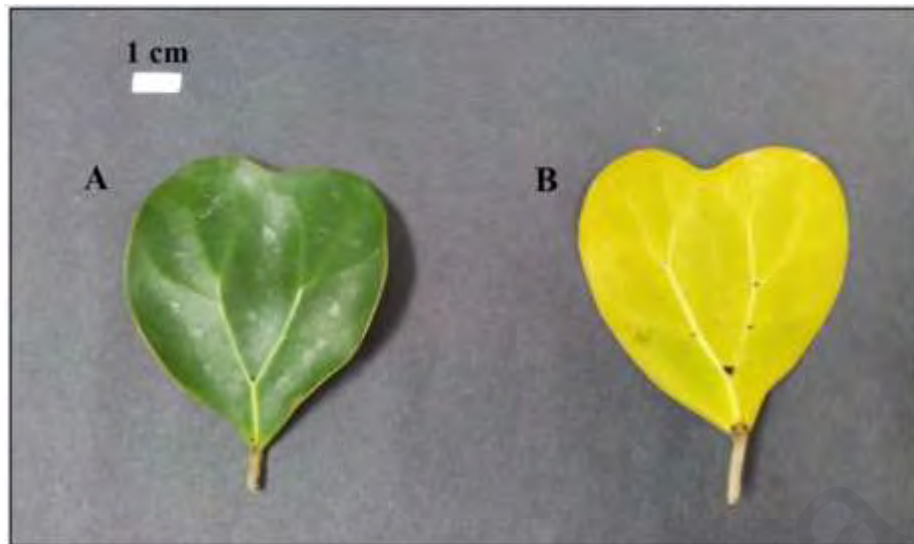
Figure 2.1: Leaf of *F. deltoidea* plant. (A) Golden spots on upper surface of leaf, and (B) Black spots between veins on bottom surface of leaf. White strip on upper left-hand corner represents 1 cm in actual size.

Figure 2.2: Cascading foliage of *F. deltoidea* plant.

this plant can be found in the jungles of Pahang, Terengganu, Kelantan, Sabah and Sarawak. It also found growing in the oil palm plantation of Selangor, Perak and Johor (Hassan & Mahmood, 2006).

The scientific name of this plant, *deltoidea*, refers to the deltoid shape of the leaves. In Malaysia, *F. deltoidea* is commonly known as 'Mas Cotek'. Other local name for it includes 'Emas Secotek', 'Serapat Angin', 'Delima Sudip', 'Telinga Gajah' and 'Telinga Beruk' among the Malays (Musa, 2005), 'Serapat' and 'Sempit-sempit' in Sabah, Sarawak and Kalimantan (Soepadmo et al., 2004), 'Tabat Barito' in Indonesia, 'Angulora' in the Phillipines and 'Kangkalibang' in Africa. Other common names for it includes 'Mistletoe fig' and 'Mistletoe rubber plant' (Starr et al., 2003). The botanical name for it is *Ficus deltoidea* Jack (Berg, 2003). It comes under the Order of Rosales and Family of Moraceae (Mulberry family). The genus *Ficus* consists of about 1000 species from pantropical and subtropical origins (Wagner et al., 1999). Table 2.1 describes the scientific classification of *F. deltoidea* (Awang et al., 2013).

Table 2.1: Scientific classification of *F. deltoidea.*

Level	Name
Kingdom	Plantae
Phylum	Magnoliophyta
Class	Magnoliopsida
Order	Rosales
Family	Moraceae
Genus	*Ficus*
Species	*Ficus deltoidea*
Binomial name	*Ficus deitoidea* Jack

2.2.1 Pharmacological and ethno medicinal uses of *F. deltoidea*

In Malaysia, *F. deltoidea* has long been used as a phytomedicine by the local community to treat a variety of ailments such as headaches and fever (Mat-Salleh & Latif, 2002), Traditionally, all parts of this plant is believed to have medicinal benefits (Wahid et al., 2010) and many studies have supported claims whereby the locals used different parts of the plants to treat various ailments.

The leaves of this plant were reported with properties such as blood glucose lowering effect (Aminudin et al., 2007; Adam et al., 2009; Aminudin et al., 2012), blood pressure lowering effect (Aminudin et al., 2012) and blood cholesterol lowering effect (Aminudin et al., 2007). Other claims on *F. deltoidea* leaves includes that it has antinociceptive and anti-inflammatory potential with reduced sensitivity to painful stimuli (Sulaiman et al., 2008; Zakaria et al., 2012), anti-adipogenic activity with potential for slimming effect (Woon et al., 2014), anticancer towards human ovarian carcinoma cell line (Akhir et al., 2011), angiogenic as it possesses ability to inhibit the formation of blood vessel (Shafaei et al., 2014) and anti-photoaging effect on skin cells (Hasham et al., 2013).

Misbah et al. (2013) reported the antidiabetic potential of the fruit extract. Fruits when chewed relieved toothache and cold. Other parts were used to treat diarrhea, gout, pneumonia and possess the ability to enhance sexual desire. Powdered roots and leaves healed wounds and sores when applied to and relieved rheumatism when applied to joints. The entire plant was reported to possess as well as an antioxidant, antiulcerogenic effect (Fatimah et al., 2009) and antimicrobial activity (Samah et al., 2012).

Based on the claims and reports by consumers, at present this plant has gained much popularity as an alternative to modern medicine as a treatment with little to no side effects. Evidently, surveys conducted in several states of Malaysia from 2004 to 2007 revealed an increase in the number of manufacturers for products such as tea, coffee, cordial juice,

extract powder, pills/capsule and massage oil with tea being most preferred (Farhana et al., 2007; Ramamurthy et al., 2014).

2.2.2   Uterotonic properties of *F. deltoidea*

Traditionally, Malay women of all reproductive ages consumed the whole plant as a herbal drink on a regular basis. This has been a practice for many generations taking it either in the form of decoction or infusion. It has been reported to act as treatment to heal and contract the muscles of uterus and vagina following parturition, restore the female body strength during confinement, improve blood circulation and aids in birth spacing (Andersen et al., 2003). Other female reproductive disorders relieved by consumption of *F. deltoidea* extracts includes irregular menstrual cycle and excessive vaginal discharge (Burkill & Haniff, 1930; Salleh & Ahmad, 2013). In Indonesia, it is used by women as a health tonic and an aphrodisiac (Bunawan et al., 2014).

2.2.3   Phytochemicals in *F. deltoidea*

Phytochemicals are natural bioactive compounds found within plants that produce certain physiological effect on human body, and thus determines its medicinal usage. *F. deltoidea* has been described to contain flavonoids (Miean & Mohamed, 2001; Sulaiman et al., 2008; Ong et al., 2011; Amiera et al., 2014; Ramamurthy et al., 2014, Woon et al., 2014), saponins and terpenes (Sulaiman et al., 2008; Amiera et al., 2014), vitexin and isovitexin (Abdullah et al., 2009) and tannins (Abdullah et al., 2009; Amiera et al., 2014). Other compounds present includes phenylsopropanoid (Abdullah et al., 2009), proanthocyanins and triterpenoids (Woon et al., 2014) as well as pholabatannins, resins and terpenoids (Amiera et al., 2014). These phytochemicals are widely known to have

pharmacological properties such as antioxidant, anti-inflammation, antitumor, antibacterial, antiviral, anti-melanogenic and cardio-protective property (Ramamurthy et al., 2014).

2.3   Proteomics

In proteomic research, the usual aims would be to determine expression of proteins, identify proteins, elucidate structure and functions of proteins. The least complex method to obtain a protein profile is using the sodium dodecyl sulphate-polyacrylamide gel electrophoresis (SDS-PAGE), followed by other more invasive methods i.e., two-dimensional electrophoresis (2-DE) with incorporation of Matrix-assisted Laser Desorption Ionization – Time of Flight (MALDI-TOF) and/or LC-Chip-MS/MS Q-TOF analysis. A standard workflow in proteomics research involves the separation of proteins, staining and visualization of protein spots, quantification and analysis of proteins as well as identification of proteins. Following SDS-PAGE, validation of proteins could be carried out using Western immunoblotting.

Since most biological function of the body involves the presence of proteins, it is hypothetical that the presence of *F. deltoidea* extract could alter or change the profile of protein present in the rat reproductive system. Therefore, the uterine tissues obtained from animals treated with *F. deltoidea* extract were subjected to proteomics technique to develop a protein profile. The separation of proteins from the protein profile using the 2-DE is crucial for the characterization and differential analysis. This would allow changes that had occurred in the investigated animals be observed and, possibly reflect the actual scenario as in female human.

2.3.1   Sodium dodecyl sulphate-polyacrylamide gel electrophoresis (SDS-PAGE)

In proteomics, SDS-PAGE is a frequently preferred preliminary method to resolve proteins in complex mixtures due to its relatively inexpensive and simple protocol. Proteins are separated based on their molecular weight (MW) in SDS-PAGE with negatively charged proteins migrating towards the positively charged anode within the polyacrylamide gel. Generally, smaller and more highly charged protein molecules migrates more rapidly than larger and less charged ones. Migration of these proteins also depends on several other factors being, concentration and composition of the separating gel, the electrophoresis buffer which produces a system for resolving proteins as well as the strength of the electrophoretic field used.

The polyacrylamide gel used are a combination of acrylamide and bisacrylamide, a cross-linking reagent. Polymerization of the gel is due to ammonium persulfate (APS) a catalyst that reacts with another catalyst, N, N, N', N'-tetramethylethylenediamine (TEMED). The resolving gels would have different porosity, ionic strengths and basic pH. Other factors include the electrophoresis buffer containing glycine that assumes a negative charge, the sample buffer contains glycerol that allows the protein samples to settle at the bottom of the gel wells. Prior to electrophoresis, proteins are denatured by boiling with anionic detergents sodium dodecyl sulphate (SDS) and beta-mercaptoethanol. Combination of both detergent and heat breaks many non-covalent bonds, disrupts disulfide bonds between cysteine residues thus dissociating them into polypeptides.

To visualize the positions of proteins, the gels can be stained with various dyes that binds non-covalently to the proteins through ionic bonds and Van der Waals interactions. The stains used also fixes the proteins making them insoluble and unable to diffuse out of the gel. Intensity of the stained bands is directly proportional to the amount of protein

in the band (Laemmli, 1970; Gelperin et al., 2005). To estimate MW a plot of log10 MW of the standard proteins against their distance migrated on the gel produces a straight line. Following that, size of the unknown proteins can be estimated by interpolating experimental values of proteins on a graph of standard proteins. There is possibility that in a complex protein sample, a single band may consist of several proteins with similar molecular weight (Phinney & Thelen, 2005; Steinberg, 2009). SDS-PAGE also demonstrates presence of substance possibly interfering with relative mobility such as salt in the sample of interest.

2.3.2   Two-dimensional Electrophoresis (2-DE)

Two-dimensional electrophoresis (2-DE) was first introduced by Klose (1975) and O'Farrell (1975) and combines the first dimension isoelectric focusing (IEF) and second dimension SDS-PAGE. The combination of two independent electrophoretic parameters being; isoelectric points (pI) and relative molecular mass (M_r) makes this method the most powerful protein separation technique (Celis et al., 1994). It has been widely used for the analysis of proteins in complex mixtures extracted from cells, tissues, or other biological samples and is readily useable in a clinical research environment. In certain clinical studies this method aided in identifying the origin of body fluids samples (i.e., spinal, serum, pleural), analyze protein phenotypes, monitor progress of certain diseases as well as discover new biomarkers for diseases in body fluids or tissue biopsies (Hochstrasser, 1997).

During the IEF phase, proteins are separated in a pH gradient using electric fields. pH of a protein at the point that it has no net electric charge is known as isoelectric point (pI). Subsequently, during the SDS-PAGE phase, separation is based on relative molecular mass (M_r). Both electrophoretic parameters, pI and M_r are indispensable for efficient

separation of proteins in complex mixtures. Prior to IEF, proteins are solubilized in rehydration buffer containing denaturing agent dithiothreitol (DTT) and urea/ thiourea. High electrical voltage during IEF then separates the denatured proteins which becomes loaded onto the gel of IPG strips. Negatively charged proteins moves towards anode whilst positive charge ones move towards the cathode, until their pI is reached.

Before going into the SDS-PAGE, the IPG strips are incubated with alkylation buffer containing iodoacetamide to prevent appearance of streaking on the polyacrylamide gels. The transfer of proteins to the gels is improved by rinsing the IPG strips with the SDS electrophoresis buffers. Agarose solution used to seal the IPG strips permits penetration and proper migration of the earlier focused proteins into the SDS polyacrylamide gels. Visualization of protein spots require the gels to be stained. The two phases of 2-DE protein separation method is considered unsurpassed as it is quite unlikely that different proteins would share similar pI and M_r. 2-DE is also able to resolve post-translationally modified proteins into multiple spots (Oh-Ishi & Maeda, 2007).

2.3.2.1 Matrix-assisted Laser Desorption Ionization – Time of Flight (MALDI-TOF)

Matrix-assisted Laser Desorption Ionization – Time of Flight (MALDI-ToF) can be used to analyze biomolecules such as peptides, oligosaccharides and nucleotides. It is a contemporary analytical method for linking gel separated proteins to entries in sequence database and could facilitate the characterization of the protein/peptide by determination of molecular weight, amino acid sequence, etc. In proteomics, mass spectrometry is usually for rapid identification of proteins following protein separation via 2-DE. This combination has been known to significantly improve high-throughput analysis (Hillenkamp et al., 1991; Karas & Krüger, 2003).

In the general principle for MALDI, the sample is first mixed with suitable matrix and applied to a metal plate. This is followed by laser irradiation of the sample along with the matrix material. Then the analyte molecules are ionized and accelerated into the mass spectrometer that is used to analyze them. Analysis is carried out using Global protein Server Explorer 3.6 software which uses MASCOT software to match MS and MS/MS data against database information. The obtained data are screened against *Rattus norvegicus* database downloaded from Swiss-Prot/TrEMBL homepage.

2.3.3   LC-MS/MS Q-ToF

Samples containing peptides can be subjected to LC-MS/MS system and Spectrum Mill software (Agilent, USA) for identification of individual proteins. The combination of the separation technique of LC allows pure compounds to enter the identification by mass spectrometry which increases the chance of successful identification for any unknown substance. Based on the principle that many compounds with identical retention characteristics have different mass spectra, any complex sample can be separated. LC-MS/MS can be applied to a wide range of biological molecules as it allows highly accurate assays to be developed through some method optimization (Ardrey, 2003).

Mass spectrometry operates by converting the analyte molecules to a charged (ionized) state. Spectrum Mill software can be set to search the UniProtKB/Swiss-Prot database for the required organism and Scaffold Proteome software will be used to validate the MS/MS analysis across grouped samples. Proteins are considered identified based on threshold of greater than 99.0% probability and contained a minimum of 2 identified peptides. Spectral counts from analyses of the various proteins with statistically significant differences ($p < 0.05$) using One-way ANOVA and then compiled. This represents protein expression changes or fold change.

2.3.4   Search Tool for the Retrieval of Interacting Genes/Proteins (STRING) database

Search Tool for the Retrieval of Interacting Genes/Proteins (STRING) database was incorporated in this study with the aim to predict protein-protein interactions. It is a collective and integrated biological database and web source of known and predicted protein-protein interactions on about 9.6 million proteins from more than 2000 organisms. STRING analysis demonstrates protein-protein interactions based on experimental data and knowledge transfer between organisms, computational prediction methods as well as interactions accumulated from other databases. STRING database has continuously been maintained since the year 2000, and the protein-protein association network is made accessible to continuously produce better protein functional associations and connectivity for any given organism (Snel et al., 2000; Franceschini et al., 2012; Szklarczyk et al., 2016). This is important in the understanding of cellular processes at the system-level by the way certain proteins influence each other's production and transcription, participate in signaling mechanisms or contribute to specific organismal functions.

In the analysis using STRING, results are displayed as a network of predicted associations for a particular group of proteins in the forms of nodes and edges. Each network node represents a single protein and the network edges represents protein-protein associations. Prediction of association are based on criterias listed as curated databases, experimentally determined, gene neighborhood, gene fusion, gene occurrence, text mining, co-expression and protein homology. Protein scores are given based on combination of existing pathway databases linked to actual evidences from experiments, gene expression data from a variety of expression experiments.

CHAPTER 3: METHODOLOGY

3.1   Materials

3.1.1   Plant materials

Fresh leaves of *F. deltoidea* were purchased from Delto Medicama Plantation (M) Sdn. Bhd., Sabak Bernam, Selangor, Malaysia.   Botanical identification and authentication was performed by a plant taxonomist at the Herbarium, Rimba Ilmu, University of Malaya (specimen voucher no.: KLU 046469).   The leaves were cleaned, air-dried at room temperature and ground into small pieces.

3.1.2   Animals

Adult ICR mice and Wistar Kyoto (WKY) rats, aged 10-12 weeks, were housed in polypropylene cages and maintained in a controlled environment with temperature of 25 ± 2°C, 12 hours of light and dark cycle and 30-70% relative humidity.   They were provided with standard food pellet and water *ad libitum*.   Handling and experimental procedures complied with the standard guidelines for use of laboratory animals and was approved by the Institutional Animal Care and Use Committee, University of Malaya (ISB/14/08/2012/KHAK (R)).   The animals were allowed time for acclimatization for 7 days prior to treatment.

3.1.3   Chemicals

Sigma Chemicals, USA

1,4-dithiothreitol (DTT), β-mercaptoethanol, Acetonitrile, Acetylcholine chloride, Acrylamide, Ammonium bicarbonate, Ammonium persulphate, Atropine sulphate, Bromophenol blue, Calcium chloride, Ethyl acetate, Ethylene diamine tetra acetic

acid (EDTA), EDTA-free protease inhibitor cocktail, D-glucose, Formaldehyde, Formic acid, Glacial acetic acid, Glutaraldehyde, Glycerol, Glycine, Iodoacetamide, Hydrochloric acid, Magnesium chloride, N,N'-methyenebisacrylamide, Potassium chloride, Potassium ferricyanide, Protease inhibitor, Silver nitrate, Sodium carbonate, Sodium chloride, Sodium dodecyl sulfate, Sodium hydrogen carbonate, Sodium thiosulphate, Tetramethyl ethylenediamine (TEMED), Tris-base, Triton X-100, Tween-20

J. Kollin, UK

Ethanol

Promega, USA

Trypsin Gold Mass Spectrometry Grade

Abcam, UK

Anti-beta-actin (ab8227), Anti-muscarinic acetylcholine receptor 2 antibody (ab109226), Conjugated goat anti-rabbit IgG Fc (HRP) (ab97200), Human brain tissue lysate (ab29467)

3.1.4 Kits and reagents

Listed below are the kits and reagents used throughout the experimentation:

ACE Kit-WST (Dojindo, Japan), Bradford assay kit (BioRad, USA), Peroxidase Stain DAB Kit (Nacalai Tesque, Japan), BLUeye Prestained Protein Ladder (GeneDireX, USA), Estradiol ELISA Kit (no.: 582251) (Cayman Chemical, USA), Progesterone

ELISA Kit (no.: 582601) (Cayman Chemical, USA), Testosterone ELISA Kit (no.: 582701) (Cayman Chemical, USA)

3.1.5 Apparatus

Listed below are various apparatus used throughout the experimentation:

<u>SDS-PAGE and Western-immunoblotting</u>

Electrophoresis Dual vertical Mini-gel unit (Model: MGC-206) (C.B.S. Scientific Co., USA), Electrophoresis Power Supply unit (Model: PSU 400/200) (Scie-Plas), Trans-Blot® Semi-Dry Transfer Cell (BioRad, USA), Image Scanner III LabScan 6.0 (GE Healthcare, USA)

<u>2-D Electrophoresis</u>

Reswelling tray (GE Healthcare, USA), Ettan DALTsix gel caster (GE Healthcare, USA), Ettan DALTsix electrophoresis unit (GE Healthcare, USA), Image Scanner III LabScan 6.0 (GE Healthcare, USA)

<u>MALDI-ToF</u>

384 well Opti-ToF MALDI sample plate (Applied Biosystems, USA), ABI 4800 plus MALDI TOF/TOF Analyzer (Applied Biosystems, USA), Speed Vacuum Concentrator (Thermoscientific, USA)

<u>LC-MS/MS Q-ToF</u>

Accurate-Mass 6550 Series Q-TOF LC-MS system (Agilent, USA), Speed Vacuum Concentrator (Thermoscientific, USA)

<u>Uterus contractility study</u>

Organ bath chamber (ADInstruments, Australia), Force transducer PowerLab recorder ML785 (ADInstruments, Australia), Data acquisition system PowerLab Chart 7.3.1 software (ADInstruments, Australia)

<u>Other common apparatus</u>

Centrifuger 5804R (Eppendorf, Germany), FreeZone Freeze dryer (Labconco, USA), Polytron homogenizer PT-MR2100 (Polytron, USA), Microplate reader ASYS UMV 340 (Biocompare, USA), Refrigerator (Memmert, Germany), Rotary evaporator R-215 (Buchi, Switzerland), Ultra-low temperature freezers (Thermo Fischer Scientific, USA), Waterbath (Memmert, Germany)

3.1.6 Consumables

96-well microplate, C-18 Zip-tip (Millipore, USA), Nitrocellulose membranes 0.45 µm (BioRad, USA), Sterile pipette tips 0.5-10 µl, 20-200 µl, 100-1000 µl (ThermoScientific, USA)

3.2 Preparation of *F. deltoidea* crude and fractionated extracts

Crude extract of *Ficus deltoidea* (FdCE) was obtained by boiling pulverized *F. deltoidea* leaves (100 g) in 1 liter distilled water for 2 hours. This was followed by addition of the same volume of distilled water and boiling was continued for another 2 hours to obtain an extract similar to the traditional preparation. The decoction was concentrated by heating at 60-70°C for several hours to a lower volume. Subsequently, the decoction was allowed to cool, filtered and freeze-dried (Labconco, USA) to give a

yield of 17.08 g (17.08% based on the dried starting weight). For preparation of the water fraction (FdWF), the FdCE was subjected to liquid-liquid separation using ethyl acetate as previously described by Misbah et al. (2013). Fractionated extracts were collected after 15-20 minutes. The FdWF was freeze-dried, whilst the ethyl acetate fraction (FdEAF) was rotary evaporated (Buchi, Switzerland). The dried sample materials were stored in air-tight containers at 24°C in a dehumidifier until required and dissolved in distilled water prior to usage.

3.3 *In vitro* bioactivity evaluation of *F. deltoidea*

3.3.1 Acetylcholinesterase inhibition assay

F. deltoidea extract and fractions were subjected to acetylcholinesterase (AChE) inhibition assay to determine the of acetylcholinesterase (AChE) activity. The potential of AChE activity in FdCE, FdWF and FdEAF contributes to its property in enhancing signal transduction. In this study, Ellman's protocol with modifications was carried out at 1.0 mg/ml concentration of FdCE, FdWF and FdEAF, with physostigmine salicylate as positive control (Nargis et al., 2013). Samples and solutions were prepared as described in Appendix A. Subsequently, the samples and solution were pipetted and mixed accordingly into 96-well microplate in triplicates. The mixtures were incubated at room temperature for 15 minutes away from sunlight. Absorbance was measured at 414 nm in a microplate reader (ELISA, USA).

3.3.2 Angiotensin-converting enzyme inhibition assay

In this experiment, FdCE, FdWF and FdEAF were subjected to Angiotensin-converting enzyme (ACE) assay to assess its ACE activity. The potential of *F. deltoidea*

extract and fractions to inhibit ACE activity can be linked to its properties in muscle contraction. This study was carried out with 1.0 mg/ml of extracts using ACE Kit-WST (Dojindo, Japan) in accordance to the manufacturer's protocol. Optical absorbance of the mixtures was read at 450 nm after 10 minutes of incubation at room temperature.

3.4   Toxicity screening on Zebrafish *(Danio rerio)*

A preliminary investigation was carried out to screen *F. deltoidea* extract and fractions for toxicity. This study was performed using Zebrafish *(Danio rerio)* in accordance to the OECD Guideline 203 (OECD, 1992). Prior to testing, the Zebrafish was acclimatized for 3 days in a controlled environment with 16 hours of light and 8 hours of dark cycle, temperature of $25 \pm 1°C$, ambient laboratory illumination and aeration. Zebrafish were divided into groups of eight fishes (n=8) and exposed to FdCE, FdWF and FdEAF at different concentrations (0.02, 0.2, 1.0 and 2.0 mg/ml). The control group of Zebrafish was exposed to water of the same volume. At every 12-hour period, the number of surviving Zebrafish was determined, and dead Zebrafish were removed. This observation was continued for a duration of 72 hours. Criteria for establishing death of the Zebrafish includes no visible movement of gills or appendages, and no reaction to gentle prodding.

3.5   *F. deltoidea* dose selection study

Based on the result obtained in the previous *F. deltoidea* toxicity screening on Zebrafish, FdCE and FdWF were further investigated, whilst FdEAF was eliminated. Subsequent experiments were carried out on female nulliparous ICR mice.

3.5.1   Oral toxicity study in ICR mice

Female ICR nulliparous mice were divided into groups based on different doses of *F. deltoidea* administered once daily for 14 days. Each group consisted of five animals (n=5) were orally administered with 50, 100 or 200 mg/kg body weight of FdCE or FdWF (accordingly listed as: CE50, CE100, CE200, WF50, WF100 and WF200 groups of mice). Mice in the control group was given water and handled identically as the test group. Observation began immediately upon the first administration of the extract and fraction and continued throughout the 14 days. The mice were observed closely for changes in their physical appearance and behavior including signs of toxicity, morbidity or death.

3.5.2   Biochemical analysis in ICR mice

The same groups of ICR mice used in Section 3.5.1 were used in this investigation. Following administration of FdCE and FdWF for 14 days, on the 15th day, the mice were sacrificed, and their blood samples were collected by cardiac puncture. Collected blood samples were centrifuged (Eppendorf 5804R, Germany) at 5,000 rpm for 5 minutes to obtain the serum for biochemical analysis. Their sera were analyzed using ADVIA 2400 Chemistry Systems (Siemens, USA). Biochemical parameters of interest were those related to kidney and liver function. Selected indicators for kidney functions were creatinine and urea, whilst for liver functions were enzymes gamma-glutamyl transferase (GGT), alanine aminotransferase (ALT) and aspartate aminotransferase (AST).

3.5.3 Hormonal analysis in ICR mice

In this investigation, six groups of female ICR mice were administered with 50, 100 and 200 mg/kg body weight of FdCE or FdWF for a duration of 14 days via oral gavage once daily. The groups were divided based on the different doses of FdCE and FdWF administered. Each group consisted of five animals (n=5). The control group was given water instead of the extract or fraction. On the 15th day, the mice were subjected to cardiac puncture and sacrificed. Their sera were analyzed for levels of progesterone, estradiol and testosterone using ELISA kits (Cayman Chemical, USA).

3.5.4 Embryo implantation study in ICR mice

Female nulliparous ICR mice were divided into 7 groups and orally administered with different doses (50, 100 and 200 mg/kg body weight) of FdCE or FdWF once daily for a duration of 14 days. Mice in the control group were given water. Each group consisted of five animals (n=5). On the 15th day, each of the female mice was placed into a cage with one male ICR mouse overnight for mating (mating ratio 1 male: 1 female). Early morning the following day, the female mice were inspected for presence of copulation plugs upon removal from the cages. Evidence of successful mating and Day-1 of gestation was marked by presence of the copulation plug. Pregnant female mice were monitored constantly in individual cages. On day-18 of gestation, the female mice were sacrificed and subjected to necropsy. Their uteri were resected and counted for numbers of embryos implanted.

3.6   Uterus contractility study in WKY rats

Based on the results obtained in Section 3.5.4, further investigation was performed using the 100 mg/kg body weight dose of FdCE and FdWF. In this study, female WKY rats, a larger rodent was chosen for the ease of experimental preparation. Female nulliparous WKY rats were divided into 3 groups (n=6). The first group received water (control), the second group received 100 mg/kg body weight of FdCE (CE100) and the third group received 100 mg/kg body weight FdWF (WF100) orally for a duration of 14 days once daily. The animals were humanely sacrificed on day-15 to obtain the uterus. The uterus was dissected from both the ovary and cervical ends and cleaned off surrounding fats and connective tissues.

Subsequently, each uterine horn was placed onto a Petri dish containing freshly prepared Locker Ringer physiological solution (NaCl 154 mM, $NaHCO_3$ 5.95 mM, KCl 5.63 mM, $MgCl_2$ 2.1 mM, $CaCl_2$ 2.16 mM and D-glucose 5.55 mM) pH 7.4 and cut into strips of approximately 10 mm. The uterine strip was mounted in an organ bath of 30 ml Locker Ringer physiological solution at $37 \pm 0.5°C$ and continuously aerated with 95% O_2 and 5% CO_2. Prior to *ex vivo* assessment using acetylcholine and atropine, each uterine strip was equilibrated for 45 minutes by which optimum resting tension was adjusted to 1.0 g while continuously washing with physiological solution at 15-minute intervals. After equilibration, uterine segments were treated with 40 mM KCl to stimulate contractions. Acetylcholine (ACh) and atropine were dispensed into the organ bath in a cumulative manner for 5 minutes at each concentration.

Uterine contractile response (mean amplitude and frequency) was captured using a PowerLab ML785 data acquisition system (ADInstruments, Australia) and analyzed using LabChart 7.3.7 software. The maximal achievable response (E_{max}), concentrations that produced 50% maximal response (EC_{50}) and 50% inhibitory response (IC_{50}), as well

as percentage relaxation for each concentration-response were computed using the Graphpad Prism 6 Software.

3.7 Analysis of blood hormones in WKY rats

In this study, female nulliparous WKY rats were divided into 3 groups of six animals (n = 6). Each group of animals were orally administered with 100 mg/kg body weight of FdCE or FdWF for a duration of 14 days once daily whilst the control group was given water. The animals were humanely sacrificed on the 15th day to obtain blood samples via cardiac puncture. Serum samples were submitted to Clinical Diagnostic Laboratory, Universiti Malaya Medical Centre for steroid hormone analysis using ADVIA Centaur Immunoassay Systems (Siemens, USA). Three steroid hormones of interest were progesterone, estradiol and testosterone.

3.8 Western-immunoblotting

The same female nulliparous groups of WKY rats used in Section 3.7 were used in this investigation. They were orally administered once daily with FdCE or FdWF at 100 mg/kg body weight or water for 14 days. Each group of animals consisted of six rats (n = 6). However, instead of blood, uterus was resected from the three different groups of rats on the 15th day. The expression of M2 muscarinic acetylcholine receptor M2 mAChR (M2 mAChR) obtained from rat uterine tissue lysate were analyzed.

3.8.1   Preparation of tissue lysate

The resected rat uteri were cleaned off surrounding fats and connective tissue, cut into segments and homogenized in lysis buffer (Tris-base 20 mM, NaCl 150 mM, EDTA 5 mM, 1% Triton X-100 and EDTA free protease inhibitor cocktail (SigmaFAST S8830)) pH 7.4, using a homogenizer (Polytron, USA), at medium speed for 30 seconds. The homogenized solution was vortexed and then centrifuged (Eppendorf, Germany) at 11,000 rpm for 20 minutes at 4°C. Supernatant was collected, and estimation of tissue lysate protein was performed using Bradford reagent with bovine serum albumin as standard (BioRad, USA). Prepared samples were stored at -80°C until further use.

3.8.2   Sodium dodecyl sulphate-polyacrylamide gel electrophoresis (SDS-PAGE)

In SDS-PAGE, polyacrylamide gels used were casted in glass plate gel casters. Gel solutions were prepared as described in Appendix B. Upon usage, the solutions for the stacking and separating gels were mixed as listed in Table 3.1.

Once prepared the separating gel was immediately pipetted into the glass plates. Distilled water was gently layered onto the separating gel to even out the gel surface. The separating gel was set aside to polymerize for approximately 1.5 hours. After the separating gel has polymerized, the stacking gel was prepared. Distilled water was replaced with the stacking gel. A gel comb was immediately inserted into the stacking gel. Approximately 1.5 hours, the polymerized gels were assembled into electrophoresis unit Model: MGC-206 (C.B.S. Scientific Co., USA).

Table 3.1: Solutions for separating gel (12.5%) and stacking gel (4%).

Solutions	Separating gel	Stacking gel
Monomer stock solution	8.34 ml	0.65 ml
4x resolving buffer	5.00 ml	-
10% SDS	0.20 ml	50.00 µl
10% APS	100.00 µl	25.00 ml
TEMED	6.60 µl	5.00 µl
4x stacking buffer	-	1.25 ml
Distilled water	6.36 ml	3.05 ml

Running buffer was poured into the electrophoresis unit until sample wells within the stacking gels were immersed. Sample buffer and uterine protein lysate previously prepared were mixed at 1:3 ratio, incubated for 5 minutes at 90-95°C before allowed to cool to room temperature. The running buffer and sample buffer were prepared as described in Appendix C. Buffer-lysate mixture containing 40 µg of protein was loaded into respective sample wells of the stacking gel layer. One of the sample wells was loaded with 3 µl of pre-stained protein ladder (GeneDireX, UK). Electrophoresis was carried out with voltage set at 60 V until protein bands migrated into the separating layer of the gel. The voltage was then increased to 120 V for separation of proteins. When the dye front reached approximately 1 cm from the gel end, electrophoresis was turned off.

3.8.3   Immunodetection

Proteins resolved in the SDS-PAGE gel were then electro-transferred onto a nitrocellulose membrane using the Trans-Blot® Semi-Dry Transfer Cell (BioRad, USA). The membrane was blocked using 3% gelatin in Tris-buffer saline-Tween (TBST) at 25°C

for 1 hour, followed by incubation with 1:1000 dilutions of rabbit monoclonal anti-M2 mAChR (ab109226, Abcam, USA) or anti-beta-actin (ab8227, Abcam, USA) at 25°C overnight. Horseradish peroxidase-conjugated goat anti-rabbit IgG Fc at 1:5000 dilution was used as secondary antibody (ab97200, Abcam, USA) and protein bands were finally developed with peroxidase stain DAB kit (Nacalai Tesque, USA). For confirmation of M2 muscarinic acetylcholine receptor (M2 mAChR) bands, 20 µg of human brain (HB) tissue lysate (Abcam: ab29467) was also analyzed. The membrane was scanned using ImageScanner III LabScan 6.0 (GE Healthcare, USA) and quantified for relative expression of the M2 mAChR bands using ImageJ software (http://imagej.nih.gov/ij/).

3.9   Matrix-assisted Laser Desorption Ionization – Time of Flight (MALDI-TOF)

Female nulliparous groups of WKY rats were used in this investigation. Each group of animals were orally administered with FdCE or FdWF at 100 mg/kg body weight or water for 14 days once daily. On the 15th day uterus of the rats was resected and subsequently prepared into tissue lysate as described in Section 3.8.1.

3.9.1   Preparation of 11% polyacrylamide gel

Glass plate gel caster for 26 cm x 28 cm sized gels was assembled according to the manufacturer's protocol. Solutions for polyacrylamide gel were prepared as described in Appendix B. Subsequently, the solutions in Appendix B were mixed as listed in Table 3.2 to produce a volume sufficient to cast 4 gels.

The gel mixture was poured into the glass plates until its level reached approximately 0.5 cm to the top. Using a dropper, water saturated butanol was gently layered onto the

gel mixture. This was to ensure even surface of the polymerized gel. Duration of at least 3 hours was allocated for gel polymerization. Once polymerized, the gel plates were removed from the gel caster and thoroughly rinsed with Milli-Q water to remove traces of butanol. Gel plates containing gels were stored in storage solution at 4℃.

Table 3.2: Solutions for 11% polyacrylamide gel.

Solutions	Volume (ml)
Monomer stock solution	133.2
4x resolving buffer	90
10% SDS	3.6
10% APS	1.8
TEMED	0.12
Distilled water	131.4

3.9.2 Rehydration of IPG strip

A specified volume of sample that contains a known amount of protein was added to urea rehydration buffer containing 10% DTT and mixed thoroughly, giving a total volume of 500 µl. Only 450 µl of the rehydration buffer (contain 100 µg/ml protein) was transferred onto each well of the reswelling tray. Subsequently, dry IPG strips (pH 4-7) 24 cm was added onto the rehydration buffer with its gel layer facing down. Dry strip cover fluid was layered over the immersed strip to prevent urea crystallization. This rehydration process was carried out for 20-24 hours to ensure the rehydration buffer was entirely absorbed by the strips. Preparation of buffers were as described in Appendix D.

3.9.3 Isoelectric Focusing (IEF)

IEF electrophoresis or first-dimension electrophoresis was carried out for 20 hours at 20°C to separate proteins based on isoelectric points (pI). When the rehydration process was complete, rehydrated IPG strips in the reswelling tray were transferred onto silica plate in Ettan IPGphor III (GE Healthcare, USA) with its gel surface facing up. Positive end of the strips was positioned on the positive side of the IPGphor III unit and vice versa. Damp paper wicks were placed on both ends of the strips prior to assembling of electrodes. A maximum of 12 strips was allowed for each run with voltage as described in Table 3.3.

Table 3.3: Voltage setting for first-dimension IEF of uterine tissue.

Steps	Condition	Voltage (V)	Time (hrs.)
1	Gradient	30	8
2	Step and hold	100	2
3	Gradient	500	1
4	Gradient	1000	1
5	Gradient	8000	1
6	Step and hold	8000	7

After completion of IEF, each strip was rinsed with Milli-Q water to remove Dry strip cover fluid. The strips were stored at -80°C in equilibration tubes with its gel surface facing in or continued with the 2-DE.

3.9.4   Equilibrium of IPG strips

Prior to 2-DE, equilibration process was carried out to saturate the IPG strips with the SDS equilibration buffer. Equilibration was carried out in two steps: reduction followed by alkylation. Ten ml of reducing solution was added to each of the equilibration tubes containing the IPG strips and incubated by gently shaking on a shaker for 15 mins. After the first equilibration, the reducing solution was decanted, and 10 ml of alkylating solution was added to each tube. Incubation was allowed for another 15 minutes before decanting the alkylating solution.

The equilibrated strips were rinsed with SDS electrophoresis buffer and then placed onto the surface of the 2-DE gels. Subsequently, pre-melted 0.5% agarose solution was pipetted into the glass plates to seal the strips. Precaution was taken to ensure a perfect migration of the protein sample by removing any bubbles. The reducing solution, alkylating solution and SDS electrophoresis buffer were prepared as described in Appendix E.

3.9.5   Two-dimensional Electrophoresis (2-DE)

2-DE was carried out on using Ettan Daltsix (GE Healthcare, USA) to separate proteins vertically according to their molecular weight (M_r, relative molecular mass). SDS electrophoresis buffer was filled into electrophoresis unit once the gels were prepared. Glass plates containing gels were loaded into the electrophoresis unit connected to electrophoresis power supply EPS 601 (GE Healthcare, USA). Electrophoresis was allowed to run as described in Table 3.4 at temperature 25°C.

Table 3.4: Voltage setting for 2-DE.

Steps	Voltage (V)	Current (mA/gel)	Time (hrs.)	Watt (W/gel)
1	80	10	1	1
2	500	40	4.5 - 6.0	13

Electrophoresis was terminated once the dye front reached approximately 1 cm to the bottom of the gel. Glass plates were removed from the electrophoresis unit and dissembled to release the gels. Upper corner of the gel was marked with a small slant cut to indicate positive end. Each gel and its pairing IPG strip were placed in a clean container that contained a known volume of fixing solution (Appendix F).

3.9.6   Silver staining

Upon completion of electrophoresis, the transparent polyacrylamide gels were removed from the glass plates and subjected to silver staining to reveal protein bands. Solutions required in silver stain protocol were prepared as described in Appendix F. The gels were immediately immersed in fixing solution for 30 minutes and then washed with distilled water for 5 minutes. Washing with distilled water was repeated twice. Subsequently, the gels were incubated in silver solution for 20 minutes followed by washing with distilled water for 1 minute to remove unbound silver. Washing was repeated one more time. Next, the gels were immersed into developing solution for a duration of 5 to 10 minutes to reveal proteins bands. Precaution was taken during this step, as once the protein bands were visible, the developing solution was immediately replaced with stopping solution for a duration of 10 minutes. Finally, the gels were washed three times in distilled water for 10 minutes each time.

3.9.7 Gel image analysis

The previously stained polyacrylamide 2-DE gels were scanned using Image Scanner III (GE Healthcare, USA) and analysis of protein expressions was carried out using Progenesis Samespot software (version 4.5). Protein spots that were altered in abundance when greater than 2.0-fold change were considered as significantly expressed and subjected for identification by MALDI-ToF.

3.9.8 Protein preparation and in-gel digestion

Following the silver stain protocol described in Section 3.9.6, protein spots within the polyacrylamide gels were revealed. Chosen protein spots were excised from polyacrylamide gels, placed into individual microcentrifuge tubes and added 100 µl of Milli-Q water to prevent them from drying. Preparation of solutions for destaining, reduction, alkylation, tryptic digestion and extraction were as described in Appendix G. In the first step, the gel plugs were subjected to destaining by continuously swirling them in 100 µl of destaining solution for 15 minutes. Following that, the destaining solution was discarded and this was carried out three times until the gel plugs were free of stains.

The subsequent preparatory phases were reduction and alkylation. Proteins in the gel plugs were reduced by exposure to 150 µl of reducing solution at 60°C for 30 minutes. This solution was allowed to cool to room temperature and then discarded. The gel plugs were then alkylated in 150 µl of alkylating solution for 20 minutes away from light. Next, the alkylating solution was discarded and replaced with 500 µl of washing solution for 20 minutes. Washing was carried out three times. Denatured proteins were concentrated by adding 50 µl of 100% acetonitrile and incubating for 15 minutes. Subsequently the gel plugs in acetonitrile were subjected to drying using Speed Vacuum Concentrator

(Thermoscientific, USA) for 30 minutes at 4°C. Dried gel plugs were subjected to digestion by incubating them in 25-50 µl of trypsin solution overnight at 37°C.

The following morning, trypsin solution was transferred to fresh microcentrifuge tubes. Extraction of proteins from the gel plugs involved incubating them in 50 µl of 50% acetonitrile for 15 minutes at room temperature. Following incubation, the 50% acetonitrile was transferred to the tubes containing the trypsin solution earlier. Subsequently 50 µl of 100% acetonitrile was added to the tubes containing gel plugs and incubated for another 15 minutes at room temperature. This solution was transferred into the tubes containing pooled solutions of the trypsin solution and 50% acetonitrile. The tubes containing extracted proteins were dried using speed vacuum for 1 hour at 4°C, and subsequently stored at -80°C for desalting procedure.

3.9.9 Desalting of extracted protein via Zip-tip

Extracted proteins stored at -80°C were reconstituted in 10 µl of 0.1% formic acid and vortexed. Desalting was performed using reverse-phase cleanup C-18 Zip-tip (Sigma, USA) and solutions (as described in Appendix H). Prior to desalting of proteins, the Zip-tips were prepared by aspirating and dispensing wetting solution and equilibrating solution repeatedly 3 times each. Precaution was taken to ensure that the column remained wet. This was followed by aspirating and dispensing 10 µl of the reconstituted proteins repeatedly 10-15 times to bind proteins to the column. Subsequently, 10 µl of washing solution was aspirated and dispensed 3 times repeatedly to rid samples from salts and impurities. Finally, proteins bound to the column was eluted by releasing contents of the column into a fresh tube containing 2 µl of fresh eluting solution. These eluted protein samples were dried using a speed vacuum and stored at -80°C until further required.

Matrix solution of 1.5 µl of volume was added to the eluted sample. Then, 0.7 µl of the sample-matrix mixture was spotted onto a MALDI sample plate (384 Opti-ToF) and allowed to dry.

3.9.10 MALDI-ToF analysis

Peptide mass spectra was obtained by MALDI-ToF/ToF mass spectrometer (Applied Biosystems, USA) in the positive ion reflector mode. All fractions were performed in single MS before MS/MS for precursor ion selection. For MS/MS spectra, the peaks were calibrated by default. Twenty most abundant precursor ions per sample were selected for subsequent fragmentation by high-energy CID. Collision energy was set to 1 keV and air was used as the collision gas. Criterion for precursor selection was a minimum S/N of 5. The mass accuracy was within 50 ppm for the mass measurement and within 0.1 Da for CID experiments. Other parameter settings for search were: trypsin, one missed cleavage, variable modification of carbamidomethyl and oxidation of methionine, peptide charge of +1 and monoisotropic. For database search, known contamination peaks such as keratin were omitted beforehand. Analysis was carried out using Global protein Server Explorer 3.6 software (Applied Biosystems) which uses MASCOT software (http://www.matrixscience.com/) to match MS and MS/MS data against database information. Data obtained were screened against *R. norvegicus* database downloaded from Swiss-Prot/TrEMBL homepage (http://www.expasy.ch/sprot).

3.10   LC-Chip-MS/MS Q-ToF

The same female nulliparous groups of WKY rats used in Section 3.7 were used in this investigation. Each group of animals were orally administered once daily with FdCE or FdWF at 100 mg/kg body weight or water for 14 days and instead of blood, uterus was resected from the rats on the 15th day. Tissue lysate was prepared according to Section 3.8.1 followed by separation of 40 µg of protein by SDS-PAGE described in Section 3.8.2.

3.10.1   Protein preparation and in-gel digestion

Proteins bands revealed by the silver stain protocol (Section 3.9.6), were cut out of the polyacrylamide gels using clean blades and placed into individual microcentrifuge tubes. Each of the gel bands was cut into smaller pieces before topping with 100 µl of Milli-Q water to prevent them from drying. These pieces of gels were subjected to protein destaining, reduction, alkylation, tryptic digestion and extraction (Section 3.9.8) by sequentially incubating them in solutions prepared as described in Appendix G. In the final step, extracted proteins in microcentrifuge tubes were dried using speed vacuum for 1 hour at 4°C and stored at -80°C for desalting procedure.

3.10.2   Desalting of extracted protein via Zip-tip

The extracted proteins previously stored at -80°C were subjected to desalting as described in Section 3.9.9 using reverse-phase cleanup C-18 Zip-tip (Sigma, USA) and solutions in Appendix H. Following the steps described in Section 3.9.9, the proteins bound to the column was eluted and then dried using a speed vacuum.   Protein samples were stored at -80°C until further required.

3.10.3   LC-MS/MS Q-ToF analysis

Dried eluted protein samples were subjected to mass spectrometry and Spectrum Mill software (Agilent, USA). These protein samples were reconstituted in 10 µl of the first LC mobile phase (0.1% formic acid in water). Peptide separation was performed using Nano-LC 1260 connected to an Accurate Mass Q-TOF 6550 containing a Chip-Cube interface Nano-ESI ion source. The peptides were enriched in a 160 nl enrichment column, and subsequently separated in a separation column (C18 reverse phase, 300 Å, 150 mm, 5 µl) with 5-80% gradient of solvent B (0.1% formic acid in acetonitrile) at a flow rate of 0.4 µl/min for 34 mins. Each mass data acquisition (8 spectra per second from 200-3000 m/z) was followed by collision induced dissociation of the 20 most intense ions. MS/MS data was acquired within the 50-3000 m/z range.

To identify the proteins, Spectrum Mill software was set up to search the UniProtKB/Swiss-Prot database for *Rattus norvegicus* (rat) and Scaffold Proteome software (version 4.4.6) was used to validate the MS/MS analysis across the grouped samples. Proteins were considered identified based on threshold of greater than 99.0% probability and contained a minimum of 2 identified peptides by Peptide Prophet algorithm with Scaffold delta-mass correction for matched peptide-spectra. Proteins with similar peptide evidence were grouped into clusters and annotated based on Gene Ontology (GO) terms from National Center for Biotechnology Information (NCBI).

For the label-free quantification in this study, the differentially expressed proteins of the untreated and treated groups were exported to Mass Profiler Professional (MPP) software to overcome false discovery complications. Analysis was based on total spectra intensity of the proteins which was considered to be entities in MPP. By setting baseline of various protein spectra as median of samples, the entities were filtered on their frequency of occurrence across replicates of each treatment. Following One-way

ANOVA with statistically significant differences ($p < 0.05$) and Benjamin-Hochberg post-test, regulated proteins with expression changes or fold change greater than (>) 1.5 was compiled.

3.11 Statistical analysis

Analysis was carried out in triplicates using One-way ANOVA. Probability level of less than 0.05 ($p < 0.05$) was considered significant and results were expressed as mean ± standard error of mean. For uterus contractility study, GraphPad Prism version 6 software was used.

CHAPTER 4: RESULTS

4.1 *In vitro* test: Inhibition of Acetylcholinesterase

When the crude extract of *F. deltoidea* (FdCE) and its water fraction (FdWF) and ethyl acetate fraction (FdEAF) were tested for acetylcholinesterase (AChE) inhibition activity, the lowest percentage of inhibition was observed in FdCE, followed by FdWF and FdEAF, respectively (Table 4.1).

Table 4.1: Effects of *F. deltoidea* extract and fractions on AChE inhibition.

Samples	% inhibition
Crude extract (FdCE)	2.11 ± 0.38
Water fraction (FdWF)	3.97 ± 0.11
Ethyl acetate fraction (FdEAF)	23.50 ± 1.38

Data are expressed as mean $\pm$ SEM (n=3); Extract/fractions were tested at 1.0 mg/ml.

Acetylcholine (ACh) is a neurotransmitter responsible for neurotransmission at nerve endings on smooth muscles (neurotransmitter junction). It diffuses across the synaptic cleft and binds onto ACh receptors on the postsynaptic membrane. ACh is then hydrolyzed by AChE into acetate and choline. Inhibition of AChE leads to accumulation of ACh in the synaptic cleft, which causes a block in neurotransmission. Efficiency of AChE in the removal of ACh ensures continuous relay of new signals (Tripathi, 2013). The above results showed that FdCE as having the lowest percentage of inhibition of AChE, and hence, has the most potential in maintaining ACh transmission.

4.2   *In vitro* test: Inhibition of Angiotensin-converting Enzyme

In this experiment, FdCE, FdWF and FdEAF were tested for their angiotensin-converting enzyme (ACE) inhibition activities. When ACE was exposed to FdCE, FdWF and FdEAF at 1.0 mg/ml for 10 mins, the highest percentage of inhibition was observed in FdCE, followed by FdWF and FdEAF, respectively (Figure 4.1).
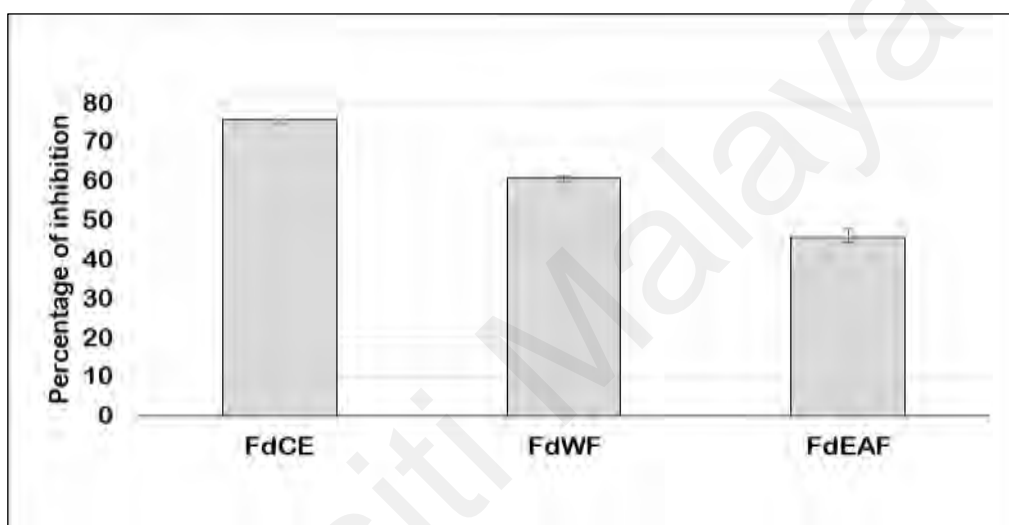
Figure 4.1: Effects of *F. deltoidea* extract and fractions on ACE inhibition. ACE inhibition assay was performed using the ACE Kit-WST protocol (Section 3.3.2). Data are expressed as mean ± SEM (n=3).

ACE increases blood pressure by causing blood vessels to constrict. It converts Angiotensin I into a vasoconstrictor, Angiotensin II. Inhibition of ACE results in a decrease of the formation of Angiotensin II, which causes dilation of blood vessels and decrease in blood pressure. The ability to inhibit ACE is proportional to the contractility potential of blood vessels (Heran et al., 2008). The above results indicated that FdCE demonstrated the highest percentage of ACE inhibition, which is suggestive of a higher potential for smooth muscle contraction and/or relaxation.

4.3 Toxicity screening on Zebrafish (*Danio rerio*)

In this preliminary study, *F. deltoidea* extract and fractions were screened for toxicity using the Zebrafish (*Danio rerio*) as a vertebrate model. The Zebrafish were exposed to FdCE, FdWF or FdEAF at different concentrations (0.02, 0.2, 1.0 and 2.0 mg/ml) for a duration of 72 hours. The Zebrafish were divided into groups of eight fishes based on each concentration tested (n=8). Water instead of extract or fraction of the same volume was used as the control. At the end of each 12-hour period, the number of surviving Zebrafish was recorded. The criteria for establishing death of the Zebrafish were no visible movement of gills or appendages, and no reaction to gentle prodding.

When the first four groups of Zebrafish were exposed to FdCE at concentrations of 0.02, 0.2, 1.0 and 2.0 mg/ml, none died throughout the 72-hour duration (Figure 4.2, panel A). Similarly, none of the Zebrafish died when they were exposed to FdWF at concentrations of 0.02, 0.2 and 1.0 mg/ml. However, one Zebrafish apparently died at the 48th hour in the group of Zebrafish exposed to 2.0 mg/ml concentration of FdWF (Figure 4,2, panel B). In the groups of Zebrafish exposed to FdEAF, none died at concentrations of 0.02 and 0.2 mg/ml. However, five Zebrafish died at the 12th hour upon exposure to FdEAF at 1.0 mg/ml concentration, whilst all of them finally died progressively at the 24th hour of exposure to FdEAF (Figure 4.2, panel C). In the case of Zebrafish exposed to 2.0 mg/ml FdEAF, all of them died at the 12th hour of exposure. As expected, the control group of Zebrafish survived throughout the 72-hour duration of experiment.
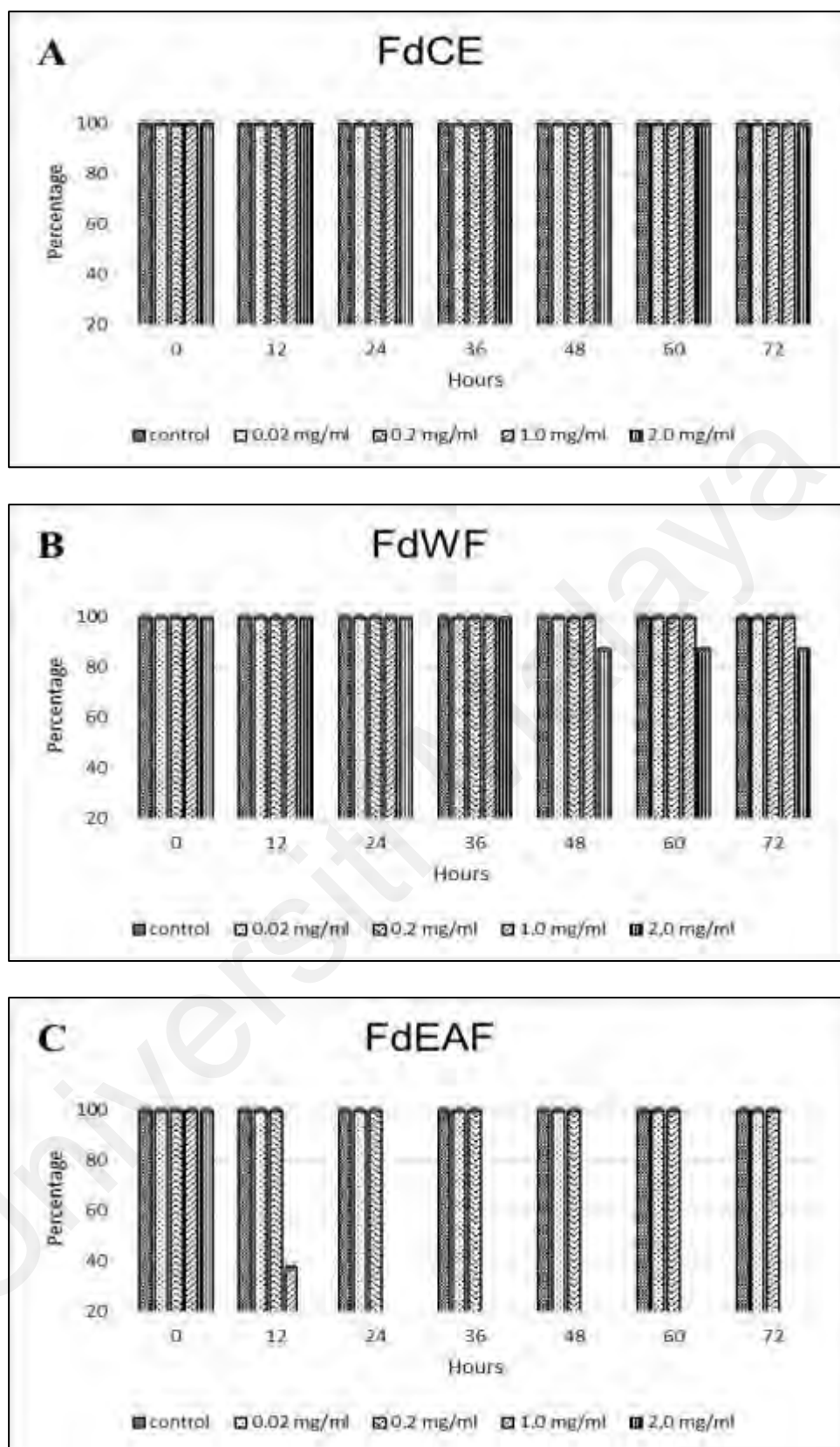
Figure 4.2: Effects of *F. deltoidea* extract and fractions on percentage survival of *Danio rerio*. (A) FdCE, (B) FdWF, (C) FdEAF. Data are expressed as mean percentage of survival ± SEM (n=8) of Zebrafish exposed to different concentrations of *F. deltoidea* extract and fractions in mg/ml.

FdEAF that was used in the preceding experiment had also contained 0.5% (v/v) DMSO as diluent. Hence, another test was set up to determine if there was a direct effect of the DMSO used on the survival of Zebrafish. In this experiment, the same volume percentage of DMSO was exposed to the Zebrafish throughout the 72-hour duration and none of them apparently died. This indicates that DMSO, at the same concentration that was used to dilute FdEAF in the earlier experiment, was not toxic and showed no effect on the survival of Zebrafish.

4.4   Dose selection of *F. deltoidea* based on Zebrafish study

The use of Zebrafish in the previous toxicity screening of extract and fractions of *F. deltoidea* was due to the fact that Zebrafish is a tractable model organism for toxicity study (Reynolds, 2013). In addition, it was considered crucial prior to analysis of the effects of the extract and fractions on higher vertebrate models on the basis for elimination as described by Zurlo et al. (1994). Based on the apparent toxic effect displayed among Zebrafish exposed to FdEAF, certain expected toxicological effects were foreseen on other animals if orally fed with the *F. deltoidea* fraction. Therefore, only FdCE and FdWF were further attested in all subsequent experiments in this study. Dose selection study was carried out in triplicates.

4.4.1   Oral toxicity study in ICR mice

Oral toxicity study was carried out to investigate if the consumption of the same daily dose of FdCE and FdWF had affected the physical appearance and behaviour of female animals. This study was performed on female nulliparous ICR mice and carried out in accordance to the OECD Guideline 407 (OECD, 1995). The mice were orally

administered with FdCE or FdWF once daily for a duration of 14 days at similar times each day. Each group consisted of five animals (n=5) and were divided based on the dosage of FdCE or FdWF administered (50, 100 and 200 mg/kg body weight). Mice in the control group were given water and handled identically as the test group. The group of mice were observed closely after administration of FdCE and FdWF for signs of toxicity, morbidity or death.

When the first three groups of female ICR mice were administered with FdCE at doses of 50, 100 and 200 mg/kg body weight, no apparent change was observed in the physical appearance and behaviour of mice throughout the dosing duration of 14 days (Table 4.2).

Table 4.2: Effects of *F. deltoidea* extract and fraction on physical appearance and behaviour of female ICR mice.

ICR Mice		Observation criteria					
Group (n=5)	Concentration of *F. deltoidea* (mg/kg body weight)	Respiratory pattern	Skin colour	Mucous membrane colour	Excretion	Behavior	Death
Control	0	Normal	NC	NC	Normal	Normal	Nil
CE50	50	Normal	NC	NC	Normal	Normal	Nil
CE100	100	Normal	NC	NC	Normal	Normal	Nil
CE200	200	Normal	NC	NC	Normal	Normal	Nil
WF50	50	Normal	NC	NC	Normal	Normal	Nil
WF100	100	Normal	NC	NC	Normal	Normal	Nil
WF200	200	Normal	NC	NC	Normal	Normal	Nil

NC: No changes

Similarly, in the groups of mice administered with FdWF at doses of 50, 100 and 200 mg/kg body weight, there was no apparent change in the physical appearance and behaviour of the mice. None of the treated animals died or exhibited any observable toxic effects. As anticipated, mice in the control group did not die or exhibit any observable toxic effects.

4.4.2   Biochemical analysis in ICR mice

In this experiment, possible toxic effects of FdCE and FdWF ingestion within female ICR mice were investigated. Several biochemical parameters related to the kidney and liver functions were selected for the analysis. Creatinine and urea were used as indicators for kidney functions, while enzymes gamma-glutamyl transferase (GGT), alanine aminotransferase (ALT) and aspartate aminotransferase (AST) were indicators for liver functions.

Six groups of female ICR mice were administered with 50, 100 and 200 mg/kg body weight of FdCE or FdWF for a duration of 14 days via oral gavage once daily. The groups were divided based on the different doses of FdCE and FdWF administered. Each group consisted of five animals (n=5). The control group was given water instead of the extract or fraction. On the 15th day, the mice were subjected to cardiac puncture and sacrificed. Collected blood samples were centrifuged to obtain the serum for biochemical analysis.

Female ICR mice administered with FdCE at doses between 50 to 200 mg/ml body weight for 14 days did not show any increase in the concentrations of creatinine and urea compared to the control group (Table 4.3). There was also no increase in the concentrations of creatinine and urea in female ICR mice given FdWF at doses between 50 to 200 mg/ml body weight, compared to the control group of mice.

Table 4.3: Effects of *F. deltoidea* extract and fraction on serum biochemical parameters of female ICR mice.

ICR Mice		Serum Profile				
Group (n=5)	Concentration of *F. deltoidea* (mg/kg body weight)	Creatinine (mol/L)	Urea (nmol/L)	GGT (IU/L)	ALT (IU/L)	AST (IU/L)
Control	0	16	9.6	≤ 3	196	1660
CE50	50	≤ 9	7.0	≤ 3	110	1382
CE100	100	≤ 9	7.7	≤ 3	235	2208
CE200	200	≤ 9	7.0	≤ 3	194	1117
WF50	50	≤ 9	6.9	≤ 3	281	1981
WF100	100	10	6.8	≤ 3	237	1646
WF200	200	16	8.3	≤ 3	333	2041

Data are expressed as mean of 3 technical replicates of pooled serum samples.

The concentrations of GGT remained the same in both groups of ICR mice administered with FdCE as well as FdWF, between 50 to 200 mg/kg body weight, compared to the control. Similarly, there was no increase in the concentrations of ALT and AST in the groups of ICR mice administered with FdCE at 50 and 200 mg/kg body weights. However, the group of ICR mice administered with FdCE at 100 mg/kg body weight showed a slight increase in the concentrations of ALT and AST when compared to the control. Nevertheless, this increase was still within the normal range and comparable to the values of the control group.

In the case of mice administered with FdWF, an increase of ALT concentrations was noted at all doses administered. The concentrations of AST were increased in the groups of mice administered with FdWF at 50 and 200 mg/kg body weight only. However, these

altered levels of ALT and AST were still within the normal range when compared to the values of the mice in the control group.

4.4.3   Hormonal analysis in ICR mice

Analysis was also carried out to investigate the possible effects of FdCE and FdWF consumption towards the serum hormones in female ICR mice. The three hormones of interest were progesterone, estradiol and testosterone. In this study, female nulliparous ICR mice were orally administered different doses (50, 100 and 200 mg/kg body weight) of FdCE or FdWF for a duration of 14 days once daily at similar times each day. Each group consisted of five animals (n=5), which were divided based on the dosage of FdCE or FdWF administered. The control group was given water and handled identically as the test groups. On the 15th day, the mice were sacrificed and blood samples were collected by cardiac puncture. Hormonal bioassay was carried out using the Cayman Chemical EIA Kits.

When the first three groups of female ICR mice were administered with FdCE at doses of 50, 100 and 200 mg/kg body weight for a duration of 14 days, there was no significant increase in the concentrations of progesterone observed compared to the control (Figure 4.3, panel A). Nevertheless, when the groups of mice were administered with FdWF at doses of 50, 100 and 200 mg/kg body weight, a significant increase in the concentration of progesterone compared to the control was observed only in the group of mice administered with 100 mg/kg body weight of FdWF.
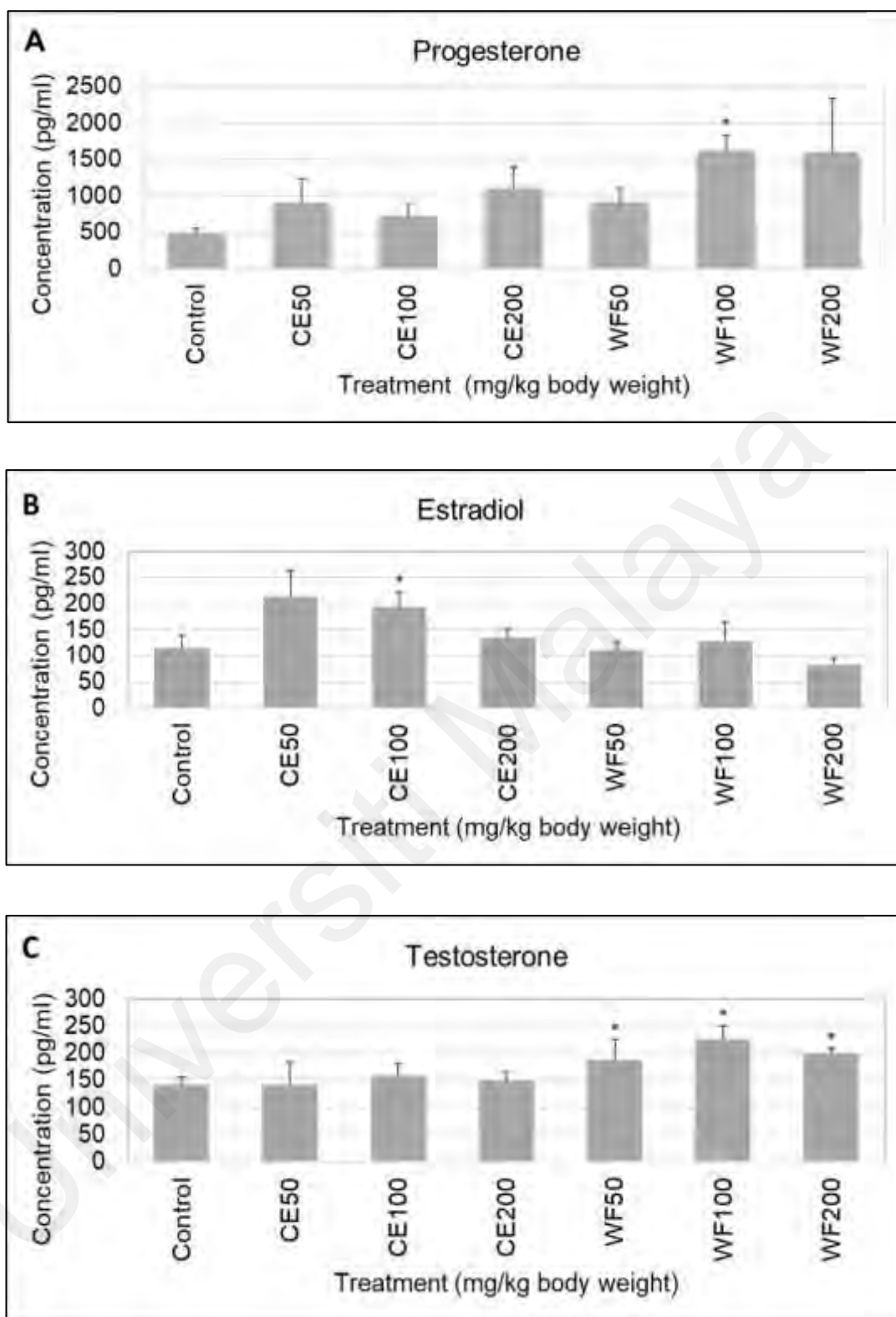
Figure 4.3: Effects of *F. deltoidea* extract and fraction on steroid hormone levels of female ICR mice. (A) Progesterone, (B) Estradiol and (C) Testosterone. Data are expressed as mean ± SEM (n=5) of 3 replicates. *Statistically significant differences between groups *(p < 0.05)* in comparison to controls were measured using Student's *t*-test.

In the groups of female ICR mice administered with FdCE at doses of 50, 100 and 200 mg/kg body weight for a duration of 14 days, increased concentrations of estradiol was observed in all the treated groups compared to the control. However, the increase was only significant in the group of mice administered with 100 mg/kg body weight of FdCE (Figure 4.3, panel B). When the groups of mice were administered with FdWF, there was apparently no significant increase in estradiol concentrations at all doses tested.

When the groups of female ICR mice were administered with FdCE at doses of 50, 100 and 200 mg/kg body weight, compared to the control there was no significant increase in testosterone levels in all doses tested (Figure 4.3, panel C). However, the concentrations of testosterone were significantly increased in all the tested doses of FdWF compared to the control.

4.4.4   Embryo implantation study in ICR mice

This study was conducted to investigate whether the consumption FdCE and FdWF had any direct effect on the number of embryo implantation within female ICR mice. The number of embryo implantation within the uterus was obtained by subjecting pregnant female ICR mice to necropsy on Day-18 of the gestation period. Each embryo implantation site represents one viable offspring conceived by the female ICR mice.

In this investigation, female ICR mice were divided into 7 groups (n=5). The treated groups of mice were orally administered with different doses (50, 100 and 200 mg/ kg body weight) of FdCE or FdWF for 14 days once daily. The control group was given water of the same volume. On the 15th day, each female mouse was put into a cage with one male mouse overnight for mating (mating ratio 1 male: 1 female).

In the early morning the following day, all the female mice were removed from the cages and inspected for presence of copulation plug. The plug serves as evidence that successful mating had taken place, and this was considered as Day-1 of the gestation period. All pregnant female mice were constantly monitored. On day-18 after successful mating, mice were subjected to necropsy and the animals' uteri were resected and embryo implantation sites were counted.

When FdCE at doses 50, 100 and 200 mg/kg body weight was administered to female ICR mice for 14 days, the number of embryo implantation increased in all groups compared to the control (Figure 4.4). The highest number of embryo implantation was in the group administered with FdCE at 100 mg/kg body weight group, followed by 50 mg/kg body weight and 200 mg/kg body weight, respectively.
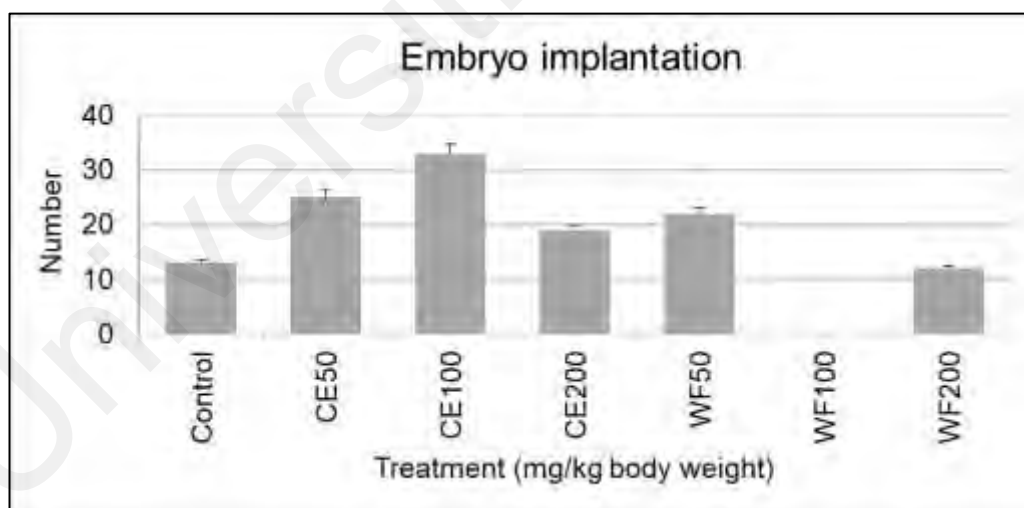
Figure 4.4: Effect of *F. deltoidea* extract and fraction on the number of embryo implantation in female ICR mice. Numbers of uterine embryo implantation are expressed as mean ± SEM of 3 total biological replicates.

In the groups of mice administered with FdWF at doses 50, 100 and 200 mg/kg body weight, increase in the number of embryo implantation were seen in the 50 mg/kg body

weight dose followed by 200 mg/kg body weight dose when compared to control. No embryo implantation was detected in the group of mice administered with FdWF at 100 mg/kg body weight. The same results were observed when the experiments were repeated twice under similar conditions.

4.5   Uterus contractility study in WKY rats

Uterus contractility is the motion of uterine smooth muscle which is termed as contractile waves or endometrial waves. These contractile waves are the tightening and shortening of the uterine muscles. This study was carried out to investigate if FdCE or FdWF consumption had any effect towards uterus contractility of female WKY rats.

In this study, female WKY rats were chosen over female ICR mice, as rats are larger rodents, thus a convenient biological model for the ease in the experimental preparation. Uteri strips of female WKY rats were mounted in the organ bath chambers and spontaneous uteri muscle contraction/release pattern were recorded by a force transducer connected to a bridge amplifier and data acquisition system.

In the previous implantation study (Section 4.4.4), lack of embryo implantation observed in the group of mice administered with 100 mg/kg body weight of FdWF whilst highest number of implantations was in the 100 mg/kg body weight of FdCE. The lack of implantation observed in the mice group administered 100 mg/kg body weight of FdWF and their altered serum progesterone levels (Section 4.4.3) are suggestive of an abortifacient effect possibly induced by uterine contraction. In view of this, subsequent further investigations were performed using the 100 mg/kg body weight dose of FdCE and FdWF.

Female nulliparous WKY rats were orally administered with 100 mg/kg body weight of FdCE or FdWF for a duration of 14 days once daily. Each group consisted of six animals (n=6). The control group was given water. On the 15th day the rats were humanely sacrificed, and an incision was made at the lower abdominal cavity to obtain the uterus. Uterine segments were then prepared as stated in Section 3.6.

Each uterine strip of approximately 10 mm were mounted in an organ bath containing Locker Ringer physiological solution and equilibrated for 45 minutes prior to *ex vivo* assessment using acetylcholine and atropine. Respective cholinergic receptor agonist and antagonist were dispensed into the organ bath in a cumulative manner for 5 minutes at each concentration. Uterine contractile response expressed as the mean amplitude and frequency was captured and computed into a dose response curve.

At the beginning of the experiment, spontaneous contractile activities of rat uterine segments were observed in the control, FdCE administered and FdWF administered groups of female WKY rats. When acetylcholine was added in a dose cumulative manner to the organ bath chamber containing rat uterine segments of the control group, increasing contractile response of the uteri segments was detected (Figure 4.5, panel A). Similarly, when acetylcholine was added to the organ bath chamber containing rat uterine segment of the FdCE and FdWF administered groups, contractile response of the uterine segments were also increased in a dose-dependent manner compared to the control. Highest contractile response was detected in the FdWF group, followed by FdCE, respectively.

Administration of atropine to the organ bath chamber in a dose cumulative manner, decreased dose-dependent contractile response was observed in the uterine segments of all groups of rats studied (Figure 4.5, panel B). Following atropine administration, the contractile response of uterine strips were almost returned to original in all groups of rats thus generally displaying the normal regulation of muscle contraction-relaxation rhythm.
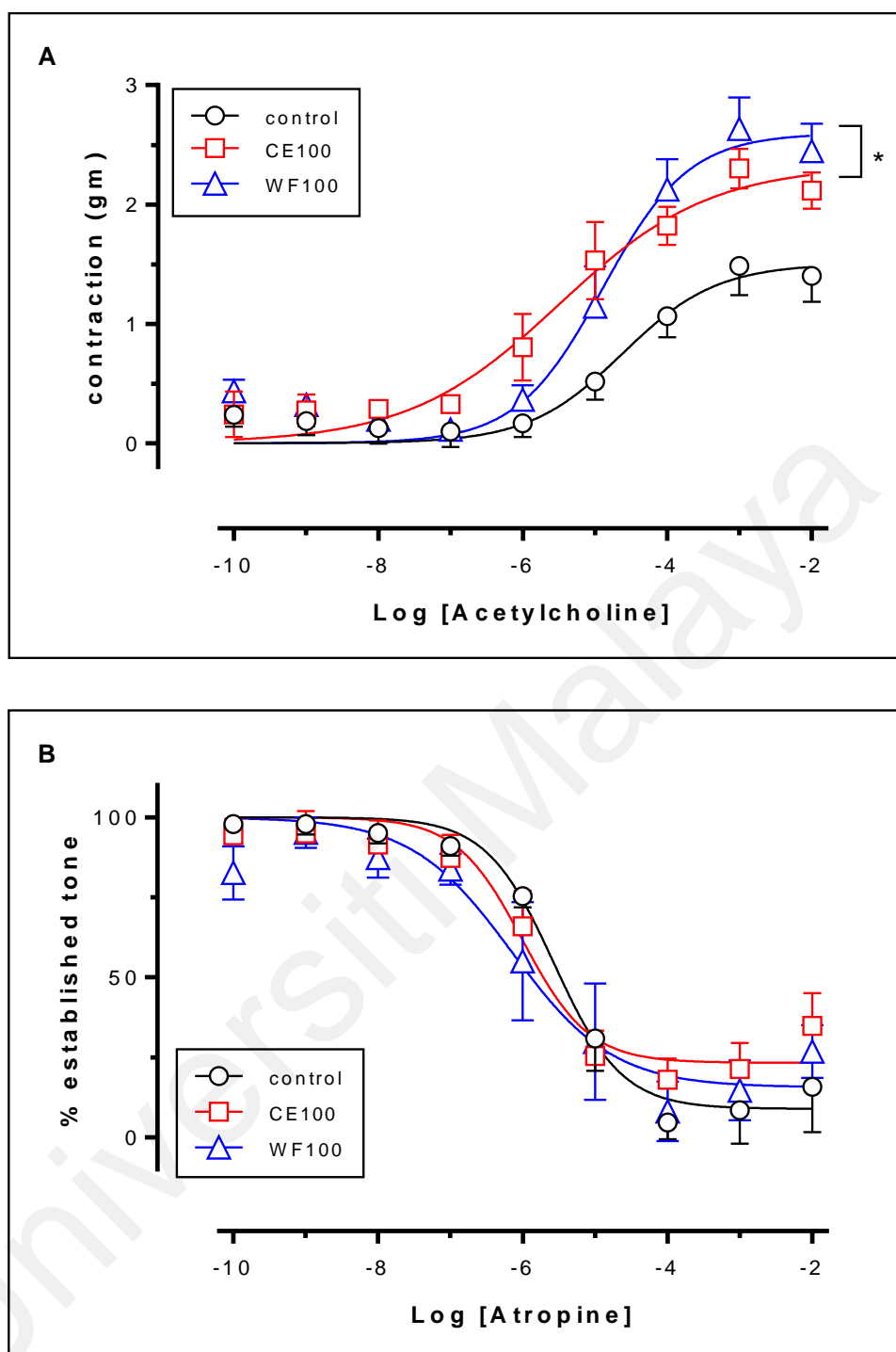
Figure 4.5: Effect of *F. deltoidea* extract and fraction on the contractile activities of rat uterine strips. (A) Dose-response curve in presence of acetylcholine, (B) Dose-response curve in presence of atropine (pre-contracted with acetylcholine). Each point represents the mean ± SEM of four experiments performed using different animals. *Statistically significant differences *(p < 0.05)* in comparison to controls were measured using two-way ANOVA.

Both WF100 and CE100 rat uterine segments demonstrated dose-response curves with higher E_{max} and lower EC_{50} values compared to the control rat uteri strips (Table 4.4). In both the 100 mg/kg body weight of FdCE and FdWF administered groups of rats, the value of E_{max} were significantly higher compared to the control, with highest E_{max} seen in the FdWF treated group. The dose-response curve of rat uteri in all three groups showed a similar pattern.

Table 4.4: Effects of *F. deltoidea* extract and fraction on the contractile activities of rat uterine strips.

Contractile activity			
	Control	**CE100**	**WF100**
EC_{50} **(mg/ml)** **SEM**	24.07×10^{-6} $\pm\ 0.30$	3.19×10^{-6} $\pm\ 0.34$	12.78×10^{-6} $\pm\ 0.19$
E_{max} **(gm)**	1.50 ± 0.17	$2.33 \pm 0.21^*$	$2.60 \pm 0.18^*$
Relaxant activity			
IC_{50} **(mg/ml)** **SEM**	2.69×10^{-6} $\pm\ 0.15$	0.99×10^{-6} $\pm\ 0.19$	0.71×10^{-6} $\pm\ 0.32$
% relaxation	8.90 ± 4.6	23.30 ± 4.8	15.60 ± 7.4

CE100: crude extract at 100ml/kg body weight; WF100: water fraction at 100 ml/kg body weight; EC_{50}: concentration that produced 50% of maximal response of acetylcholine induced uterine contractions; E_{max}: maximum value for contractile activity of rat uteri strips subjected to acetylcholine; IC_{50}: concentration that produced 50% of inhibitory response of atropine on acetylcholine-induced sustained uterine contractions; SEM: standard error mean of four experiments. *Statistically significant differences *(p < 0.05)* in comparison to controls were measured using two-way ANOVA.

4.6 Analysis of blood hormones in WKY rats

In this study, female nulliparous WKY rats were divided into 3 groups that consisted of six animals (n=6). Each group of animals were orally administered with 100 mg/kg body weight of FdCE or FdWF for a duration of 14 days once daily. The control group was given water. On the 15th day, blood samples were collected from the animals via cardiac puncture. Serum samples were sent to Clinical Diagnostic Laboratory, University Malaya Medical Centre for hormone analysis using ADVIA Centaur Immunoassay Systems (Siemens, USA). The three steroid hormones of interest were progesterone, estradiol and testosterone.

When the various groups of female WKY were estimated for the steroid hormones, the levels of serum progesterone were significantly increased compared to the control in the group of rats administered with 100 mg/kg body weight of FdWF (Figure 4.6, panel A). On the other hand, the levels of serum estradiol and testosterone appeared marginally higher in both the 100 mg/kg body weight of FdCE and FdWF administered groups of rats compared to the control rat group (Figure 4.6, panel B and C). These results are generally comparable to those obtained in the earlier study (Section 4.4.3) involving female nulliparous ICR mice.
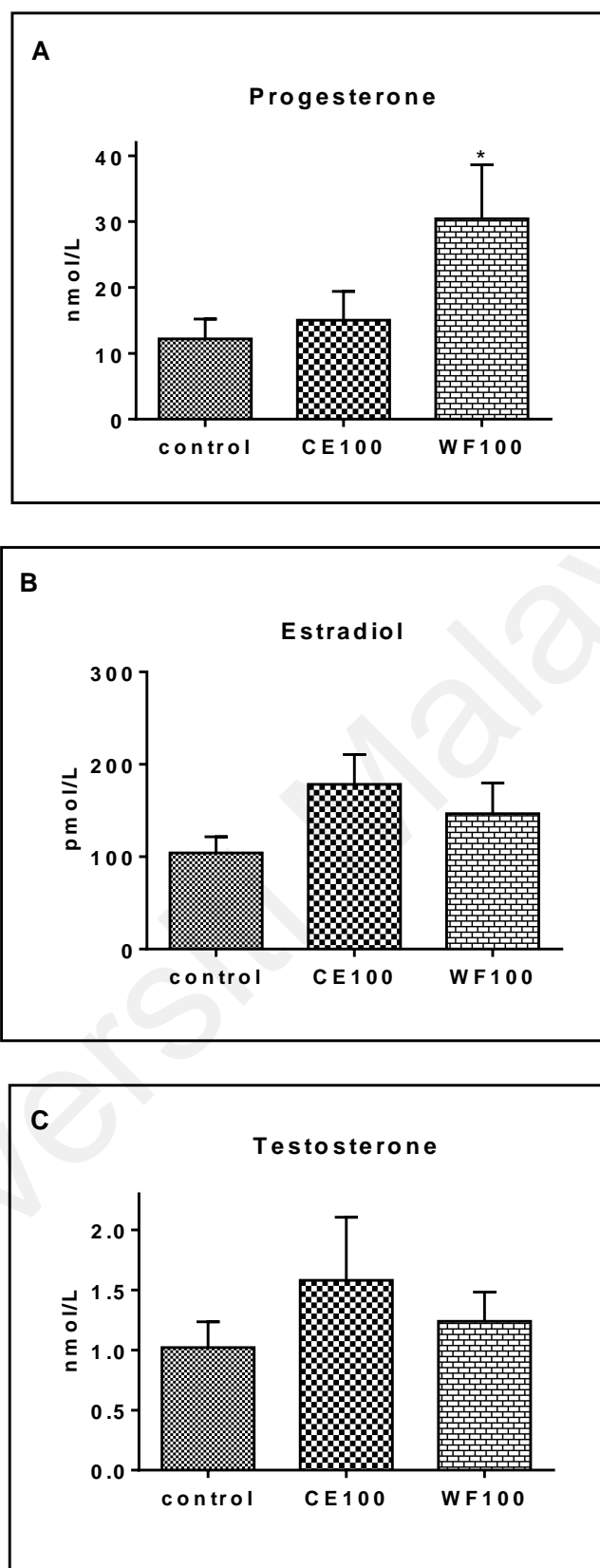
Fig 4.6. Effects of *F. deltoidea* extract and fraction on steroid hormone levels in rat serum. (A) Progesterone, (B) Estradiol and (C) Testosterone. Determination of steroid hormone levels were performed in triplicates. Data are expressed as mean ± SEM. *Statistically significant differences between groups ($p < 0.05$) in comparison to controls were measured using one-way ANOVA.

63

4.7　Immunoblotting analysis of rat uterine tissue

Muscarinic acetylcholine receptors (mAChRs) play a vital role during muscle contraction. Contractile function in smooth muscle of uterus is known to involve a mixed population of mAChRs subtypes M2 and M3. This study was carried out to investigate whether consumption of FdCE or FdWF had any effect on the uterine tissue density of M2 mAChRs.

This investigation involved the same female nulliparous groups of WKY rats that were treated with FdCE or FdWF (Section 4.6). Instead of blood, uterus was resected from the three different groups of rats, which had been orally administered with water or 100 mg/kg body weight of FdCE or FdWF once daily for a duration of 14 days.

Cleaned uterine segments were prepared to yield uterine tissue lysate according to the method described in Section 3.8.1. The tissue lysate protein was subjected to protein separation using SDS-PAGE. Proteins resolved in the SDS-PAGE gel were electro-transferred onto nitrocellulose membrane and subsequently quantified for relative expression of the M2 mAChR bands.

Immunoblotting analysis of rat uterine tissues detected presence of M2 mAChR bands near the 63 kDa region of the nitrocellulose membrane (Figure 4.7, panel A). Identity of the M2 mAChR was confirmed when similar bands were also detected in the human brain (HB) tissue lysate. For the purpose of quantitation, the intensity of the M2 mAChR bands detected in the uterine tissues of the all the groups of rats were normalized to the levels of their housekeeping β-actin protein, which appeared close to the 48 kDa region of the nitrocellulose membrane. Compared to the control group of rats, there was a significant increase in the relative intensities of the M2 mAChR bands in the uterine tissues of the FdWF administered animals, whilst the relative intensity of similar bands in the group of FdCE treated rats were not significantly different (Figure 4.7, panel B).
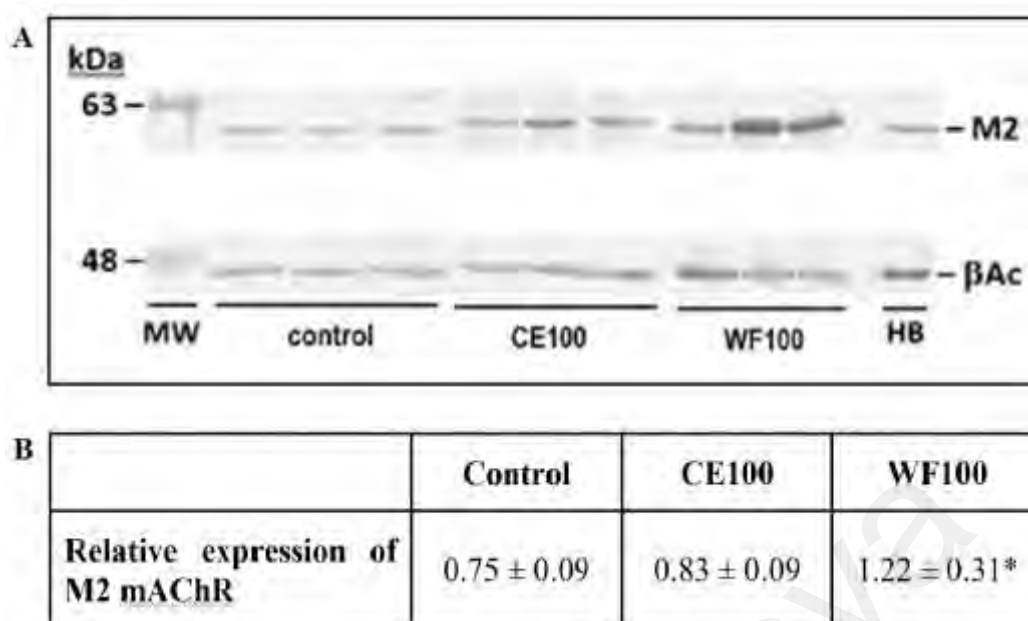
Figure 4.7: Immunoblotting of M2 mAChR in rat uterine tissues. (A) Presence of M2 mAChR was detected near the 63 kDa region and confirmed by similar appearance of bands in human brain tissue lysate (HB). (B) Relative expression of 52 kDa M2 mAChR (M2) bands was normalized to the levels of their housekeeping β-actin (βAc). Expression fold is expressed as mean ± SEM of pooled uterine tissues. MW refers to molecular weight. *Statistically significant difference ($p < 0.05$) between groups in comparison to control was measured using the Student's t-test.

4.8   2-D Electrophoresis of rat uterine tissue

In this study, uterine tissues were obtained from female WKY rats treated with 100 mg/kg body weight of FdWF for a duration of 14 days via oral gavage once daily. Another group of female WKY rats that were given water was used as a control. On day 15th, uteri were resected from all the rats and uterine tissue lysate was prepared as described in Section 3.8.1. The tissue lysate protein was then subjected to 2-DE, with the use of precast IPG strips (pH 4-7) to IEF and 11% polyacrylamide gels for the second-dimension separation. Representative 2DE gels of the control and WF100-treated group of rats used to determine relative abundance of proteins are shown in Figure 4.8. Protein spots were revealed when the gels were subjected to silver staining protocol as described in Section 3.9.1.
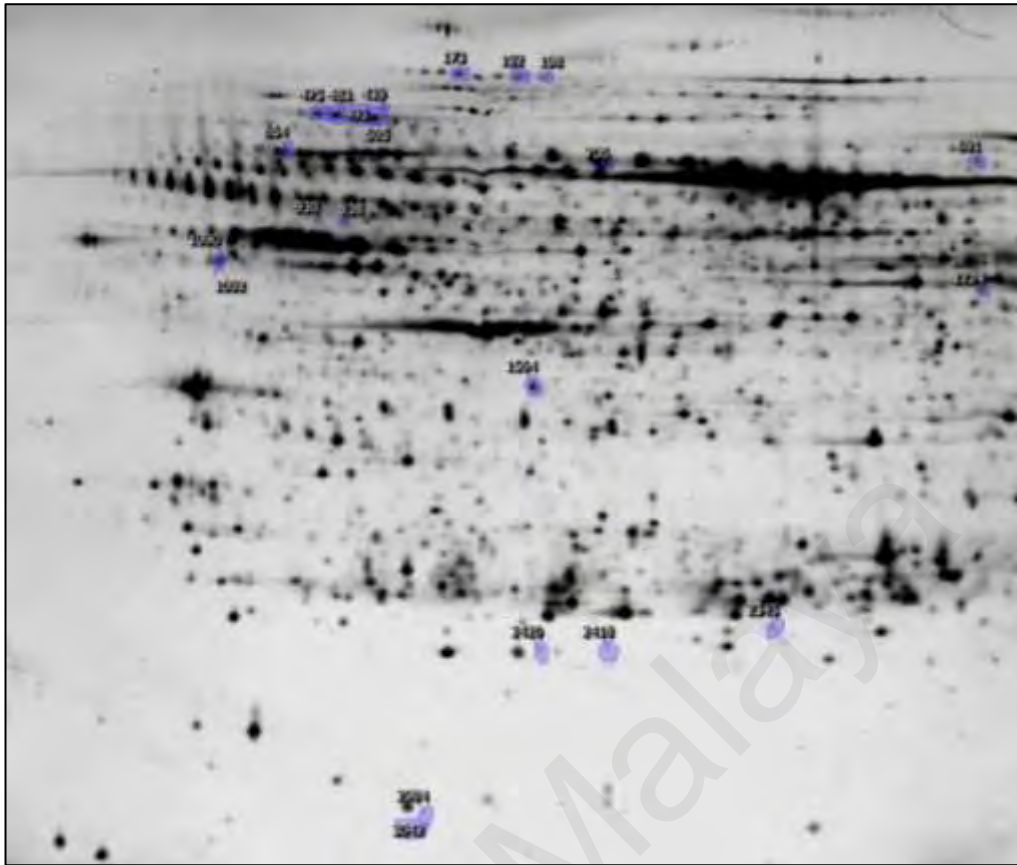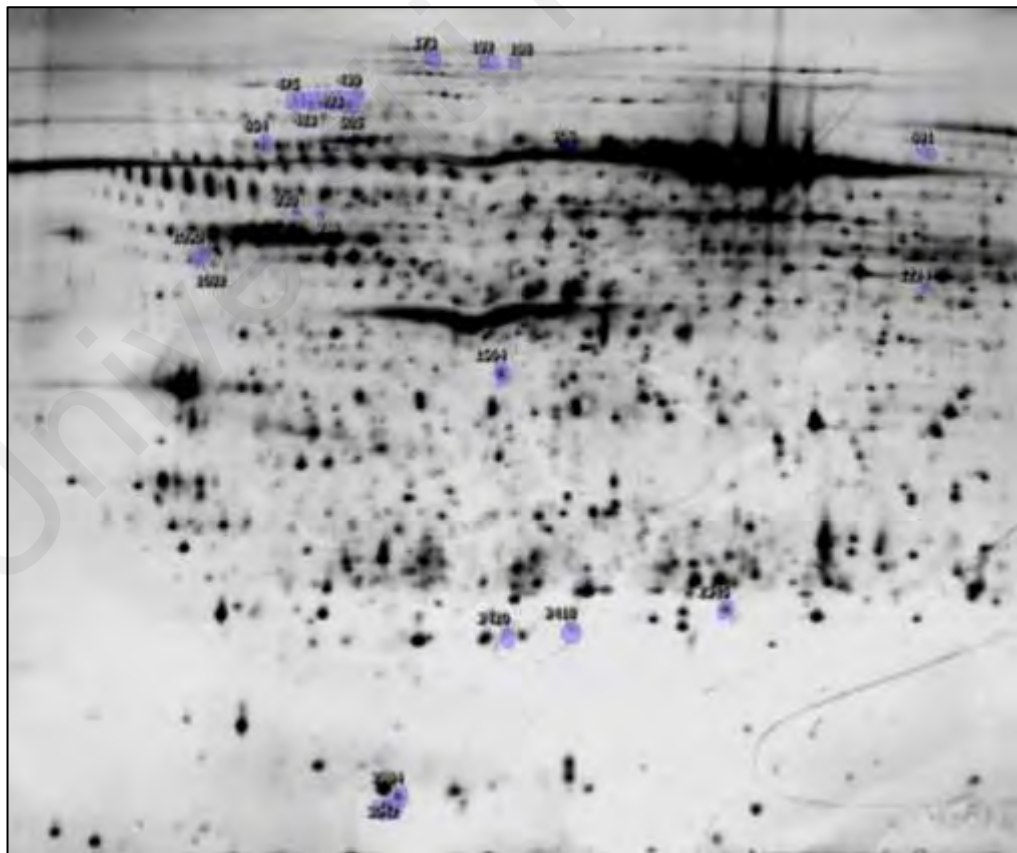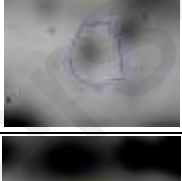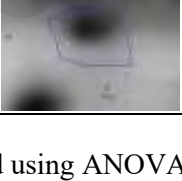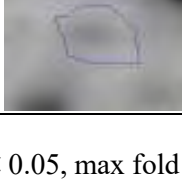
Figure 4.8: Images of representative 2DE gels used to determine relative abundance of proteins. (A) control, and (B) WF100-treated rats.

When the stained gels were scanned using Image Scanner III and analysed using Progenesis Samespot (version 4.5) software, significant changes in the proteome expression of the WF100 treated groups of rats, relative to controls, were generally detected. The expression dynamic was calculated based on the ratio of the WF100-treated groups against the control group. A total of 6 proteins appeared to be altered in abundance when greater than 2.0-fold change was set as the cut-off point ($p < 0.05$) (Table 4.5). The majority of the proteins with altered abundance observed to be down-regulated in the WF100 treated group of rats. Two of these proteins appeared to be up-regulated while four proteins were down-regulated when the rats were treated with WF100. These six proteins with altered abundance were then subjected to MALDI-ToF analysis and database query (Section 4.8.1) for identification.

Table 4.5: The expression dynamic of matched uterine protein spots of interest.

No.	Spot no.	Control	WF100	Mean Fold Change
Control versus WF100-treated rats (representative protein spots)				
1	2416			2.70
2	2413			2.13
3	752			-2.00
4	1025			-2.02
5	1050			-2.08
6	1344			-2.49

Data was analysed using ANOVA p-value < 0.05, max fold change ≥ 2.0.

4.8.1   MALDI-ToF analysis

Following 2-DE, the six protein spots with altered abundance were subjected to MALDI-ToF analysis and database query. The software for mass spectrometry, Mascot (http://www.matrixscience.com/), was used to identify proteins from the primary sequence databases of *R. norvegicus* (rat). In this analysis, a MOWSE score greater than 52 was considered as significantly identified. However, none of the six protein spots demonstrated a significant score although one, i.e, E3 ubiquitin-protein ligase, demonstrated a MOWSE score of 52 (Table 4.6). There were two other spots with their highest scores also indicating E3 ubiquitin-protein ligase. Another protein spot with a considerably high score was likely potassium voltage-gated channel subfamily S member 1 (KCNS1).

Table 4.6: MALDI-ToF analysis of differentially expressed uterine proteins.

Spot no.	Protein Name	Swissprot/ Accession no.	MOWSE Protein Score	Matched peptide	Sequence coverage (%)	Experimental		Theoretical	
						MW	pI	MW	pI
1344	E3 ubiquitin-protein ligase (RN181)	Q6AXU4	52	2/8	25.5	53,665	6.7	19,674	5.7
2416	E3 ubiquitin-protein ligase (RN181)	Q6AXU4	40	2/29	6.9	20,332	4.7	46,063	5.7
2413	E3 ubiquitin-protein ligase (RN181)	Q6AXU4	35	2/29	6.9	20,379	4.9	161,856	5.7
1025	(F-actin)-methionine sulfoxide oxidase (MICAL2)	D4A1F2	20	2/38	5.3	65,637	5.0	111,220	8.8
752	NADH dehydrogenase (ubiquinone) 1 beta subcomplex subunit 1 (NDUB1)	P0DN35	10	1/29	3.4	74,892	5.47	6,994	4.9
1050	Potassium voltage-gated channel subfamily S member 1 (KCNS1)	O88758	47	8/16	50.0	64,776	5.0	55,564	6.7

MOWSE score greater than 52 was considered significantly identified; pI: Isoelectric point; MW: Molecular weight.

4.9   LC-MS/MS Q-TOF and Label free quantification of rat uterine tissue proteins

In the first part of this study, two groups of female WKY rats were either administered with 100 mg/kg body weight of FdCE or FdWF for a duration of 14 days via oral gavage once daily. The control group was given water instead of the extract or fraction. Each group consisted of five animals (n=5). On day 15th, uterus was resected from all the rats and prepared according to the method described in Section 3.6.3 to yield uterine tissue lysate. The rat uterine tissue lysate protein was then separated by SDS-PAGE and gels were developed by silver staining. This was followed by in-gel tryptic digestion of the protein and ZipTip clean-up procedures, performed according to the methods described in Sections 3.9.8 and 3.9.9, respectively.

Processed samples containing peptides from the control and treated groups of rats (denoted as: control, CE100 and WF100) were subjected to LC-MS/MS system and Spectrum Mill software (Agilent, USA) analyzes as described in Section 3.10.3. In order to identify individual proteins, the Spectrum Mill was set up to search the UniProtKB/Swiss-Prot database for *R. norvegicus* (rat) and Scaffold Proteome software (version 4.4.6) was used to validate the MS/MS analysis across grouped samples. Proteins were considered identified based on threshold of greater than 99.0% probability and contained a minimum of 2 identified peptides. Spectral counts from analyses of the various proteins with statistically significant differences *(p < 0.05)* using One-way ANOVA with Benjamin-Hochberg post-test were compiled to represent protein expression changes or fold change.

In the present study, a total of 833 proteins from 483 clusters were identified from uterine tissues of female WKY rats that were subjected to LC-MS/MS analysis. Among these proteins, 380 were commonly detected in all uterine tissue samples analyzed, while

83, 20 and 29 proteins were exclusively detected in the control, CE100 and WF100 samples, respectively (Figure 4.9). CE100 and WF100 apparently demonstrated 31 common uterine tissue proteins, while 24 were commonly detected in CE100 and control, and 138 were commonly detected in WF100 and control.
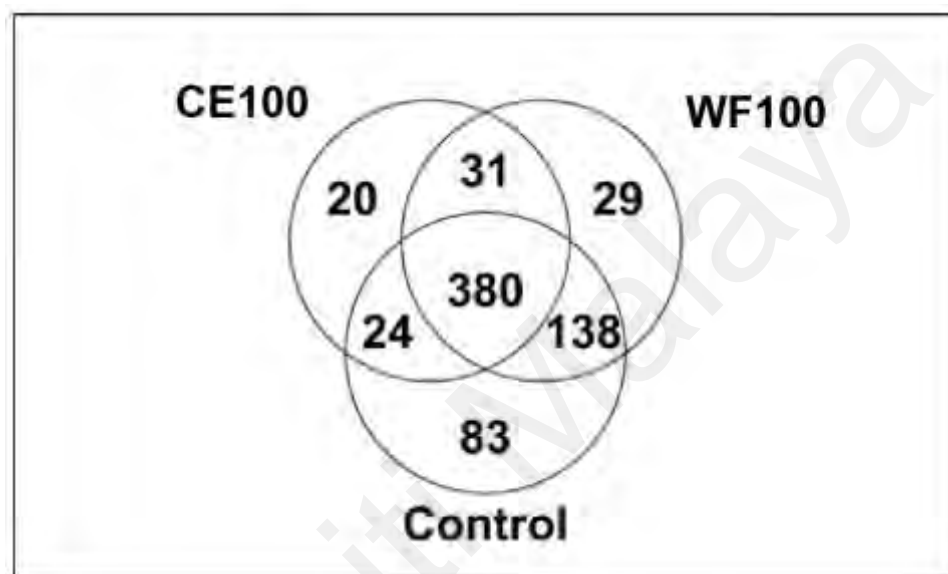
Figure 4.9: Number of identified proteins in rat uterine tissues.

4.9.1 Functional annotation of identified rat uterine tissue proteins based on Gene Ontology

Using the developed gene ontology (GO) tool which has been made available in Scaffold software (version 4.4.6) (http://www.proteomesoftware.com/products/scaffold/), functional annotation statements about a specific gene product may be derived. Each GO annotation is an association between a gene and a GO term. In the present study, identified rat uterine tissue proteins were analyzed using GO terms as annotated by the National Center for

Biotechnology Information (NCBI) (Ashburner *et al*., 2000), based on the following three domains for *R. norvegicus*:

1. Biological Process – pathways and larger processes made up of the activities of multiple gene products
2. Cellular Component – localization in the cell where gene products are active
3. Molecular Function – molecular activities of gene product

The results of the present study showed that the majority of the identified rat uterine proteins (27.08%) had unknown Biological Process function (Figure 4.10, panel A). This was followed by proteins involved in Cellular Process (14.86%), Metabolic Process (9.64%), Biological Regulation (9.38%), Response to Stimulus (7.27%) and Developmental Process (7.16%). Similarly, the functions of the majority of identified uterine proteins that were associated with Cellular Component (21.96%) as well as Molecular Function (36.25%) were also unknown (Figure 4.10, panels B and C). Many of the uterine proteins identified to be associated with the Cellular Component were those localised in the Cytoplasm (12.70%), Intercellular Organelle (12.60%), Extracellular Region (9.25%) or Organelle Part (9.12%), while those associated with Molecular Function were mainly involved in Molecular Function (23.55%), Binding (18.31%) and Catalytic Activity (10.62%).
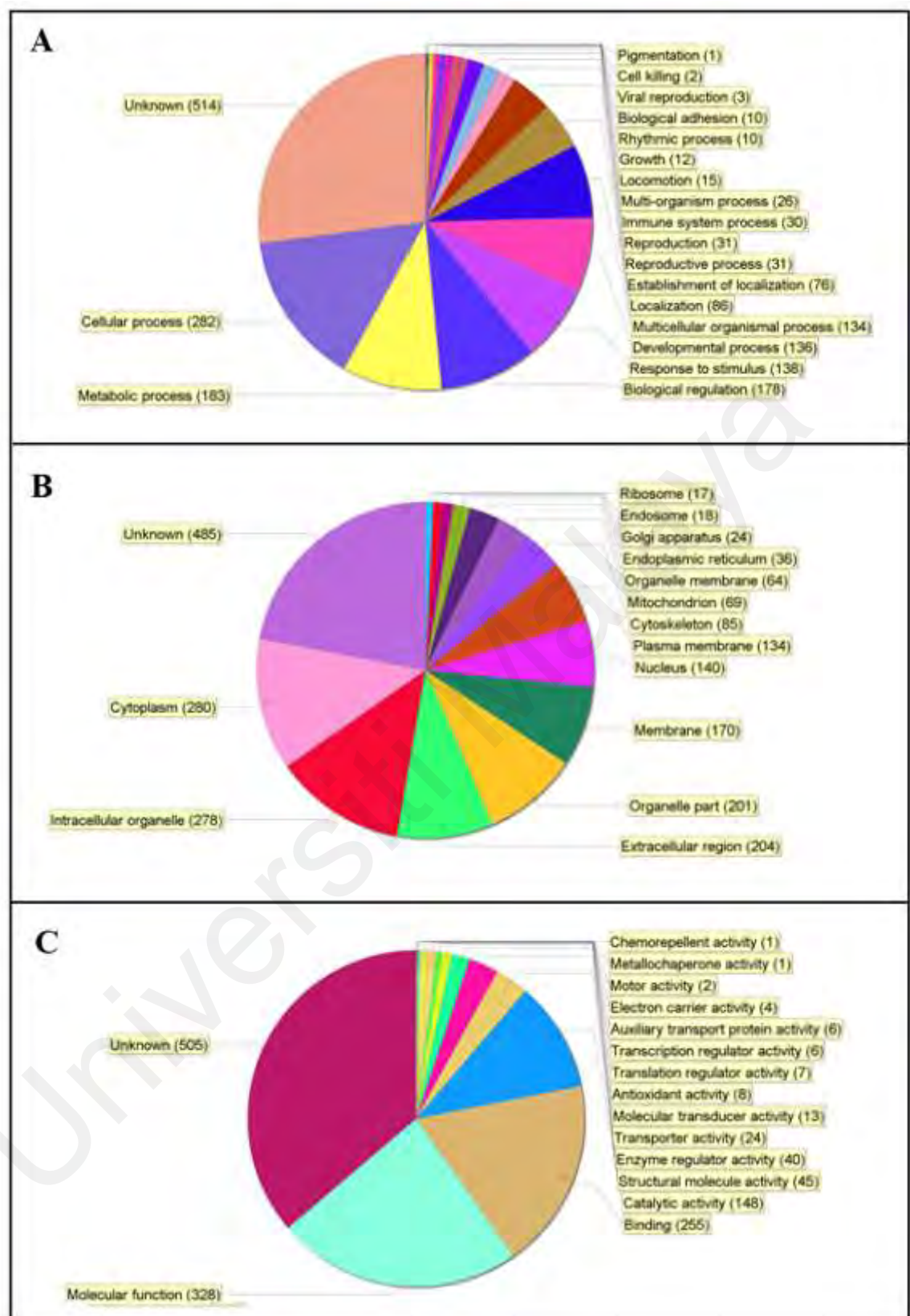
Figure 4.10: Categorization of rat uterine tissue proteins based on GO. (A) Biological Process, (B) Cellular Component and (C) Molecular Function.

In the case of Biological Process, the functions of proteins can be further categorized into Biological Adhesion, Biological Regulation, Cell Killing, Cellular Process, Developmental Process, Establishment of Localization, Growth, Immune System Process, Localization, Locomotion, Metabolic Process, Multi-organism Process, Multicellular Organismal Process, Reproduction, Reproductive Process, Response to Stimulus, Rhythmic Process and Viral Reproduction.

In a subsequent analysis that was performed, proteins were compiled based on their levels of expression or fold change. Proteins with significant expression changes greater than 1.5-fold change ($p < 0.05$) were considered as differentially regulated (up- or down-regulated). One hundred and twenty-nine proteins met the criteria of altered abundance with fold changes greater than 1.5 with a majority of them decreased in abundance (Table 4.7). Out of the 129 proteins, 29 were exclusively altered in the group of rats treated with CE100, whilst 15 were altered only in animals treated with WF100. The remaining 85 proteins, on the other hand, were altered in both groups of CE100- and WF100-treated rats. This denotes that among the 129 altered abundant proteins, 114 were proteins present in CE100 treated rats and 100 present in WF100 rats (Figure 4.11).
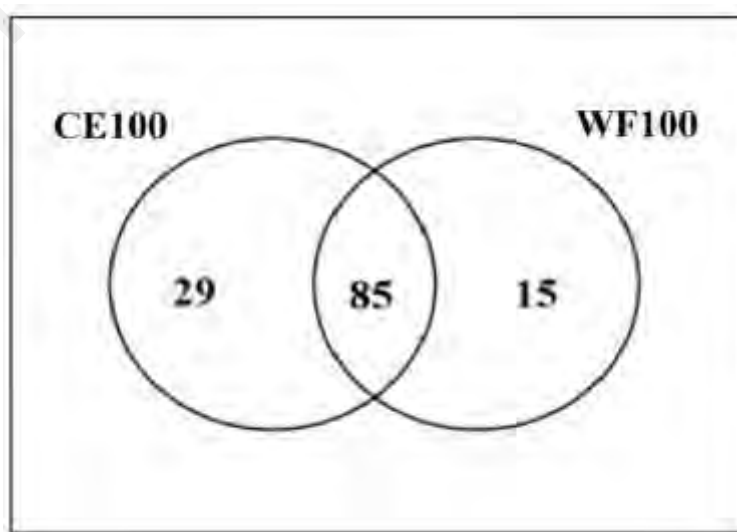
Figure 4.11: Venn diagrams of proteins with expression changes greater than 1.5-fold change.

Table 4.7: Identification of rat uterine proteins with altered abundance at greater than 1.5-fold change.

No.	Protein	Swiss-Prot ID	Mass	p value	CE100 vs control		WF100 vs control	
					Fold Change	Log Fold Change	Fold Change	Log Fold Change
1	Keratin, type I cytoskeletal 42	Q6IFU7	50554.6	1.35E-11	34816.80	18.40	39681.54	15.28
2	Keratin, type II cytoskeletal 6A	Q4FZU2	59590.3	0.00167855	182109.81	17.47	478.28	8.90
3	Alcohol dehydrogenase 1	F1LSR9	40669.8	6.66E-13	48994.49	15.58	12518.59	13.61
4	Nucleolin	Q5U328	77332.1	2.36E-12	32347.75	14.98	27284.72	14.74
5	Splicing factor proline/glutamine rich (Polypyrimidine tract binding protein associated)	Q4KM71	75599.5	1.21E-11	26892.61	14.71	14675.83	13.84
6	Plastin 3 (T-isoform), isoform CRA_a	F1LPK7	71261.2	6.75E-11	24158.90	14.56		
7	Type II keratin Kb25	A7M777	57360.8	1.51E-08	18575.22	14.18		
8	Procollagen-lysine,2-oxoglutarate 5-dioxygenase 2	D3ZQR7	87637.2	0.00321369	10460.16	13.35	324.98	8.34
9	Protein Hnrnpab	Q9QX81	36346.3	0.00195685	16.44	4.04	13242.00	13.69
10	Histone H2B	D3ZNH4	15492.7	8.13E-06	-4.86	2.28	3.27	1.71
11	Transgelin	P31232	22659.5	8.74E-05	4.47	2.16	1.85	0.89
12	Polyubiquitin-C	Q63429	91199.3	4.33E-04	2.21	1.15		
13	Protein disulfide-isomerase A3	P11598	57078.7	2.47E-06	1.75	0.81		
14	Keratin, type II cytoskeletal 1	Q6IMF3	65229.1	5.87E-06	1.73	0.79		
15	Enolase 1, (Alpha)	Q5EB49	47499.4	0.00160775	1.67	0.74		
16	Endoplasmin	A0A0A0MY09	93183.7	3.17E-07	1.64	0.71		
17	Annexin A2	Q07936	38962.8	4.03E-04	1.61	0.69		
18	Annexin	Q6IMZ3	76154.2	3.08E-04	1.51	0.59		
19	Citrate synthase, mitochondrial	Q8VHF5	52208.2	0.00175167	1.50	0.58		
20	Heat shock protein HSP 90-beta	P34058	83622	0.00340444	-1.51	-0.60		

Table 4.7, continued.

No.	Protein	Swiss-Prot ID	Mass	p value	CE100 vs control		WF100 vs control	
					Fold Change	Log Fold Change	Fold Change	Log Fold Change
21	Protein disulfide-isomerase A6	Q63081	48571.9	1.24E-04	-1.65	-0.73	-1.73	-0.79
22	Alpha-2-HS-glycoprotein	F1LM19	38834.5	1.41E-07	-1.77	-0.83	-4.81	-2.26
23	78 kDa glucose-regulated protein	P06761	72516.8	4.38E-04	-1.78	-0.84		
24	Histone H4	P62804	11367.1	4.98E-07	-1.81	-0.86	-3.21	-1.68
25	Adenosylhomocysteinase	Q6P743	48200.8	1.03E-04	-1.89	-0.91	-2.27	-1.18
26	Calreticulin	P18418	48165.7	0.00356688	-2.00	-1.00		
27	Alpha-1-inhibitor 3	P14046	165139.6	6.23E-05	-2.10	-1.07	-2.53	-1.34
28	Hemopexin	P20059	52091.7	7.87E-05	-2.27	-1.18	-2.20	-1.13
29	Protein Mylk	D3ZFU9	217533.3	2.47E-04	-2.68	-1.42		
30	Creatine kinase B-type	P07335	43009.8	0.00164845	-4.12	-2.04	-1.98	-0.99
31	Hemoglobin alpha, adult chain 2	B1H216	15499.4	1.09E-06	-4.15	-2.05	-6.00	-2.58
32	Hemoglobin subunit beta-2	P11517	16096.2	1.19E-06	-6.30	-2.65	-5.78	-2.53
33	Ceruloplasmin	P13635	121637.2	1.28E-04	-7.94	-2.99	-1.82	-0.87
34	Histone H3.1	Q6LED0	155179	7.83E-07	-10.61	-3.41	-3.47	-1.79
35	Tubulin alpha-1B chain	Q6P9V9	50835.4	4.30E-06	-14.46	-3.85	-1.58	-0.66
36	Alpha-actinin-4	Q9QXQ0	105369.6	0.00312007	-20.63	-4.37	333.31	8.38
37	Glyceraldehyde-3-phosphate dehydrogenase	M0R660	36067.6	0.00349064	-27.46	-4.78	-27.46	-4.78
38	Protein Arhgap1	D4A6C5	50679	0.00335326	-1700.67	-10.73	-1.57	-0.65
39	Proteasome (Prosome, macropain) activator subunit 1	Q6P9V7	28805.6	2.99E-09	-7920.86	-12.95	-7920.86	-12.95
40	6-phosphogluconolactonase	G3V8D5	31163.2	1.88E-16	-9220.19	-13.17	-9220.19	-13.17

No.	Protein	Swiss-Prot ID	Mass	p value	CE100 vs control		WE100 vs control	
					Fold Change	Log Fold Change	Fold Change	Log Fold Change
41	14-3-3 protein gamma	P61983	28473.3	1.68E-07	-9269.81	-13.18	2.67	1.42
42	Clathrin heavy chain	F1M779	193324.8	3.24E-11	-9418.11	-13.20	-9418.11	-13.20
43	N(G),N(G)-dimethylarginine dimethylaminohydrolase 2	Q6MG60	30029.7	1.26E-12	-9611.73	-13.23	-9611.73	-13.23
44	60S ribosomal protein L13	P41123	24366.1	2.93E-09	-9734.54	-13.25	-9734.54	-13.25
45	Electron transfer flavoprotein subunit alpha, mitochondrial	P13803	35293	6.30E-09	-9963.67	-13.28	-9963.67	-13.28
46	Purine nucleoside phosphorylase	P85973	32586.6	5.36E-09	-10201.77	-13.32	-10201.77	-13.32
47	40S ribosomal protein S8	B2RYR8	24490	1.97E-12	-10807.25	-13.40	-10807.25	-13.40
48	14-3-3 protein beta/alpha	P35213	28168	3.29E-10	-11556.62	-13.50	3.10	1.63
49	Peptidyl-prolyl cis-trans isomerase	Q6AYQ9	23066.1	1.82E-10	-14506.20	-13.82	-14506.20	-13.82
50	Protein Serpina4	Q5M8C3	48160.3	6.60E-10	-15703.83	-13.94	-15703.83	-13.94
51	3-alpha-hydroxysteroid dehydrogenase	P23457	37540.4	2.05E-08	-15858.31	-13.95	-15858.31	-13.95
52	Heterogeneous nuclear ribonucleoprotein A3	Q6URK4	39879.5	5.34E-12	-16056.79	-13.97	1.78	0.83
53	Myl9 protein	B0BMS8	19910.9	1.61E-07	-16394.65	-14.00	2.26	1.18
54	Low molecular weight phosphotyrosine protein phosphatase	Z4YNF4	18944.1	1.24E-11	-16860.19	-14.04	-16860.19	-14.04
55	Procollagen, type VI, alpha 2, isoform CRA_a	F1LNH3	110798.7	1.23E-11	-19621.53	-14.26		
56	Destrin	Q7M0E3	18818.5	4.86E-11	-19860.96	-14.28	1.65	0.73
57	Apolipoprotein A-I	P04639	30118.7	0.00243954	-20736.20	-14.34	2.70	1.43
58	Tubulin alpha-1C chain	Q6AYZ1	50621.1	0.00327084	-20841.74	-14.35	-69.86	-6.13
59	Nucleoside diphosphate kinase B	P19804	17396.8	1.37E-12	-21481.89	-14.39		

Table 4.7, continued.

No.	Protein	Swiss-Prot ID	Mass	p value	CE100 vs control		WF100 vs control	
					Fold Change	Log Fold Change	Fold Change	Log Fold Change
60	Plasma protease C1 inhibitor	Q6P734	55838.5	3.82E-11	-21884.64	-14.42		
61	Prothrombin	P18292	71836.9	0.00192888	-22704.47	-14.47	-1642.77	-10.68
62	Selenium-binding protein 1	Q8VIF7	53101.7	7.33E-09	-23411.08	-14.51	-23411.08	-14.51
63	T-complex protein 1 subunit gamma	Q6P502	61216.5	3.32E-17	-25240.09	-14.62	-25240.09	-14.62
64	Ptges3 protein	B2GV92	19006.4	2.01E-14	-26039.26	-14.67	-26039.26	-14.67
65	Eukaryotic translation initiation factor 4A1	Q6P3V8	46381.4	0.00259831	-27139.63	-14.73	-92.59	-6.53
66	Rho GDP-dissociation inhibitor 1	Q5XI73	23464	0.00206418	-27160.44	-14.73	-1524.95	-10.57
67	Cysteine and glycine-rich protein 1	P47875	21468.9	7.13E-10	-27226.34	-14.73	10.18	3.35
68	Prohibitin	P67779	29876.6	1.49E-10	-27262.96	-14.73	-27262.96	-14.73
69	Methylmalonate-semialdehyde dehydrogenase [acylating], mitochondrial	Q02253	58263	1.15E-15	-27606.71	-14.75	-27606.71	-14.75
70	6-phosphogluconate dehydrogenase, decarboxylating	Q7TP11	121777.5	8.83E-12	-27720.53	-14.76	-27720.53	-14.76
71	Actin-related protein 2/3 complex subunit 3	B2GV73	20763.5	1.01E-10	-27783.17	-14.76	-27783.17	-14.76
72	Guanine deaminase	Q9JKB7	51470.6	1.30E-13	-29040.22	-14.83	-29040.22	-14.83
73	Protein LOC100362751	D4A4D5	11705.8	3.72E-12	-29099.02	-14.83		
74	Isoform M2 of Pyruvate kinase PKM	P11980-2	58350.3	1.11E-14	-29559.04	-14.85		
75	Acidic (Leucine-rich) nuclear phosphoprotein 32 family, member A	Q5PPI9	28736.2	9.30E-11	-30187.17	-14.88		
76	Phosphoglycerate mutase 1	P25113	28945.6	2.25E-10	-31756.48	-14.95	-31756.48	-14.95
77	Protein LOC100362339	D4A6G6	16117.3	1.54E-12	-31910.22	-14.96		
78	Protein LOC100911847	Q6PDV6	16443.6	0.00319862	-32401.57	-14.98	-32401.57	-14.98

Table 4.7, continued.

No.	Protein	Swiss-Prot ID	Mass	p value	CE100 vs control		WF100 vs control	
					Fold Change	Log Fold Change	Fold Change	Log Fold Change
79	Serine (Or cysteine) proteinase inhibitor, clade H, member 1, isoform CRA_b	Q5RJR9	46674.8	2.33E-15	-32473.40	-14.99	-32473.40	-14.99
80	Protein Vps35	G3V8A5	92524.1	8.48E-15	-33046.50	-15.01	-33046.50	-15.01
81	60S ribosomal protein L7	P05426	30385.8	8.75E-12	-33418.15	-15.03	-33418.15	-15.03
82	Aspartate aminotransferase, mitochondrial	P00507	47712.8	3.23E-11	-34930.88	-15.09	-2.34	-1.23
83	Carbonic anhydrase 3	P14141	29716.1	7.98E-14	-35810.47	-15.13	-35810.47	-15.13
84	Isoform 2 of NADH-cytochrome b5 reductase 3	P20070-2	35093.1	1.54E-11	-36003.11	-15.14	-36003.11	-15.14
85	Protein LOC100909878	D3ZLL8	14968.3	1.07E-07	-36101.01	-15.14	-36101.01	-15.14
86	Protein Ppp2r1a	Q5X134	66120.2	8.94E-15	-37307.41	-15.19	-37307.41	-15.19
87	Glutamate dehydrogenase 1, mitochondrial	P10860	61757.1	5.99E-10	-39951.32	-15.29		
88	Glucose-6-phosphate isomerase	Q6P6V0	62997	3.05E-09	-40201.88	-15.29	-2.99	-1.58
89	Calponin-1	Q08290	33514.2	1.29E-11	-40428.99	-15.30		
90	Hnrpk protein	Q5D059	51312.6	0.00323914	-40985.59	-15.32		
91	Aa1249	Q7TMA9	117828.7	1.18E-14	-41655.90	-15.35	-41655.90	-15.35
92	Actin-related protein 3	Q4V7C7	47812.7	0.0028149	-44829.83	-15.45	-1834.21	-10.84
93	Dihydropyrimidinase-related protein 2	P47942	62675.8	1.42E-08	-45456.18	-15.47	-2.81	-1.49
94	Peptidyl-prolyl cis-trans isomerase B	P24368	23859.2	1.80E-10	-46152.79	-15.49		
95	Chloride intracellular channel protein 1	Q6MG61	27322.6	0.00311391	-47690.22	-15.54	-1843.94	-10.85
96	14-3-3 protein epsilon	P62260	29344.6	9.90E-10	-48613.65	-15.57		
97	Stress-induced-phosphoprotein 1	R9PXW7	63295.7	1.35E-13	-49083.89	-15.58	-49083.89	-15.58
98	RCG45400	G3V7C6	50286.6	1.43E-14	-55322.36	-15.76		
99	Protein Snrpd3	M0R907	14030.1	1.26E-09	-56008.58	-15.77	-56008.58	-15.77

Table 4.7, continued.

No.	Protein	Swiss-Prot ID	Mass	p value	CE100 vs control		WF100 vs control	
					Fold Change	Log Fold Change	Fold Change	Log Fold Change
100	Heterochromatin protein 1-binding protein 3	F1M6V1	61306.3	9.67E-16	-65992.29	-16.01	-65992.29	-16.01
101	Histone H1.5	D3ZBN0	22648.8	1.62E-15	-69358.51	-16.08	1.53	0.61
102	Tropomyosin alpha-3 chain	Q63610	29234.3	1.33E-09	-70806.36	-16.11		
103	LOC500183 protein	Q4KM66	26033.6	7.02E-12	-73356.82	-16.16	1.67	0.74
104	Ferritin light chain 1	P02793	20805.2	0.00320459	-74825.39	-16.19	-111.29	-6.80
105	Ezrin	P31977	69503.7	5.28E-14	-78564.77	-16.26	-2.34	-1.23
106	Alpha globin	Q63910	15581.4	7.66E-16	-87774.75	-16.42	-87774.75	-16.42
107	Dipeptidyl peptidase 2	Q9EPB1	55683.9	2.48E-15	-87885.76	-16.42	-5.59	-2.48
108	D-dopachrome decarboxylase	P80254	13247.1	1.33E-10	-107282.26	-16.71	-107282.26	-16.71
109	Alpha-1B-glycoprotein	Q9EPH1	57162.5	2.24E-16	-110127.23	-16.75	-4.86	-2.28
110	ATP synthase subunit f, mitochondrial	D3ZAF6	105009.2	1.20E-22	-114317.80	-16.80	-114317.80	-16.80
111	Histone H1.0	P43278	20884.6	0.00285679	-114388.70	-16.80		
112	Myosin light chain 3	P16409	22269.9	0.0031681	-117631.59	-16.84	-213.25	-7.74
113	Protein LOC100360905	D3ZIY5	19373.8	1.64E-14	-157804.88	-17.27	-157804.88	-17.27
114	Histone H2A type 4	Q00728	14283.4	4.96E-15	-1072056.90	-20.03	-1072056.90	-20.03
115	SP130	Q63555	88545.7	4.11E-12			19055.86	14.22
116	Ras-related C3 botulinum toxin substrate 1	Q6RUV5	21849.1	0.00160716			16640.28	14.02
117	Ubiquitin-like modifier-activating enzyme 1	Q5U300	118983.8	3.05E-14			7225.46	12.82
118	Glutathione peroxidase 1	P04041	22326	0.00341304			15.90	3.99
119	L-lactate dehydrogenase	B5DEN4	36735.1	0.00256761			2.10	1.07
120	Malate dehydrogenase, mitochondrial	P04636	36139.3	1.89E-05			1.71	0.77

Table 4.7, continued.

No.	Protein	Swiss-Prot ID	Mass	p value	CE100 vs control		WF100 vs control	
					Fold Change	Log Fold Change	Fold Change	Log Fold Change
121	Gelsolin	Q68FP1	86465.4	3.82E-05			-1.53	-0.61
122	Lymphocyte cytosolic protein 1	Q5X138	70748.5	4.41E-04			-1.56	-0.64
123	Serum albumin	P02770	70726.5	1.21E-08			-1.61	-0.69
124	Serine protease inhibtior A3K	P05545	46788.9	0.00214481			-1.97	-0.98
125	Serotransferrin	P12346	78561.8	0.00226074			-2.13	-1.09
126	Alpha-1-antiproteinase	P17475	46306.1	1.25E-04			-2.33	-1.22
127	Brain-specific alpha actinin 1 isoform	Q6T487	106097	0.00380025			-2.45	-1.29
128	Heat shock cognate 71 kDa protein	P63018	71098	5.36E-05			-3.13	-1.65
129	Protein disulfide-isomerase	P04785	57349.6	3.84E-08			-3.27	-1.71

Proteins were significantly regulated at $p < 0.05$. The symbol (-) indicates down-regulation.

Out of these 100 proteins present in WF100 rats, 9 were apparently consistently up-regulated, with another 66 consistently down-regulated in both groups of CE100- and WF100-treated and 10 proteins were not consistently up- or down-regulated in both the treated group of rats. On the other hand, 6 proteins were up- and 9 were down-regulated exclusively in the WF100 treated group of rats (Table 4.8).

When the proteins with altered abundance were analyzed based on their functions, the following results were generated. Approximately 49.69% of the up-regulated proteins in the WF100 group were apparently involved in Other Processes. This was followed by those involved in Cellular Process (14.72%), Biological Regulation (9.20%), Developmental Process (8.59%), Response to Stimulus (7.36%), Multicellular Organismal Process (6.13%) and Metabolic Process (4.92%) (Figure 4.12, panel A).

A similar trend was observed for the down-regulated proteins of WF100 group, with 45.82% of the proteins involved in Other Processes, 15.27% involved in Cellular Process, 9.45% involved in Biological Regulation, 5.82% involved in Developmental Process, 7.27% involved in Response to Stimulus, 6.55% involved in Multicellular Organismal Process and 9.82% involved in Metabolic Process (Figure 4.12, panel B).

Table 4.8: Uterine proteins that were altered in abundance at greater than 1.5-fold change in group of rats treated with WF100.

No.	Protein	Swiss-Prot ID	Mass	p value	CE100 vs control		WF100 vs control	
					Fold Change	Log Fold Change	Fold Change	Log Fold Change
1	Keratin, type I cytoskeletal 42	Q6IFU7	50554.6	1.35E-11	346816.80	18.40	39681.54	15.28
2	Keratin, type II cytoskeletal 6A	Q4FZU2	59590.3	0.00167855	182109.81	17.47	478.28	8.90
3	Alcohol dehydrogenase 1	F1LSR9	40669.8	6.66E-13	48994.49	15.58	12518.59	13.61
4	Nucleolin	Q5U328	77332.1	2.36E-12	32347.75	14.98	27284.72	14.74
5	Splicing factor proline/glutamine rich (Polypyrimidine tract binding protein associated)	Q4KM71	75599.5	1.21E-11	26892.61	14.71	14675.83	13.84
6	Procollagen-lysine,2-oxoglutarate 5-dioxygenase 2	D3ZQR7	87637.2	0.00321369	10460.16	13.35	324.98	8.34
7	Protein Hornpab	Q9QX81	36346.3	0.00195685	16.44	4.04	13242.00	13.69
8	Histone H2B	D3ZNH4	15492.7	8.13E-06	4.86	2.28	3.27	1.71
9	Transgelin	P31232	22659.5	8.74E-05	4.47	2.16	1.85	0.89
10	Protein disulfide-isomerase A6	Q63081	48571.9	1.24E-04	-1.65	-0.73	-1.73	-0.79
11	Alpha-2-HS-glycoprotein	F1LM19	38834.5	1.41E-07	-1.77	-0.83	-4.81	-2.26
12	Histone H4	P62804	11367.1	4.98E-07	-1.81	-0.86	-3.21	-1.68
13	Adenosylhomocysteinase	Q6P743	48200.8	1.03E-04	-1.89	-0.91	-2.27	-1.18
14	Alpha-1-inhibitor 3	P14046	165139.6	6.23E-05	-2.10	-1.07	-2.53	-1.34
15	Hemopexin	P20059	52091.7	7.87E-05	-2.27	-1.18	-2.20	-1.13
16	Creatine kinase B-type	P07335	43009.8	0.00164845	-4.12	-2.04	-1.98	-0.99
17	Hemoglobin alpha, adult chain 2	B1H216	15499.4	1.09E-06	-4.15	-2.05	-6.00	-2.58
18	Hemoglobin subunit beta-2	P11517	16096.2	1.19E-06	-6.30	-2.65	-5.78	-2.53
19	Ceruloplasmin	P13635	121637.2	1.28E-04	-7.94	-2.99	-1.82	-0.87
20	Histone H3.1	Q6LED0	15517.9	7.83E-07	-10.61	-3.41	-3.47	-1.79

Table 4.8, continued.

No.	Protein	Swiss-Prot ID	Mass	p value	CE100 vs control		WE100 vs control	
					Fold Change	Log Fold Change	Fold Change	Log Fold Change
21	Tubulin alpha-1B chain	Q6P9V9	50835.4	4.30E-06	-14.46	-3.85	-1.58	-0.66
22	Alpha-actinin-4	Q9QXQ0	105369.6	0.00312007	-20.63	-4.37	333.31	8.38
23	Glyceraldehyde-3-phosphate dehydrogenase	M0R660	36067.6	0.00349064	-27.46	-4.78	-27.46	-4.78
24	Protein Arhgap1	D4A6C5	50679	0.00335326	-1700.67	-10.73	-1.57	-0.65
25	Proteasome (Prosome, macropain) activator subunit 1	Q6P9V7	28805.6	2.99E-09	-7920.86	-12.95	-7920.86	-12.95
26	6-phosphogluconolactonase	G3V8D5	31163.2	1.88E-16	-9220.19	-13.17	-9220.19	-13.17
27	14-3-3 protein gamma	P61983	28473.3	1.68E-07	-9269.81	-13.18	2.67	1.42
28	Clathrin heavy chain	F1M779	193324.8	3.24E-11	-9418.11	-13.20	-9418.11	-13.20
29	N(G),N(G)-dimethylarginine dimethylaminohydrolase 2	Q6MG60	30029.7	1.26E-12	-9611.73	-13.23	-9611.73	-13.23
30	60S ribosomal protein L13	P41123	24366.1	2.93E-09	-9734.54	-13.25	-9734.54	-13.25
31	Electron transfer flavoprotein subunit alpha, mitochondrial	P13803	35293	6.30E-09	-9963.67	-13.28	-9963.67	-13.28
32	Purine nucleoside phosphorylase	P85973	32586.6	5.36E-09	-10201.77	-13.32	-10201.77	-13.32
33	40S ribosomal protein S8	B2RYR8	24490	1.97E-12	-10807.25	-13.40	-10807.25	-13.40
34	14-3-3 protein beta/alpha	P35213	28168	3.29E-10	-11556.62	-13.50	3.10	1.63
35	Peptidyl-prolyl cis-trans isomerase	Q6AYQ9	23066.1	1.82E-10	-14506.20	-13.82	-14506.20	-13.82
36	Protein Serpina4	Q5M8C3	48160.3	6.60E-10	-15703.83	-13.94	-15703.83	-13.94
37	3-alpha-hydroxysteroid dehydrogenase	P23457	37540.4	2.05E-08	-15858.31	-13.95	-15858.31	-13.95
38	Heterogeneous nuclear ribonucleoprotein A3	Q6URK4	39879.5	5.34E-12	-16056.79	-13.97	1.78	0.83
39	Myl9 protein	B0BMS8	19910.9	1.61E-07	-16394.65	-14.00	2.26	1.18

Table 4.8, continued.

No.	Protein	Swiss-Prot ID	Mass	p value	CE100 vs control		WF100 vs control	
					Fold Change	Log Fold Change	Fold Change	Log Fold Change
40	Low molecular weight phosphotyrosine protein phosphatase	Z4YNF4	18944.1	1.24E-11	-16860.19	-14.04	-16860.19	-14.04
41	Destrin	Q7M0E3	18818.5	4.86E-11	-19860.96	-14.28	1.65	0.73
42	Apolipoprotein A-I	P04639	30118.7	0.00243954	-20736.20	-14.34	2.70	1.43
43	Tubulin alpha-1C chain	Q6AYZ1	50621.1	0.00327084	-20841.74	-14.35	-69.86	-6.13
44	Prothrombin	P18292	71836.9	0.00192888	-22704.47	-14.47	-1642.77	-10.68
45	Selenium-binding protein 1	Q8VIF7	53101.7	7.33E-09	-23411.08	-14.51	-23411.08	-14.51
46	T-complex protein 1 subunit gamma	Q6P502	61216.5	3.32E-17	-25240.09	-14.62	-25240.09	-14.62
47	Ptges3 protein	B2GV92	19006.4	2.01E-14	-26039.26	-14.67	-26039.26	-14.67
48	Eukaryotic translation initiation factor 4A1	Q6P3V8	46381.4	0.00259831	-27139.63	-14.73	-92.59	-6.53
49	Rho GDP-dissociation inhibitor 1	Q5XI73	23464	0.00206418	-27160.44	-14.73	-1524.95	-10.57
50	Cysteine and glycine-rich protein 1	P47875	21468.9	7.13E-10	-27226.34	-14.73	10.18	3.35
51	Prohibitin	P67779	29876.6	1.49E-10	-27262.96	-14.73	-27262.96	-14.73
52	Methylmalonate-semialdehyde dehydrogenase [acylating], mitochondrial	Q02253	58263	1.15E-15	-27606.71	-14.75	-27606.71	-14.75
53	6-phosphogluconate dehydrogenase, decarboxylating	Q7TP11	121777.5	8.83E-12	-27720.53	-14.76	-27720.53	-14.76
54	Actin-related protein 2/3 complex subunit 3	B2GV73	20763.5	1.01E-10	-27783.17	-14.76	-27783.17	-14.76
55	Guanine deaminase	Q9JKB7	51470.6	1.30E-13	-29040.22	-14.83	-29040.22	-14.83
56	Phosphoglycerate mutase 1	P25113	28945.6	2.25E-10	-31756.48	-14.95	-31756.48	-14.95
57	Protein LOC100911847	Q6PDV6	16443.6	0.00319862	-32401.57	-14.98	-32401.57	-14.98

Table 4.8, continued.

No.	Protein	Swiss-Prot ID	Mass	p value	CE100 vs control		WF100 vs control	
					Fold Change	Log Fold Change	Fold Change	Log Fold Change
58	Serine (Or cysteine) proteinase inhibitor, clade H, member 1, isoform CRA b	Q5RJR9	46674.8	2.33E-15	-32473.40	-14.99	-32473.40	-14.99
59	Protein Vps35	G3V8A5	92524.1	8.48E-15	-33046.50	-15.01	-33046.50	-15.01
60	60S ribosomal protein L7	P05426	30385.8	8.75E-12	-33418.15	-15.03	-33418.15	-15.03
61	Aspartate aminotransferase, mitochondrial	P00507	47712.8	3.23E-11	-34930.88	-15.09	-2.34	-1.23
62	Carbonic anhydrase 3	P14141	29716.1	7.98E-14	-35810.47	-15.13	-35810.47	-15.13
63	Isoform 2 of NADH-cytochrome b5 reductase 3	P20070-2	35093.1	1.54E-11	-36003.11	-15.14	-36003.11	-15.14
64	Protein LOC100009878	D3ZLL8	14968.3	1.07E-07	-36101.01	-15.14	-36101.01	-15.14
65	Protein Ppp2r1a	Q5XI34	66120.2	8.94E-15	-37307.41	-15.19	-37307.41	-15.19
66	Glucose-6-phosphate isomerase	Q6P6V0	62997	3.05E-09	-40201.88	-15.29	-2.99	-1.58
67	Aa1249	Q7TMA9	117828.7	1.18E-14	-41655.90	-15.35	-41655.90	-15.35
68	Actin-related protein 3	Q4V7C7	47812.7	0.0028149	-44829.83	-15.45	-1834.21	-10.84
69	Dihydropyrimidinase-related protein 2	P47942	62675.8	1.42E-08	-45456.18	-15.47	-2.81	-1.49
70	Chloride intracellular channel protein 1	Q6MG61	27322.6	0.00311391	-47690.22	-15.54	-1843.94	-10.85
71	Stress-induced-phosphoprotein 1	R9PXW7	63295.7	1.35E-13	-49083.89	-15.58	-49083.89	-15.58
72	Protein Snrpd3	M0R907	14030.1	1.26E-09	-56008.58	-15.77	-56008.58	-15.77
73	Heterochromatin protein 1-binding protein 3	F1M6V1	61306.3	9.67E-16	-65992.29	-16.01	-65992.29	-16.01
74	Histone H1.5	D3ZBN0	22648.8	1.62E-15	-69358.51	-16.08	1.53	0.61
75	LOC500183 protein	Q4KM66	26033.6	7.02E-12	-73356.82	-16.16	1.67	0.74
76	Ferritin light chain 1	P02793	20805.2	0.000320459	-74825.39	-16.19	-111.29	-6.80
77	Ezrin	P31977	69503.7	5.28E-14	-78564.77	-16.26	-2.34	-1.23

Table 4.8, continued.

No.	Protein	Swiss-Prot ID	Mass	p value	CE100 vs control		WF100 vs control	
					Fold Change	Log Fold Change	Fold Change	Log Fold Change
78	Alpha globin	Q63910	15581.4	7.66E-16	-87774.75	-16.42	-87774.75	-16.42
79	Dipeptidyl peptidase 2	Q9EPB1	55683.9	2.48E-15	-87885.76	-16.42	-5.59	-2.48
80	D-dopachrome decarboxylase	P80254	13247.1	1.33E-10	-107282.26	-16.71	-107282.26	-16.71
81	Alpha-1B-glycoprotein	Q9EPH1	57162.5	2.24E-16	-110127.23	-16.75	-4.86	-2.28
82	ATP synthase subunit f, mitochondrial	D3ZAF6	10509.2	1.20E-22	-114317.80	-16.80	-114317.80	-16.80
83	Myosin light chain 3	P16409	22269.9	0.0031681	-117631.59	-16.84	-213.25	-7.74
84	Protein LOC100360905	D3ZJY5	19373.8	1.64E-14	-157804.88	-17.27	-157804.88	-17.27
85	Histone H2A type 4	Q00728	14283.4	4.96E-15	-1072056.90	-20.03	-1072056.90	-20.03
86	SPI20	Q63555	88545.7	4.11E-12			19055.86	14.22
87	Ras-related C3 botulinum toxin substrate 1	Q6RUV5	21849.1	0.00160716			16640.28	14.02
88	Ubiquitin-like modifier-activating enzyme 1	Q5U300	118983.8	3.05E-14			7225.46	12.82
89	Glutathione peroxidase 1	P04041	22326	0.00341304			15.90	3.99
90	L-lactate dehydrogenase	B5DEN4	36735.1	0.00256761			2.10	1.07
91	Malate dehydrogenase, mitochondrial	P04636	36139.3	1.89E-05			1.71	0.77
92	Gelsolin	Q68FP1	86465.4	3.82E-05			-1.53	-0.61
93	Lymphocyte cytosolic protein 1	Q5XI38	70748.5	4.41E-04			-1.56	-0.64
94	Serum albumin	P02770	70726.5	1.21E-08			-1.61	-0.69
95	Serine protease inhibitor A3K	P05545	46788.9	0.00214481			-1.97	-0.98
96	Serotransferrin	P12346	78561.8	0.00226074			-2.13	-1.09
97	Alpha-1-antiproteinase	P17475	46306.1	1.25E-04			-2.33	-1.22

Table 4.8, continued.

No.	Protein	Swiss-Prot ID	Mass	p value	CE100 vs control		WF100 vs control	
					Fold Change	Log Fold Change	Fold Change	Log Fold Change
98	Brain-specific alpha actinin 1 isoform	Q6T487	106097	0.00380025			-2.45	-1.29
99	Heat shock cognate 71 kDa protein	P63018	71098	5.36E-05			-3.13	-1.65
100	Protein disulfide-isomerase	P04785	57349.6	3.84E-08			-3.27	-1.71

Proteins were significantly regulated at $p < 0.05$. The symbol (-) indicates down-regulation.
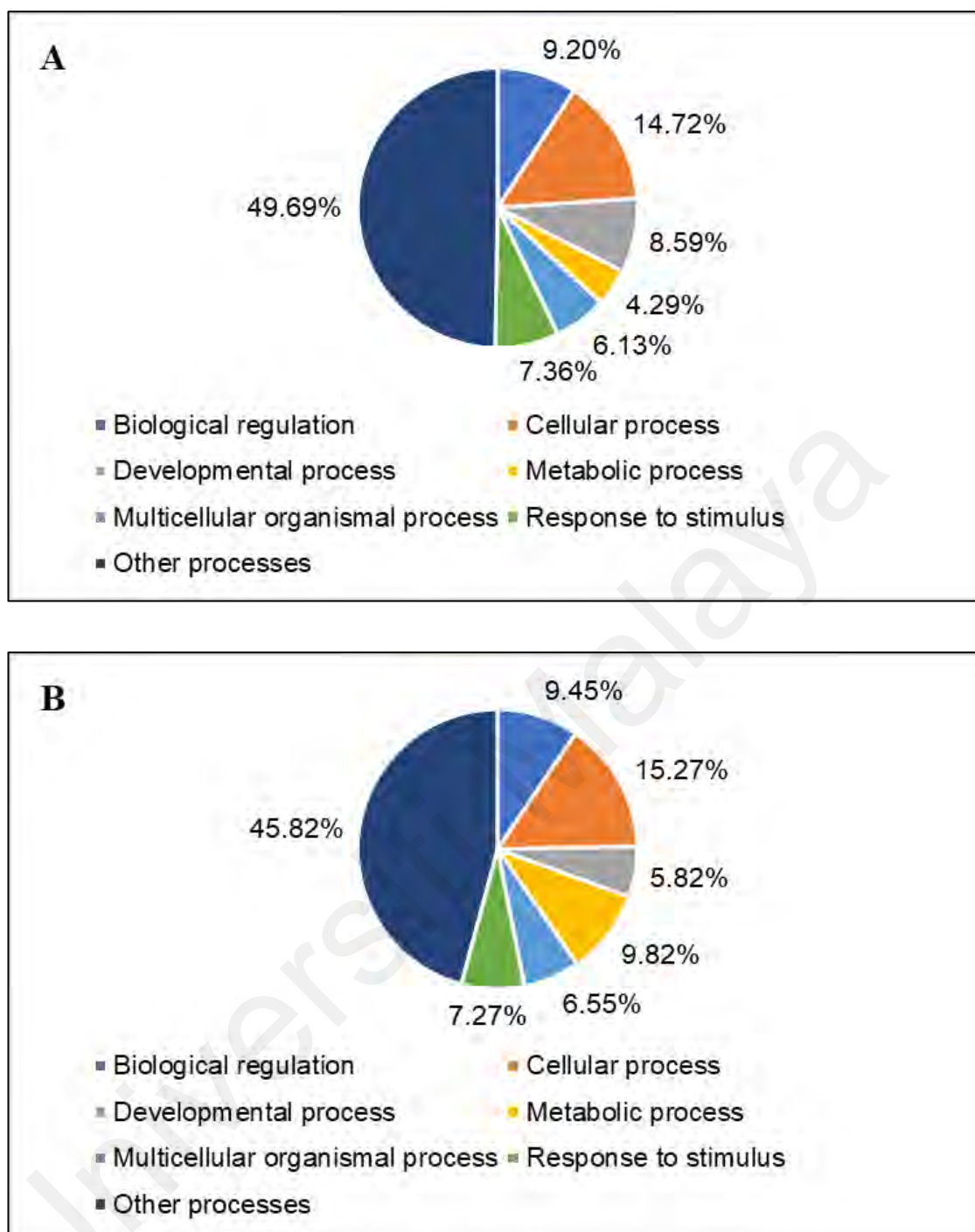
Figure 4.12: Proteins with altered abundance in rats treated with WF100 categorized under Biological Process. These proteins demonstrated expression changes greater than 1.5-fold (A) Up-regulated proteins, (B) Down-regulated proteins.

4.9.2   Protein network analysis of rat uterine tissue using Search Tool for the Retrieval of Interacting Genes/Proteins (STRING) database

In this analysis, protein-protein interaction was predicted using STRING database (version 10.5). STRING analysis demonstrated protein-protein interactions based on physical and functional association from knowledge transfer between organisms, computational prediction as well as interactions accumulated from other databases. When protein names were submitted into the STRING database for *R. norvegicus* (rat), results were displayed as a network, which portrayed predicted associations for a particular group of proteins in the forms of nodes and edges. Each network node represents a single protein and the network edges represents protein-protein associations. Prediction of association was based on criteria listed as curated databases, experimentally determined, gene neighborhood, gene fusion, gene occurrence, text mining, co-expression, protein homology, set as at medium confidence of 0.4. Figure 4.13 describes the color-coded keys to the nodes and links used in the subsequent networks identified.
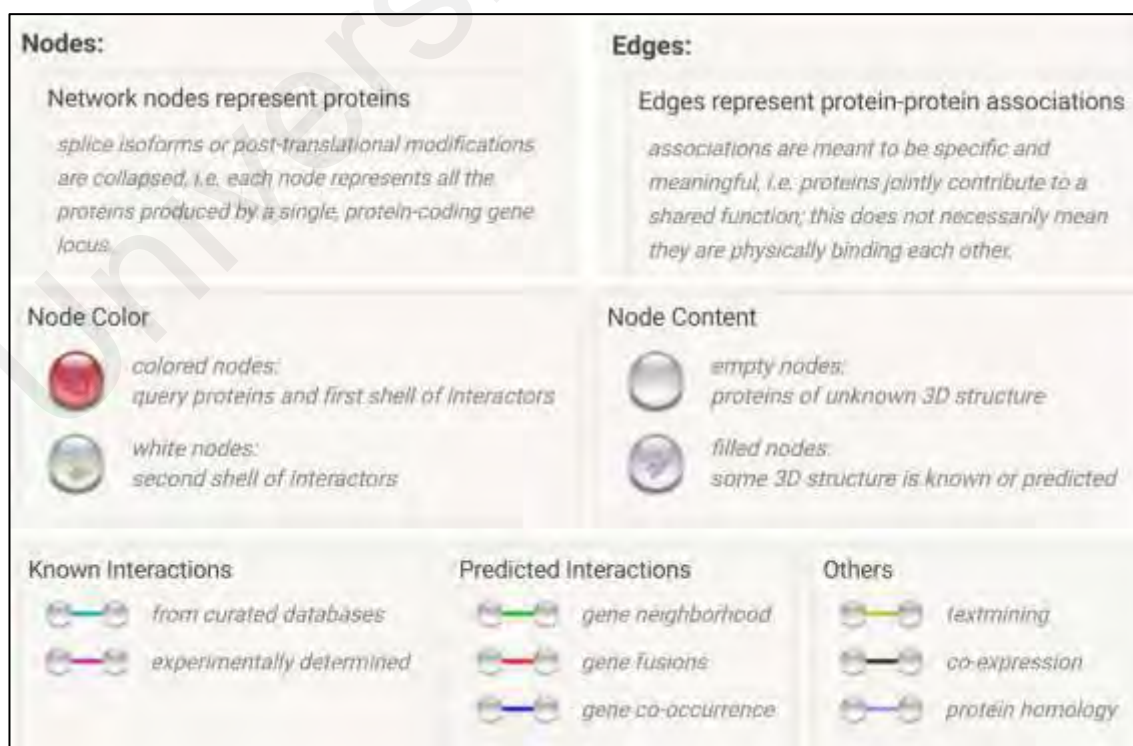

Figure 4.13: Color-coded keys to the nodes and links used in STRING.

In the case of proteins that were up-regulated in rats treated with WF100, 6 networks involving 16 out of 24 proteins were displayed. The first network involved Actn4 (alpha-actinin-4), Dstn (destin), Igkc (immunoglobulin kappa constant), Myl9 (myosin regulatory light polypeptide 9), Rac1 (Ras-related C3 botulinum toxin substrate 1) and Tagln (transgelin). A second network involved 2 proteins including Hist1h2bo (histone cluster 1, H2bo) and Hist1h1b (histone H1.5). In another network involving 2 other proteins were Adh1c (alcohol dehydrogenase 1) and Mdh2 (malate dehydrogenase, mitochondrial). There was also three other networks which involved links between 2 proteins – Sfpq (splicing factor, proline- and glutamine-rich) and Hnrnpab (heterogenous nuclear ribonucleoprotein A/B); Ywhab (14-3-3 protein beta/alpha) and Ywhag (14-3-3 gamma); and lastly between Hnrnpu (heterogenous nuclear ribonucleoprotein U) and Hnrpa3 (heterogenous nuclear ribonucleoprotein A3) (Figure 4.14).

Figure 4.14: Protein-protein interactions among up-regulated proteins in rats treated with WF100.

Refer Figure 4.13 for color-coded keys to the nodes and links in the networks.

Among the proteins that were down-regulated in rats treated with WF100, 55 out of 71 proteins were displayed in 2 networks when analysed using STRING. One of the networks involved proteins Hist2h4 (histone H4), Hist1h2aa (histone H2a type 4, Hp1bp3 (heterochromatin protein 1-binding protein 3) and LOC679994 (histone H3.1). The other network displayed consisted of several sub-network interactions, with an apparent sub-network involving Tuba1c (tubulin alpha-1C chain), Tuba1b (tubulin alpha-1A chain), Cort (cortistatin), Cct3 (T-complex protein 1 subunit gamma), Hspa8 (heat shock 70 kDa protein 8), Pdia6 (protein disulphide-isomerase A6), Ppic (peptidyl-prolyl cis-trans isomerase C), Ptges3 (prostaglandin E synthase 3), Phb (prohobitin) and Eif4a1 (eukaryotic initiation factor 4A-1) (Figure 4.15).
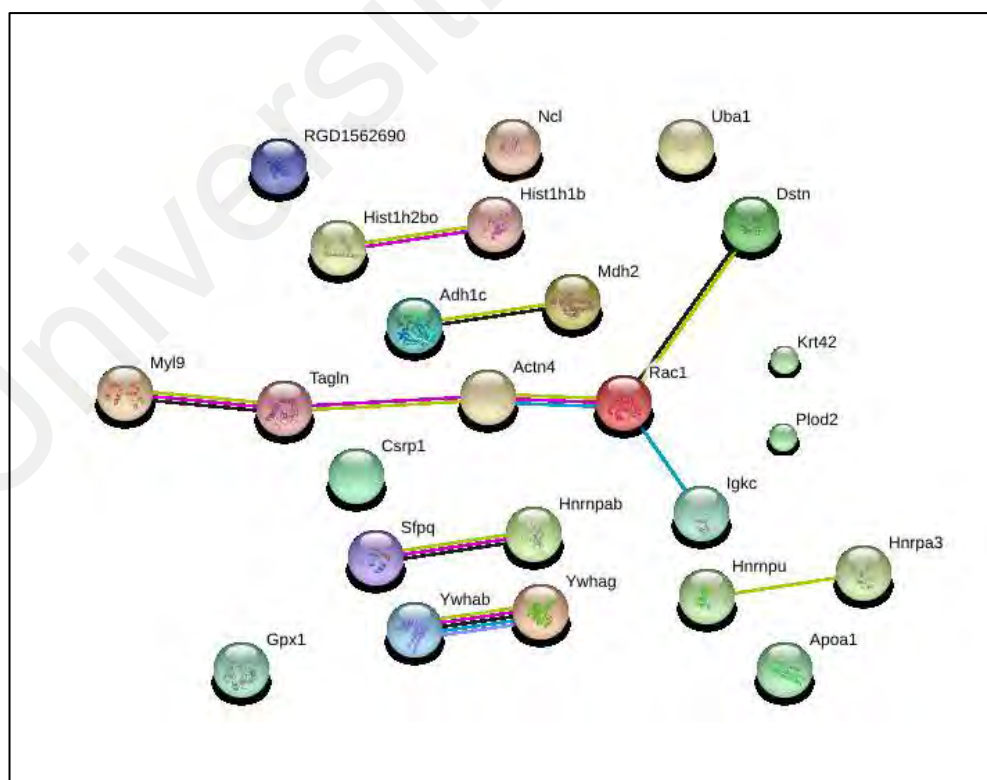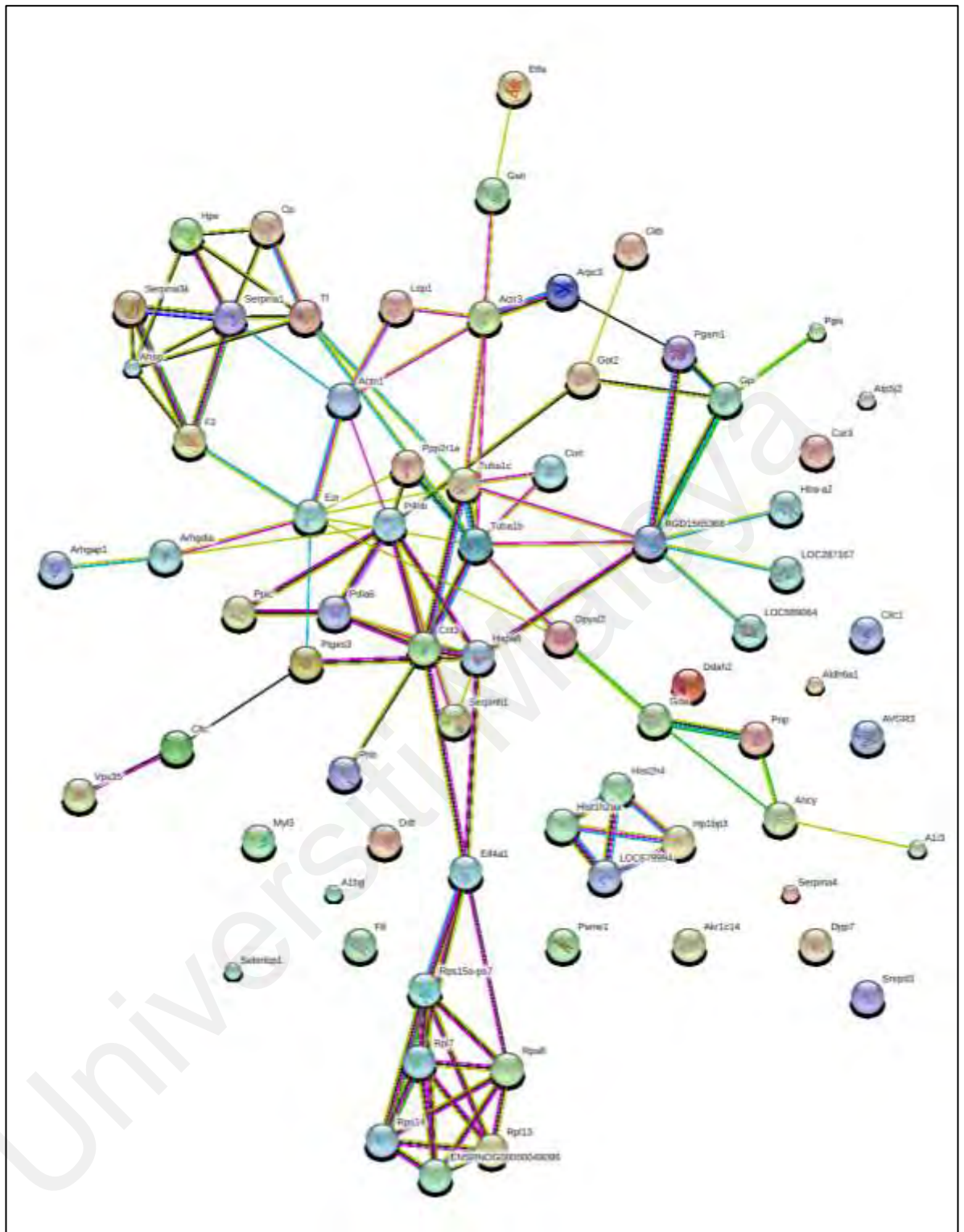
Figure 4.15: Protein-protein interactions among down-regulated proteins in rats treated with WF100.

Refer Figure 4.13 for color-coded keys to the nodes and links in the networks.

CHAPTER 5: DISCUSSION

The use of *F. deltoidea* as postpartum treatment is often described in the Malay folklore. Continuous usage of this plant by women until the present time is a strong indication of the potent effect of the plant. The plant is orally consumed in the form of a decoction to stimulate contraction of the uterus and to restore it to its pre-birthing condition. In the first part of the study, leaf extracts of *F. deltoidea* were initially prepared in a manner similar to the traditional practice. The extracts were given orally to female rodents to assess the underlying mechanisms of their uterotonic action, reflected by the amplitude and frequency of rhythmic contractions of the smooth muscle of the uterus. Biochemical changes brought about by the *F. deltoidea* leaf extracts were monitored based on alteration of serum steroid hormone levels and density of M2 mAChR in the uterine tissue extracts.

Uterine smooth muscle continuously undergoes spontaneous rhythmic contractions that change in amplitude and frequency. Implantation, which occurs when the blastocyst-stage embryo adheres to the endometrial epithelial cells of the uterus, is crucial for a viable pregnancy. Whilst a forceful uterine contraction is needed during childbirth, a similar strong contraction that occurs may impede the implantation of embryos during prenatal development and lead to abortion (Pamplona-Roger, 2005; Kamatenesi-Mugisha & Oryem-Origa, 2007). This abortifacient effect is known to be induced by some herbs (Nikolajsen et al., 2011; Larsen et al., 2016) and occurred through the actions of steroid hormones (Kaingu et al., 2012). In the present study, similar abortifacient effect was exclusively detected in mice treated with WF100 and shown to be associated with significant increased levels of serum progesterone. The abortifacient effect also explains the use of *F. deltoidea* for birth spacing in the Malay traditional medicine. Despite the biologically adverse effect, however, both the WF as well as CE of *F. deltoidea* did not

appear to cause any change in the physical appearance and behavior of mice. Normal levels of serum biomarkers for kidney and liver functions additionally indicated that both CE and WF were generally nontoxic.

The results of the organ bath study further confirmed the effects of *F. deltoidea* on uterine contractility. WKY rats treated with CE100 and WF100 were shown to display changes in both amplitude and frequency of the uterine contractile response compared to similar parameters observed in control animals. The E_{max} for uterine segments of rats treated with WF100 was 1.7 times higher than that displayed by the control rats, whilst their EC_{50} was markedly reduced. However, based on the E_{max} and EC_{50} values attained, the uterine segments of CE100-treated rats displayed weaker uterotonic effect but with increased frequency compared to the WF100-treated animals. These differences were most likely due to presence of other compounds in CE that may have interfered with the uterine contractile functions.

In this study, treatment with the leaf extracts of *F. deltoidea* on WKY rats did not appear to cause significant changes in the levels of serum testosterone and estradiol between the three different groups of female WKY rats (Figure 4.6). Highest levels of both testosterone and estradiol were apparently observed in the CE100 rat group, followed by those treated with WF100. Testosterone, in females, is a very powerful gynecogen with dual estrogenic and progestogen effects (Abarbanel, 1940). Testosterone alone results in contractions which resemble those seen after simultaneous administration of estradiol and progesterone (Wilson & Kurzrok, 1938).

However, the levels of progesterone were significantly higher in the WF100-treated rat group but not significantly different in the CE100-treated group of rats. In humans, there is certain importance in maintaining the proper levels of estradiol and progesterone. Both steroid hormones were reported to have compromising effects in restoring the uterus

to a 'normal' state of contractility compared to estradiol only therapy (Gibson & Saunders, 2013; Turgut et al., 2014). Both estrogen and progesterone fluctuate characteristically throughout menstrual cycle and influences uterine contractility in specific manner to develop uterine endometrium, transport of sperm and prepare for implantation of blastocyst (Mueller et al., 2006). Hence, the results of this study suggest that the oral intake of the *F. deltoidea* leaf extracts may regulate steroid hormones as they were able to improve the levels of both progesterone and estradiol in the rats, with no suppressive effect.

mAChRs play a vital role during muscle contraction. In the smooth muscle, mAChRs can be divided into subtypes M1, M2, M3, M4 and M5 depending on tissue or organ. A mixed population of these subtypes is often present in many smooth muscle tissues. However, the contractile function of the uterus of rats has been shown to involve only the M2 and M3 mAChR subtypes (Pennefather et al., 1994; Munns & Pennefather, 1998). In the present study, analysis of the expression of the M2 mAChR showed highest relative intensity of the receptor protein bands in the WF100-treated groups of rats compared to those untreated, followed by rats treated with CE100. These changes in protein intensities were comparable to the altered strength of uterine contraction achieved when the rats were treated with WF100 and CE100.

In the second part of the study an attempt in generating further supporting evidence that associates rat smooth muscle uterine contraction with the consumption of WF100 was made using the gel-based proteomics analysis. However, the analysis of uterine tissue samples of rats with and without WF100 treatment by 2-DE detected the significant altered abundance of only six proteins. Unfortunately, when these proteins were further subjected to MALDI-ToF analysis, none was considered affirmatively identified based on the scores that were generated, although two protein spots demonstrated high scores

that associate them with E3 ubiquitin-protein ligase and potassium voltage-gated channel subfamily S member 1. However, these uterine proteins are not directly associated with smooth muscle contraction. In this study, the failure of 2-DE to resolve and identify proteins of altered abundance may be due to the relative minute quantity of the uterine proteins that were analyzed. Even though 2DE and MALDI-ToF remains as a method of choice for protein separation and quantification, there is a need for a relatively high amount of protein sample (IJsselstijn et al., 2013; Megger et al., 2013). Hence, an alternative proteomics analysis platform was then explored.

The final part of the present study was focused on a liquid-based proteomics analysis of the uterine lysate proteins, which was prepared by homogenizing uterine tissues in lysis buffer and subjected to SDS-PAGE separation. Staining and in-gel digestion were carried out before the tissue protein samples were finally subjected to analysis by LC-MS/MS and Spectrum Mill software. This resulted in the identification of 833 proteins, with 380 of these proteins commonly detected in all groups of rat uterine tissue samples. Some of these proteins could have possibly be involved in the mechanisms that led to the abortifacient effect observed in the earlier implantation study.

In order to identify proteins (or enzymes) that may be involved in the WF100-induced abortifacient effects, the uterine proteins were subsequently analyzed based on differences of expression levels between rats treated with WF100 with the controls. For this purpose, a difference of at least 1.5-fold change was considered as significantly different. At this chosen cut-off point, a total of 100 proteins were found to be differentially regulated in rats treated with WF100. The majority of these proteins showed reduction in their expression levels. In the case of the WF100-treated rats, 15 uterine tissue proteins were identified exclusively within the group, whilst 85 uterine tissue proteins were also commonly detected in the group of rats treated with CE100.

Some of these 100 proteins may have contributed to the abortifacient effect observed in the mice that was earlier discussed, and this appeared to be correlated with significant increase in the serum progesterone levels. Hence, identifying the proteins that are present and significantly altered in expression in the uterine tissues of rats treated with WF100 became a focus. This include proteins exclusively regulated with WF100 as well as the ones commonly present in both the CE100 and WF100.

To further investigate the identified uterine proteins that were significantly altered in a consistent manner in the rats that were treated WF100, annotation via Gene Ontology (GO) was applied. The GO tool, which was a bioinformatics effort initiated in 1999 to provide an ontology (controlled shared vocabulary) of defined terms to represent specific gene product attributes according to their biological processes, molecular functions and cellular components across a defined species. The GO annotations (Biological Process, Molecular Function and Cellular Components) were connected into nodes of networks and were linked to other protein database including UniProtKB/Swiss-Prot (Ashburner et al., 2000).

When the identified uterine proteins of interest were subjected to GO, approximately 27% had unknown functional annotation under the Biological Process. About 22% of proteins under the Cellular Component and 36% proteins under the Molecular Function were also with unknown functional annotation. Most of the proteins that were functionally annotated within the Biological Process were involved in Cellular Process, Metabolic Process, Biological Regulation, Response to Stimulus and Developmental Process. Uterine proteins that were associated with Cellular Component were those present in the Cytoplasm, Intercellular Organelle, Extracellular Region and Organelle Part, whilst uterine proteins associated with Molecular Function may be further categorized into those with Binding and Catalytic Activity.

When the 100 uterine proteins of interest were further sub-grouped into those being up-and down-regulated when the rats were treated with WF100, similar results were generated, with slight differences in the percentage of protein distribution. Most of the uterine proteins that were upregulated were associated with Cellular Process (14.7%). This was followed by those associated with Biological Regulation (9.2%), Developmental Process (8.6%), Response to Stimulus (7.4%), Multicellular Organismal Process (6.1%) and Metabolic Process (4.9%). A slightly different distribution pattern was apparently observed for the down-regulated uterine proteins, with the majority associated with Cellular Process (15.3%), followed by Metabolic Process (9.8%), Biological Regulation (9.5%), Response to Stimulus (7.3%), Multicellular Organismal Process (6.6%) and Developmental Process (5.8%).

STRING provides both database and web source of known and predicted proteins to protein functional connectivity for a given organism. Analysis by STRING demonstrated protein to protein interactions in the form of protein networks. When STRING analysis was performed on the 25 rat uterine proteins of interest that were up-regulated by WF100, 6 protein-protein interaction networks were generated involving 16 proteins. The main network that was displayed involved interactions between 6 proteins (Figure 5.1), which included Ras-related C3 botulinum toxin substrate, destrin, immunoglobulin kappa constant, alpha-actinin-4, transgelin and myosin regulatory light polypeptide 9. This network appears to focus on Ras-related C3 botulinum toxin substrate 1 as a central protein, which were connected with three different edges. One edge was extended to destrin while another to immunoglobulin kappa constant. The third edge involved a network involving Ras-related C3 botulinum toxin substrate with alpha-actinin-4, followed by transgelin and ended at myosin regulatory light polypeptide 9.
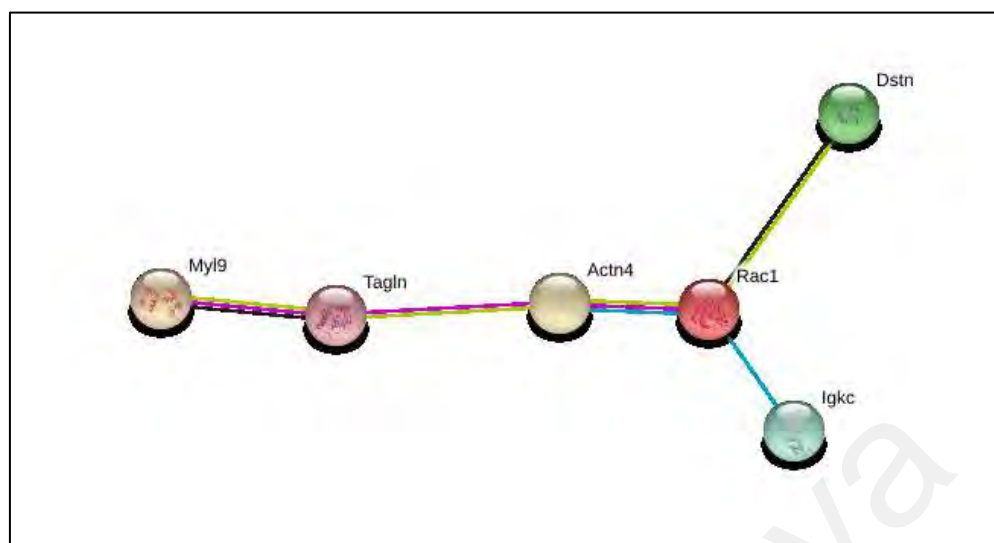
Figure 5.1: Interactions of up-regulated proteins in rats treated with WF100 – Major network. Actn4: alpha-actinin-4, Dstn: destrin, Igkc: immunoglobulin kappa constant, Myl9: myosin regulatory light polypeptide 9, Rac1: Ras-related C3 botulinum toxin substrate 1, Tagln: transgelin.

Other networks that were also displayed apparently involved interactions between two proteins (Figure 5.2). A total of five minor networks were shown, four of which involved nuclear regulatory proteins and one on enzymes. The enzymic network comprised interactions between alcohol dehydrogenase 1 and malate dehydrogenase mitochondrial. Alcohol dehydrogenase 1 is an enzyme that detoxifies blood by breaking ethanol into acetaldehyde which is then converted into acetate and other molecules easily utilized by cells. Malate dehydrogenase mitochondrial also known as malate dehydrogenase 2, on the other hand, is an enzyme that catalyzes reversible transformation of malate to oxaloacetate in many metabolic pathways by utilizing NAD/NADH as coenzyme (Fahien et al., 1988; Gelpi et al., 1992; Minarik et al., 2002; Ait-El-Mkadem et al., 2017). The enzyme has a crucial role in cellular energy metabolism and ATP production by shuttling malate-aspartate between the mitochondria and the cytosol. Hence, this network generally illustrates the minor alteration in rat metabolic processes when the animals consumed WF100 (Figure 5.2, panel A).
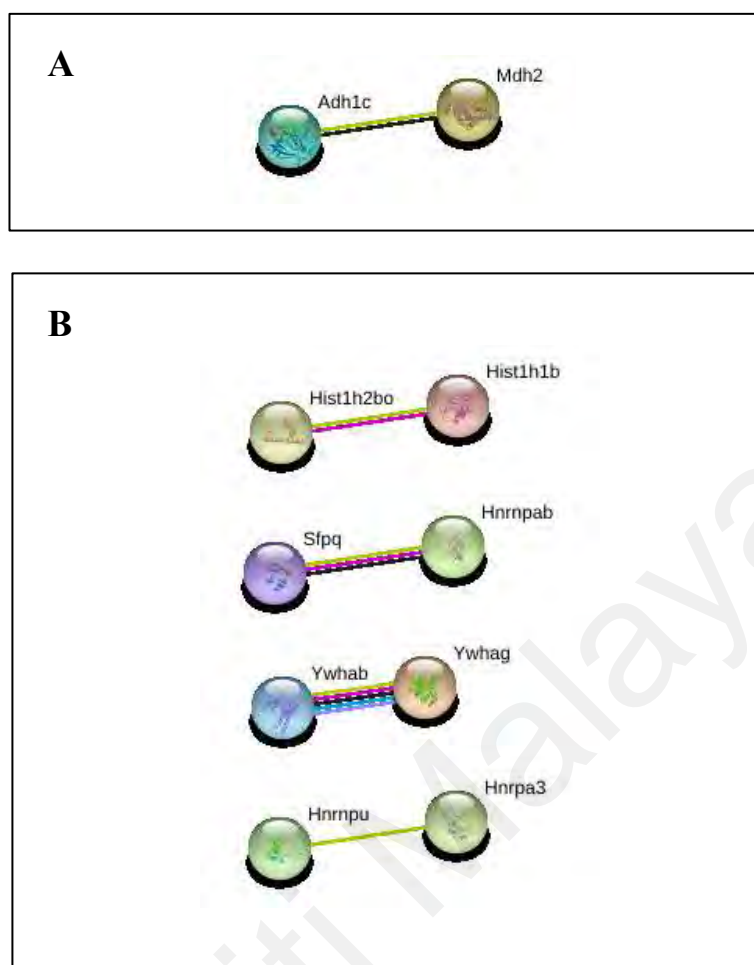
Figure 5.2: Interactions of up-regulated proteins in rats treated with WF100 – Minor network. (A) Enzyme network – Adh1c: alcohol dehydrogenase 1, Mdh2: malate dehydrogenase, mitochondrial.   (B) Nuclear regulatory protein network – Hist1h1b: histone H1.5, Hist1h2bo: histone cluster 1 H2bo, Hnrnpab: heterogeneous nuclear ribonucleoprotein A/B, Hnrnpu: heterogeneous nuclear ribonucleoprotein U, Hnrpa3: heterogeneous nuclear ribonucleoprotein A3, Sfpq: splicing factor, proline- and glutamine-rich, Ywhab: 14-3-3 protein beta/alpha, Ywhag: 14-3-3 protein gamma.

The other four minor networks involved interactions between (i) histone cluster 1 H2B family member O and histone cluster 1 H1 family member B, (ii) splicing factor, proline- and glutamine-rich and heterogenous nuclear ribonucleoprotein A/B, (iii) heterogenous nuclear ribonucleoprotein U and heterogenous nuclear ribonucleoprotein A3, and (iv) 14-3-3 protein beta/alpha and 14-3-3 gamma (Figure 5.2, panel B). Histones are generally nuclear proteins, whilst histone cluster 1 is a complex subfamily of related nuclear proteins.   Histone cluster 1 H2B family member O is a core component of the

nucleosomes that wraps DNA into chromatin. This protein is essential in DNA replication, DNA repair, chromosomal stability as well as regulation of transcription (Woodcock et al., 2006). On the other hand, histone cluster 1 H1 family member B, also known as histone H1.5, is a core component of chromatin fibers. It is a linker protein that connects the nucleosomes, which are required for stabilizing nucleosome chains into higher-order chromatin structures. Through chromatin remodeling, nucleosome spacing and DNA methylation, histone H1.5 acts as a regulator of gene transcription, DNA repair and cell proliferation (Li et al., 2012; Hergeth & Schneider, 2015; Izzo & Schneider, 2016).

Splicing factor, proline- and glutamine-rich, a component of the second minor network, is a multifunctional nuclear protein involved in regulating transcription. This includes DNA rearrangements and mRNA processing, i.e., RNA polymerase II enhancer sequence-specific DNA binding, core promoter binding and polyadenylation process. The protein is also an essential factor required for pre-mRNA splicing as well as in chromatin binding and chromosome organization (Patton et al., 1993; Lutz et al., 1998; Shav-Tal & Zipori, 2002). These functions contribute to the complexity of mRNA-dependent gene expression control within a cell. In the STRING analysis, splicing factor, proline- and glutamine-rich was displayed to interact with heterogenous nuclear ribonucleoprotein A/B, which are proteins involved in controlling transcription, RNA processing and mRNA translation (He & Smith, 2009). Heterogenous nuclear ribonucleoproteins are generally the most abundant nuclear proteins in eukaryotes. These complexes of RNA and proteins, modulates transcription, regulates gene expression by post-transcriptional modification of newly synthesized pre-mRNA into mature mRNA (mRNA splicing, capping, polyadenylation, mRNA stability as well as turnover), nucleocytoplasmic transport of mRNA and translation (Dreyfuss et al., 1993; Martinez-Contreras et al., 2008; Han et al., 2010). Some are also involved in DNA repair and

chromatin remodeling. Their functions in general are based on nucleic acid binding properties, recognizing RNA strands and single strand DNA sequences. Certain heterogeneous nuclear ribonucleoproteins of the A/B family have been reported to enhance the smooth muscle cell differentiation from stem cells both *in vitro* as well as *in vivo* (Wang et al., 2012; Choi et al., 2013; Huang et al., 2013).

The third minor network displayed by STRING analysis involved an interaction between two different heterogeneous nuclear ribonucleoproteins A3 and U. Heterogeneous nuclear ribonucleoproteins A3 is a telomere-binding protein. An experiment conducted by Huang et al. (2008) showed that the nuclear protein inhibited extension of telomerase *in vitro*, thus, suggesting that it is involved in telomere length maintenance *in vivo*. On the other hand, heterogeneous nuclear ribonucleoprotein U, also known as scaffold attachment factor, binds to RNA and DNA and transcriptionally initiate and regulate gene expression (Fackelmayer & Richter, 1994; Göhring & Fackelmayer, 1997).

The final minor network displayed by the STRING analysis demonstrated a network between 14-3-3 protein beta/alpha and 14-3-3 gamma protein. 14-3-3 proteins are a family of adaptor proteins that participate in many cellular processes. They play an important role in signal transduction that leads to cell proliferation. Both 14-3-3 protein beta/alpha and 14-3-3 gamma proteins are involved in the regulation of many general and specialized signaling pathways. Binding to their interaction partners, usually by recognition of phosphoserine or phosphothreonine motifs causes formation of protein-protein complexes which modulates activity of the binding partner (Rosenquist et al., 2000; Yang et al., 2006). An important role of 14-3-3 gamma protein in cell proliferation was seen in human vascular smooth muscle cells, which was induced by growth factors (Fu et al., 2000).

When taken together, the display of these four minor networks by STRING in general reflects the effects of WF100 on the genes that codes for nuclear regulatory proteins in the rat uterus, at the transcription and translation levels. The enhanced production of these specific nuclear proteins can be seen by the STRING analysis to be associated with smooth muscle cells differentiation and functions.

In the major network displayed by STRING, Ras-related C3 botulinum toxin substrate 1, which is a plasma membrane-associated signaling G-protein, appears to play a central role (Figure 5.1). The G-protein is one of the most studied members of the Rho family of GTPases and are known to induce different types of actin filament formation, branching and organization. These processes are known to regulate vesicle movements, which results in exocytosis as well as endocytosis (Jaffe & Hall, 2005; Sylow et al., 2016). In its first interaction within the major network, the Ras-related C3 botulinum toxin substrate 1 was demonstrated to have a linkage with an edge protein, immunoglobulin kappa constant, which is one of the light chain components of the immunoglobulin molecules. Hence, the data derived from the STRING analysis imply signaling that may have activated the humoral immune system (Janeway et al., 1996; Maverakis et al., 2015).

In its second interaction within the major network, the Ras-related C3 botulinum toxin substrate 1 was linked to another edge protein, destrin, which is an actin regulatory protein required for normal cell growth and proliferation. A member of the cofilin family/actin-depolymerizing protein, destrin severs actin filaments (F-actin) and binds to actin monomers (G-actin). This family of proteins is responsible for depolymerization of actin filaments and enhancing its turnover rate *in vivo* (Kuure et al., 2010). Depolymerization and severing of actin filaments produce new actin monomers which are essential in cell cytokinesis, cell shape and cell survival. In dividing cells, actin depolymerization is important in chromosome congression, cleavage plane-orientation and furrow formation

(Lénárt et al., 2005; Kuure et al., 2010). The interaction between Ras-related C3 botulinum toxin substrate 1 and destrin is believed to be antagonistic. The lack of destrin causes defective cytoskeletal changes due to the accumulation (Ikeda et al., 2003; Van Troys et al, 2008) or shortage of actin filaments (Chi et al., 2009; Kuure et al., 2010), and disrupts normal cell organization and proliferation.

In its final interaction within the major network, the Ras-related C3 botulinum toxin substrate 1 was shown to interact with a series of proteins leading to the final edge. This involves sequential interactions between Ras-related C3 botulinum toxin substrate 1 with alpha-actinin-4, transgelin and myosin regulatory light polypeptide 9, respectively. This network appears to demonstrate a direct link between the rat uterine proteins involved in smooth muscle contraction that were up-regulated when the animals were treated with WF100.

The first protein that interacted with Ras-related C3 botulinum toxin substrate 1 in this network is alpha-actinin-4, an F-actin cross-linking protein that anchors actin to a variety of intracellular structures. This non-muscle isoform of actin-binding protein has multiple roles in different cell types (Sjöblom et al., 2008; Foley & Young, 2013). It is seen in the structure of the tight junction (Nakatsuji et al., 2008) and is involved in directed vesicular trafficking of proteins within a cell, or between cells (Kumeta et al., 2010). It is also a cytoskeletal protein that maintains cell structure and morphology (Djinovic-Carugo et al., 2002). Other than that, alpha-actinin-4 is known to be involved in nuclear-receptor mediated transcriptional regulation by estrogen and vitamin D which allows activation of target genes (Mangelsdorf & Evans, 1995; Mangelsdorf et al., 1995; Francis et al., 2003; Chakraborty et al., 2006; Khurana et al., 2011; Khurana et al., 2012). This controls the aspects of cell differentiation, proliferation and development. As Ras-related C3 botulinum toxin substrate 1 is known to stimulate the branching of new actin filaments,

its interaction with alpha-actinin-4 is believed to induce the formation of actin filament branching, and thus, affects the transport of substances via actin-cytoskeleton vesicular movement (Kumeta et al., 2010; Sylow et al., 2016).

Following the interaction of Ras-related C3 botulinum toxin substrate 1 with alpha-actinin-4 in this network, the latter protein was also shown to interact with transgelin, an actin-crosslinking/gelling protein found in smooth muscles. Transgelin belongs to the calponin family and known to be involved in calcium-independent smooth muscle contraction (Lawson et al., 1997; Yang et al., 2007). It is a specific marker of smooth muscle differentiation in the uterus and appears useful for distinguishing smooth muscle tumors (Assinder et al., 2009; dos Santos Hidalgo et al., 2011). Nuclear-receptors mediated transcriptional regulation by alpha-actinin-4 may have asserted certain effect on transgelin and this may possibly contributed to the increase in myosin regulatory light polypeptide 9, which was also displayed as the terminal protein within this major network. This final edge protein plays an important role in the regulation of smooth muscle cell contractile activity. Myosin light chains belongs to a large family of calcium binding proteins. Myosin being a structural component of muscle shares common features of ATP hydrolysis (ATPase enzyme activity), actin binding and kinetic energy transduction potential (Kumar et al., 1989). Activation of myosin regulatory light chain by myosin light chain kinase modulates ATPase activity of myosin heads (Lazar & Garcia, 1999). Association of myosin light chains with the neck region of myosin heavy chains is necessary for myosin to function. Both transgelin and myosin regulatory light polypeptide 9, in general, are actin cross-linking proteins of the smooth muscle. Hence, this major network of proteins, when taken together, can be concluded to reflect the protein interactions that are affected by WF100 during smooth muscle contraction. This is compatible with the earlier data on the effects WF100 on uterine contractility which appeared to be associated with the termination of pregnancy.

When STRING analysis was performed on 75 uterine proteins of interest that were down-regulated by WF100, two protein-protein interaction networks were generated involving a total of 56 proteins. The first network displayed interactions between 4 proteins which includes histone H2A type-4, histone H4 osteogenic growth peptide, histone H3.1 and heterochromatin protein 1-binding protein 3, and appears to focus on nuclear proteins (Figure 5.3). Another is a major network that involves interactions between 52 proteins (Figure 5.4).
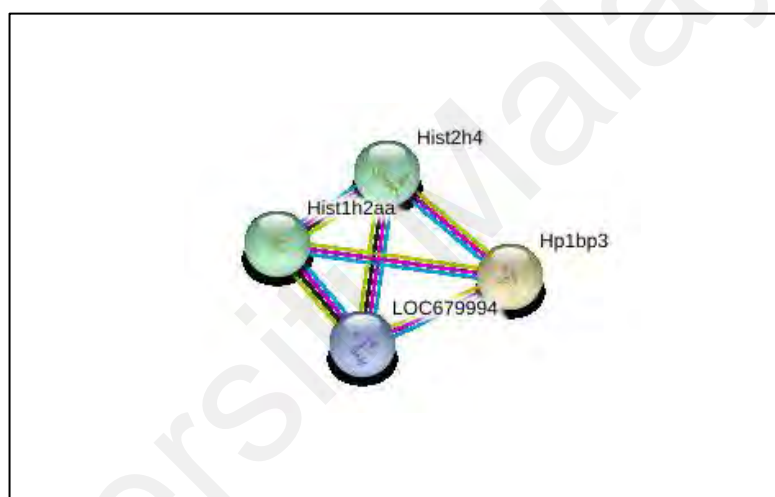
Figure 5.3: Interactions of proteins that were down-regulated in rats treated with WF100 – Minor network. Hist1h2aa: histone H2A type 4, Hist2h4: histone H4 osteogenic growth peptide, Hp1bp3: heterochromatin protein 1-binding protein 3, LOC679994: histone H3.1.

In the first network (Figure 5.3), nuclear proteins histone H2A type-4 was seen to be connected to histone H4 osteogenic growth peptide, histone H3.1 and heterochromatin protein 1-binding protein 3. Histones are generally core components of the nucleosome, which is the particle that wraps and compacts DNA into chromatin. Histones play a central role in the regulation of transcription, DNA replication, DNA repair and chromosomal stability. Heterochromatin protein 1-binding protein 3 on the other hand is

a component of heterochromatin. It has been identified as a novel subtype of linker histone H1 with crucial roles in cell viability and growth. Efficiency in regulation of cell cycle and proliferation is maintained by DNA repair, recombination and regulation (Dutta et al., 2014; Garfinkel et al., 2015). This network of nuclear proteins is probably related to the structure of chromatin and the modulation of gene expression.

Among the down-regulated proteins, the major network that was displayed consisted of 52 proteins. For convenience of the discussion, this network was further divided into five subnetworks. In the first subnetwork (Figure 5.4A), alpha-1-antiproteinase was considered as the central protein with edges connecting it to various other blood proteins (i) alpha-1-antiproteinase and alpha-2-HS-glycoprotein precursor, (ii) alpha-1-antiproteinase and ceruloplasmin isoform 1 precursor, (iii) alpha-1-antiproteinase and prothrombin precursor, (iv) alpha-1-antiproteinase and hemopexin, (v) alpha-1-antiproteinase and serotransferrin, and finally (vi) alpha-1-antiproteinase and serine protease inhibitor A3K. The central protein, alpha-1-antiproteinase belongs to the serpin superfamily. It inhibits various protease enzymes including serine protease (DeMeo & Silverman, 2004; Kolarich et al., 2006). In this subnetwork, several precursors are linked to alpha-1-antiproteinase including alpha-2-HS-glycoprotein precursor, ceruloplasmin isoform 1 precursor and prothrombin precursor. Protein precursors are inactive proteins that can be turned into active forms by post-translational modification. Alpha-2-HS-glycoprotein is a carrier-glycoprotein involved in endocytosis, whilst ceruloplasmin and prothrombin are copper-carrying and coagulation factor glycoproteins, respectively. The other two carrier proteins linked to alpha-1-antiproteinase in this subnetwork are hemopexin and serotransferrin. Hemopexin has an important role as a heme-binding glycoprotein that binds to free heme and transports them to the liver during hemoglobin degradation process. This prevents iron loss, iron-induced oxidative damage and maintains iron level in the body (Tolosano & Altruda, 2002). Serotransferrin, which is
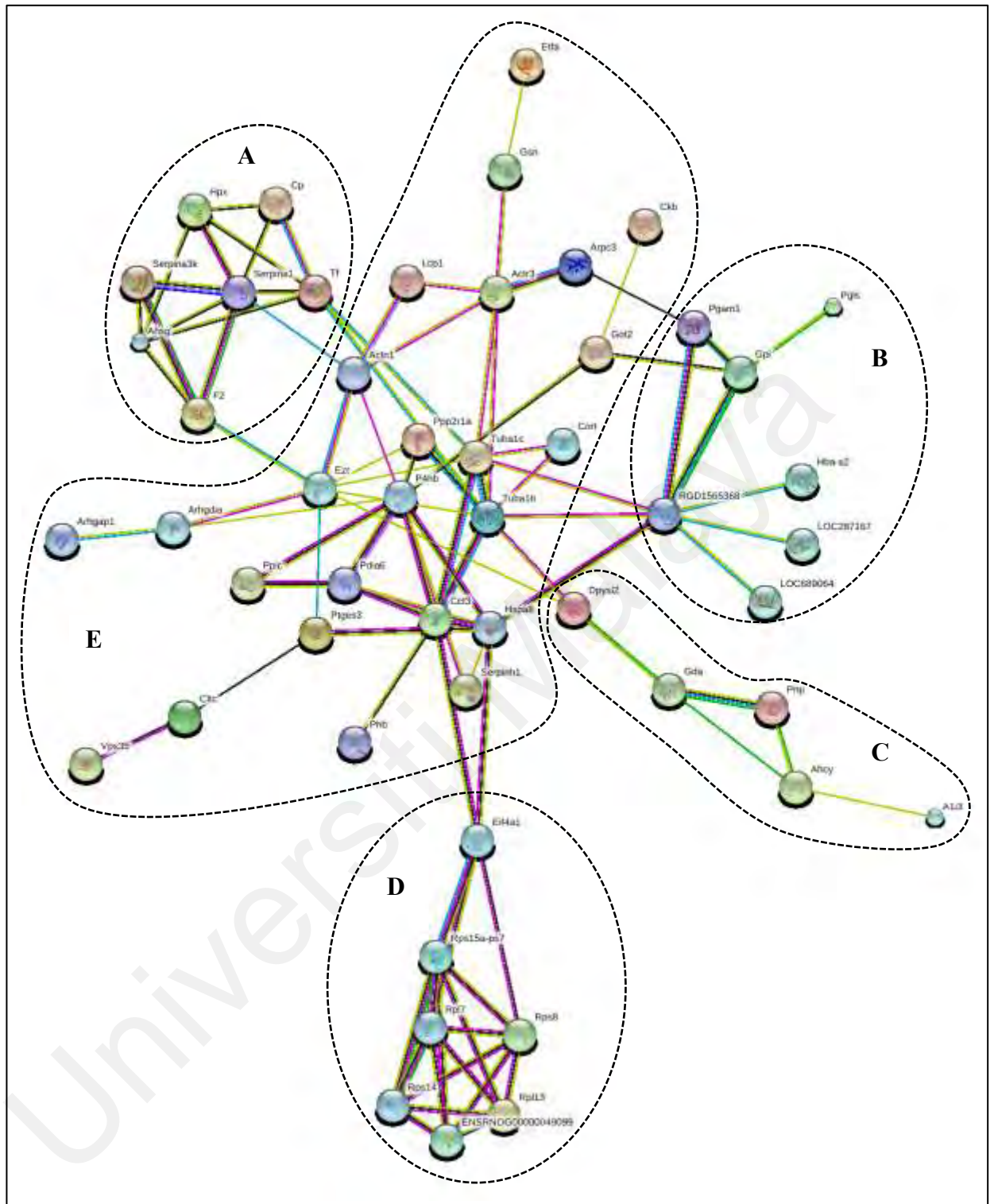
Figure 5.4: Interactions of proteins that were down-regulated in rats treated with WF100 – Major network. Interactions are further divided into five subnetworks A-E. (A) Ahsg: alpha-2-HS-glycoprotein, Cp: ceruloplasmin isoform 1 precursor, F2: prothrombin precursor, Hpx: hemopexin, Serpina1: Alpha-1-antiproteinase, precursor, Serpina3k: serine protease inhibitor A3K, Tf: serotransferrin. (B) Gpi: glucose 6-phosphate isomerase, Hba-a2: Hemoglobin subunit alpha-1/2, LOC287167: globin, alpha, LOC689064: Hemoglobin subunit beta-2, Pgam1: phosphoglycerate mutase 1, Pgls: 6-phosphogluconolactonase, RGD1565368: uncharacterized protein. (C) Ahcy: adenosylhomocysteinase, A1i3: alpha-1-

inhibitor 3 precursor, Dpysl2: dihydropyrimidinase-related protein 2, Gda: guanine deaminase, Pnp: purine nucleoside phosphorylase. (D) Eif4a1: eukaryotic initiation factor 4A-I, ENSRNOG00000049099: protein LOC100360905, Rpl7: 60S ribosomal protein L7, Rpl13: 60S ribosomal protein L13, Rps8: 40S ribosomal protein S8, Rps14: 40S ribosomal protein S14, Rps15a-ps7: uncharacterized protein. (E) Actn1: alpha-actinin-1, Actr3: actin-related protein 3, Arhgap1: Rho GTPase activating protein 1, Arhgdia: Rho GDP-dissociation inhibitor 1, Arpc3: actin-related protein 2/3 complex subunit 3, Cct3: T-complex protein 1 subunit gamma, Cltc: clathrin heavy chain 1, Ckb: creatine kinase B-type, Cort: cortistatin Cortistatin-29 Cortistatin-14, Etfa: electron transfer flavoprotein subunit alpha, mitochondrial, Ezr: ezrin, Got2: aspartate aminotransferase, mitochondrial, Gsn: gelsolin, Hspa8: heat shock 70kDa protein 8, Lcp1: plastin-2, Pdia6: protein disulfide-isomerase A6, Phb: prohibitin, Ppp2r1a: serine/threonine-protein phosphatase 2A 65 kDa regulatory subunit A alpha isoform, Ppic: peptidyl-prolyl cis-trans isomerase C precursor, Ptges3: prostaglandin E synthase 3, P4hb: protein disulfide-isomerase, Serpinh1: serpin H1 precursor, Tuba1b: tubulin alpha-1A chain, Tuba1c: tubulin alpha-1C chain, Vps35: maternal embryonic message 3.

also known as transferrin or siderophilin is an iron-binding glycoprotein that controls the level of free iron in body fluids by transporting ferric ions from sites of storage to regions of iron metabolism (MacGillivray et al., 1998; Cheng et al., 2004). The final protein linked to alpha-1-antiproteinase in this subnetwork is serine protease inhibitor A3K, which functions like alpha-1-antiproteinase by inhibiting trypsin. When taken together, this first protein subnetwork appears to involve interactions between various blood proteins that were down-regulated in uterine tissue of female rats administered with WF100. These proteins were likely down-regulated since they are irrelevant to uterine smooth muscle contraction.

The second subnetwork that was displayed from the STRING analysis appears to focus on an uncharacterized protein with five connecting protein edges: (i) globin, alpha, (ii) hemoglobin subunit alpha-1/2, (iii) hemoglobin subunit beta-2, (iv) glucose 6-phosphate isomerase, and finally (v) phosphoglycerate mutase 1, (Figure 5.4B). Globin alpha, hemoglobin subunit alpha-1/2 and hemoglobin subunit beta-2 are generally globular proteins involved in the transport of oxygen from the lungs to various peripheral tissues,

whilst the remaining edges are metabolic enzymes. One of the edge proteins, glucose-6-phosphate isomerase, was apparently shown to have interactions with phosphoglycerate mutase 1 as well as 6-phosphogluconolactonase. Whilst both the former enzymes are involved in glycolysis as well as gluconeogenesis, the latter is associated with the NADPH and ribose generating pentose phosphate pathway (Kugler & Lakomek, 2000). Hence this connectivity is generally reflective of the direct or indirect effects of smooth muscle contraction that is exerted by WF100 on energy metabolism.

In the third subnetwork interaction, dihydropyrimidinase-related protein 2 was shown to have a sequential interaction with guanine deaminase, adenosylhomocysteinase and finally with alpha-1-inhibitor 3 precursor (Figure 5.4C). The connectivity between guanine deaminase and adenosylhomocysteinase can either occur directly or via purine nucleoside phosphorylase. The majority of the proteins associated in this subnetwork are obviously intracellular enzymes involved in the nucleotide metabolism pathways. Hence, the STRING-displayed interaction is generally a reflection of the shutting down of the nucleotide metabolism in uterine tissues that was exposed to WF100 as the primary focus was to exert the smooth muscle contraction.

The fourth subnetwork of uterine proteins that was down-regulated when the rats was administered with WF100 apparently involved a cluster of seven ribosomal proteins, which appeared to centralize on 40S ribosomal protein S8 (Figure 5.4D). In this subnetwork, 40S ribosomal protein S8 was displayed to have interactions with (i) eukaryotic initiation factor 4A-I, (ii) 60S ribosomal protein L7, (iii) 40S ribosomal protein S14, (iv) 60S ribosomal protein L13, (v) Protein LOC100360905 and finally (vi) an uncharacterized protein. Eukaryotic ribosomes are generally organelles that consist of a small subunit (40S) and a large subunit (60S), which are the site for protein synthesis.

Hence, this subnetwork clearly depicts the silencing of the expression of ribosomal proteins that are not associated with smooth muscle contraction.

The fifth and final subnetwork comprised complex interactions between twenty-five uterine proteins that were down-regulated (Figure 5.4E). Among these are several energy transduction enzymes, which includes creatinine kinase B-type, Rho GTPase activating protein 1, Rho GDP-dissociation inhibitor 1, electron transfer flavoprotein subunit alpha, mitochondrial and aspartate aminotransferase, mitochondrial as well as proteins that are not related to smooth muscle contractions like clathrin heavy chain 1, cortistatin Cortistatin-29 Cortistatin-14 and maternal embryonic message 3. These uterine proteins were likely down-regulated because they are irrelevant to uterine smooth muscle contraction. There also appeared to be several regulatory proteins involved in this subnetwork such as serpin H1 precursor, prohibitin, serine/threonine-protein phosphatase 2A 65 kDa regulatory subunit A alpha isoform and heat shock 70 kDa protein 8 which are known to inhibit the synthesis of proteins, DNA and cell division respectively. Also quite clearly shown in this complex subnetwork are interactions between cytoskeletal and structural proteins: alpha-actinin-1, actin-related protein-3, actin-related protein 2/3 complex subunit 3, tubulin alpha-1A chain and tubulin alpha-1C chains, as well as their regulatory proteins: gelsolin, ezrin and plastin-2. T-complex protein 1 subunit gamma and peptidyl-prolyl cis-trans isomerase C precursor catalyzes folding of proteins, along with protein disulphide-isomerase which specifically constructs and rearrange disulphide bonds (Moretti & Laurindo, 2017). These proteins were most likely down-regulated in uterine tissues of rats administered with WF100 because of cytoskeletal and structural functions which are not pertinent to muscle contraction. Perhaps the most interesting protein that was shown to be down-regulated in this subnetwork is prostaglandin E synthase 3 which is involved in biosynthesis of this specific type of eicosanoid that inhibits smooth muscle contraction. Based on the muscle contraction effect that was

induced after consumption of WF100, the expression of prostaglandin E synthase has to be inhibited as the enzyme is involved in the formation of prostaglandin E, which is known for its role in inducing contraction of the smooth muscle of the uterus, and consequently the ability to induce parturition and abortion (O'Brien, 1995; Ruan et al., 2011).

In summary, analysis by STRING on the up-regulated group of proteins, revealed six protein-protein interaction networks. One was a main network with Ras-related C3 botulinum toxin substrate 1 as a central protein that was interconnected to three edges. The first edge connected the central protein to destrin whilst the second edge was connected to immunoglobulin kappa constant. The third edge connected Ras-related C3 botulinum toxin substrate 1 to a series of proteins in the sequence of alpha-actinin-4, transgelin and myosin light chain polypeptide 9. In this network, a notable interaction was between the central protein to alpha-actinin-4, an actin cross-linking protein. Transgelin and myosin regulatory light chain polypeptide 9 are known for their involvement in calcium-independent smooth muscle contraction of the uterus, by which transgelin is an actin-crosslinking protein in smooth muscles while myosin regulatory light chain polypeptide 9 is a smooth muscle regulatory protein. In this network the interconnectivity between the series of proteins possibly led to the increased in contractility of rat uterus administered with WF100, which thus correspond accordingly to the number of embryo implantation attained by this group. Four out of the five remaining networks presented interactions among two nuclear regulatory proteins. The first network was between histone proteins, histone cluster 1 H2bo and histone H1.5. The second network was among a multifunctional nuclear protein, splicing factor, proline- and glutamine-rich and heterogenous nuclear ribonucleoprotein A/B, whilst the third was between heterogenous nuclear ribonucleoprotein U and heterogenous nuclear ribonucleoprotein A3. Interaction of two adaptor proteins, 14-3-3 protein beta/alpha and

14-3-3 gamma was displayed in the fourth network. The fifth was an enzymic network between alcohol dehydrogenase 1 and malate dehydrogenase mitochondrial with important roles in detoxifying blood and cellular energy production respectively.

STRING analysis on down-regulated group of proteins displayed one minor and one major protein-protein interaction network. The minor network consisted of interactions among nuclear proteins, that consist of three histones and a heterochromatin whilst the elaborated major network consisted a variation of protein and therefore divided into 5 subnetworks. Displayed in the first subnetwork were interactions between blood proteins alpha-2-HS-glycoprotein precursor, ceruloplasmin isoform 1 precursor, prothrombin precursor, hemopexin, serotransferrin and serine protease inhibitor A3K with alpha-1-antiproteinase as the central protein. Three globular proteins being globin alpha, hemoglobin subunit alpha-1/2, hemoglobin subunit beta-2, and two metabolic enzymes, glucose 6-phosphate isomerase and phosphoglycerate mutase 1 appeared to be connected to an uncharacterized protein in the second subnetwork. In the third subnetwork of down-regulated uterine proteins, interactions appeared to be between a series of intracellular enzymes such as dihydropyrimidinase-related protein 2, guanine deaminase, adenosylhomocysteinase, alpha-1-inhibitor 3 precursor and purine nucleoside phosphorylase. Seven eukaryotic ribosomal proteins i.e., eukaryotic initiation factor 4A-I, 60S ribosomal protein L7, 40S ribosomal protein S14, 60S ribosomal protein L13, LOC100360905 protein, including an uncharacterized protein was connected to the central protein of the fourth subnetwork that is 40S ribosomal protein S8. In the fifth subnetwork, interactions between multiple proteins with various functions was exhibited which includes energy transduction enzymes (creatinine kinase B-type, Rho GTPase activating protein 1, Rho GDP-dissociation inhibitor 1, electron transfer flavoprotein subunit alpha, mitochondrial and aspartate aminotransferase, mitochondrial), regulatory proteins (serpin H1 precursor, prohibitin, serine/threonine-protein phosphatase 2A 65

kDa regulatory subunit A alpha isoform and heat shock 70 kDa protein 8), cytoskeletal and structural proteins (alpha-actinin-1, actin-related protein-3, actin-related protein 2/3 complex subunit 3, tubulin alpha-1A chain and tubulin alpha-1C chains), regulatory proteins for the cytoskeletal and structural proteins (gelsolin, ezrin and plastin-2), proteins that catalyzes folding and rearrangement (T-complex protein 1 subunit gamma and peptidyl-prolyl cis-trans isomerase C precursor) as well as proteins that are not related to smooth muscle contractions (clathrin heavy chain 1, cortistatin Cortistatin-29 Cortistatin-14 and maternal embryonic message 3). One thought-provoking protein within the fifth subnetwork was prostaglandin E synthase 3 owing to its known function in deterring smooth muscle contraction of the uterus. The observed network for down-regulated proteins displayed a consistent relevance in their roles which has no relevance to smooth muscle contraction. Thus, depicts the deregulation in their expression following administration of WF100 to female rats.

In this study, the primary aim of STRING analysis was to provide evidence at the protein levels that supports the hypothesis that the smooth muscle uterine contraction that was observed in the rats was due to consumption of WF100. Clearly from the STRING analysis, the observed protein interaction networks that was displayed appeared to be interconnected from the functional point of view, i.e., to induce and sustain smooth muscle uterine contraction. When taken together, the consumption of WF100 by the rats appeared to have led to a concerted action to induce the upregulated expression of proteins that are direct- and indirectly involved in uterine smooth muscle contraction, whilst those that inhibit the action as well as those that are not concerned with smooth muscle contraction were seen to be down-regulated. In the networks involving up-regulated proteins, alpha-actinin-4, transgelin and myosin regulatory light polypeptide 9 appeared to be of direct importance in uterine smooth muscle contraction, whilst in the network of down-regulated proteins prostaglandin E synthase 3 seemed to be directly relevant.

CHAPTER 6: CONCLUSION

This study described the effect of *F. deltoidea* leaf crude extract and water fraction consumption on uterus of female nulliparous ICR mice and WKY rats. The former was subjected to embryo implantation study which showed highest number of implantations in the group of mice treated with 100 mg/kg body weight of FdCE and no implantation of embryo in the group of mice administered with 100 mg/kg body weight of FdWF. Measurement in the levels of steroid hormones revealed an increase in progesterone, estrogen and testosterone after the animals were given FdCE and FdWF. Progesterone levels were seen highest in the group of mice treated with 100 mg/kg body weight of WF100, whilst estradiol levels were highest in the group treated with 100 mg/kg body weight of FdCE. Alteration in the levels of steroid hormones seemed to correspond to the number of embryos that were implanted in the uterus of ICR mice. Blood samples of the ICR mice were also examined for toxicity and biochemical analysis. None of the treated animals died or exhibited any observable toxic effect. Biochemical analysis revealed normal levels of serum biomarkers for kidney and liver functions indicating that *F. deltoidea* is generally nontoxic. Subsequent analysis of the expression of the M2 mAChR showed highest relative intensity of the receptor protein bands in the WF100-treated groups of rats compared to those untreated, followed by rats treated with CE100, which were comparable to the altered strength of uterine contraction.

Proteomics analysis of uterine proteins of rats treated with WF100 revealed a total of 833 proteins initially detected by LC-MS/MS, with 380 of these proteins commonly detected in all groups of rat uterine tissue samples. A total of 100 proteins were later found to be differentially regulated in rats treated with WF100, with the majority of these proteins showing reduction in their expression levels. When analyzed using STRING, the rat uterine proteins that appeared up-regulated by WF100 displayed six protein-

protein interaction networks involving 16 proteins. Whilst many of the protein-protein interaction networks are generally associated with general proteins with structural and regulatory functions, the study also highlighted a network involving Ras-related C3 botulinum toxin substrate 1 with alpha-actinin-4, which was also shown to interact with transgelin, an actin-crosslinking/gelling protein that may have induced smooth muscle contraction that lead to the abortifacient effects on the rats. Similarly, when STRING analysis was performed on uterine proteins of interest that were down-regulated by WF100, two protein-protein interaction networks were generated involving a total of 56 proteins. One of the networks displayed showed interactions with prostaglandin E synthase 3, which is involved in biosynthesis of this specific type of eicosanoid that inhibits smooth muscle contraction. This enzyme appeared to have been down-regulated so as to induce uterine muscle contraction, inhibit implantation of embryo and allow abortion. Hence, the protein interaction networks obtained from the STRING analysis exhibited that consumption of WF100 by the rats may have led to an orchestrated effect of induced smooth muscle uterine contraction which hindered embryo implantation at the protein level.

REFERENCES

Abarbanel, A. R. (1940). Rationale for the use of testosterone propionate in the immediate treatment of excessive uterine bleeding. *American Journal of Obstetrics and Gynecology*, *39*(2), 243-254.

Abdullah, Z., Hussain, K., Zhari, I., Rasadah, M. A., Mazura, P., Jamaludin, F., & Sahdan, R. (2009). Evaluation of extracts of leaf of three *Ficus deltoidea* varieties for antioxidant activities and secondary metabolites. *Pharmacognosy Research*, *1*(4), 216-223.

Adam, Z., Hamid, M., Ismail, A., & Khamis, S. (2009). Effect of *Ficus deltoidea* extracts on hepatic basal and insulin-stimulated glucose uptake. *Journal of Biological Sciences*, *9*(8), 796-803.

Ait-El-Mkadem, S., Dayem-Quere, M., Gusic, M., Chaussenot, A., Bannwarth, S., François, B., ... & Serre, V. (2017). Mutations in MDH2, encoding a Krebs cycle enzyme, cause early-onset severe encephalopathy. *The American Journal of Human Genetics*, *100*(1), 151-159.

Akhir, N. A. M., Chua, L. S., Majid, F. A. A., & Sarmidi, M. R. (2011). Cytotoxicity of aqueous and ethanolic extracts of *Ficus deltoidea* on human ovarian carcinoma cell line. *British Journal of Medicine and Medical Research*, *1*(4), 397-409.

Alotaibi, M. (2014). The physiological mechanism of uterine contraction with emphasis on calcium ion. *Calcium Signaling*, *1*(2), 101-119.

Amiera, Z. U. R., Nihayah, M., Wahida, I. F., & Rajab, N. F. (2014). Phytochemical characteristic and uterotonic effect of aqueous extract of *Ficus deltoidea* leaves in rat uterus. *Pakistan Journal of Biological Sciences*, *17*(9), 1046-1051.

Aminudin, N., Sin, C. Y., Chee, E. S., Nee, K. I., & Renxin, L. (2007). Blood glucose lowering effect of *Ficus deltoidea* aqueous extract. *Malaysian Journal of Science*, *26*(1).

Aminudin, N., Abdullah, N. A. H., Misbah, H., Karsani, S. A., Husain, R., Hoe, S. Z., & Hashim, O. H. (2012). Treatment with captopril abrogates the altered expression of alpha1 macroglobulin and alpha1 antiproteinase in sera of spontaneously hypertensive rats. *Proteome Science*, *10,* Article #17.

Andersen, J., Nilsson, C., de Richelieu, T., Fridriksdottir, H., Gobilick, J., Mertz, O., & Gausset, Q. (2003). Local use of forest products in Kuyongon, Sabah, Malaysia. *ASEAN Review of Biodiversity and Environmental Conservation (ARBEC)*, 1-18.

Ardrey, R. E. (2003). *Liquid chromatography-mass spectrometry: An introduction* (Vol. 2). John Wiley & Sons, US.

Ashburner, M., Ball, C. A., Blake, J. A., Botstein, D., Butler, H., Cherry, J. M., ... & Harris, M. A. (2000). Gene Ontology: Tool for the unification of biology. *Nature Genetics*, *25*(1), 25-29.

Assinder, S. J., Stanton, J. A. L., & Prasad, P. D. (2009). Transgelin: An actin-binding protein and tumour suppressor. *The International Journal of Biochemistry & Cell Biology*, *41*(3), 482-486.

Awang, N. A., Hasan, S. M. Z., & Shafie, M. S. B. (2013). Morphological study of *Ficus deltoidea* Jack in Malaysia. *Journal of Agricultural Science and Technology. B*, *3*(2B), 144-150.

Bafor, E. E., Omogbai, E. K., & Ozolua, R. I. (2009). Evaluation of the uterotonic activity of the aqueous leaf extract of *Ficus exasperata* Vahl (Moraceae). *Research Journal of Medicinal Plant*, *3*(2), 34-40.

Berg, C. C. (2003). Flora Malesiana precursor for the treatment of Moraceae 3: Ficus subgenus Ficus. *Blumea-Biodiversity, Evolution and Biogeography of Plants*, *48*(3), 529-550.

Brickell, C., & Zuk, J. D. (1997). *The American horticultural society. AZ Encyclopaedia of Garden Plants*. (pp.14-18). NY: DK Publishing Inc.

Bunawan, H., Amin, N. M., Bunawan, S. N., Baharum, S. N., & Mohd Noor, N. (2014). *Ficus deltoidea* Jack: A review on its phytochemical and pharmacological importance. *Evidence-Based Complementary and Alternative Medicine*, *2014*. Article #902734.

Burkill, I. H., & Haniff, M. (1930). *Malay Village Medicine: Prescriptions Collected*, 6(2):165-273, University Press.

Celis, J. E., Ratz, G., Basse, B., Lauridsen, J. B., & Celis, A. (1994). High-resolution two-dimensional gel electrophoresis of proteins: Isoelectric focusing and nonequilibrium pH gradient electrophoresis (NEPHGE). In *Cell Biology* (pp. 222-230). Academic Press.

Chakraborty, S., Reineke, E. L., Lam, M., Li, X., Liu, Y., Gao, C., ... & Kao, H. Y. (2006). α-Actinin 4 potentiates myocyte enhancer factor-2 transcription activity by antagonizing histone deacetylase 7. *Journal of Biological Chemistry*, *281*(46), 35070-35080.

Cheng, Y., Zak, O., Aisen, P., Harrison, S. C., & Walz, T. (2004). Structure of the human transferrin receptor-transferrin complex. *Cell*, *116*(4), 565-576.

Chi, X., Michos, O., Shakya, R., Riccio, P., Enomoto, H., Licht, J. D., ... & Mendelsohn, C. (2009). Ret-dependent cell rearrangements in the Wolffian duct epithelium initiate ureteric bud morphogenesis. *Developmental Cell*, *17*(2), 199-209.

Choi, H. S., Lee, H. M., Jang, Y. J., Kim, C. H., & Ryu, C. J. (2013). Heterogeneous nuclear ribonucleoprotein A2/B1 regulates the self-renewal and pluripotency of human embryonic stem cells via the control of the G1/S transition. *Stem Cells*, *31*(12), 2647-2658.

Choppin, A., Stepan, G. J., Loury, D. N., Watson, N., & Eglen, R. M. (1999). Characterization of the muscarinic receptor in isolated uterus of sham operated and ovariectomized rats. *British Journal of Pharmacology*, *127*(7), 1551-1558.

DeMeo, D. L., & Silverman, E. K. (2004). α1-Antitrypsin deficiency· 2: Genetic aspects of α1-antitrypsin deficiency: Phenotypes and genetic modifiers of emphysema risk. *Thorax*, *59*(3), 259-264.

Djinovic-Carugo, K., Gautel, M., Ylänne, J., & Young, P. (2002). The spectrin repeat: A structural platform for cytoskeletal protein assemblies. *FEBS letters*, *513*(1), 119-123.

dos Santos Hidalgo, G., Meola, J., e Silva, J. C. R., de Paz, C. C. P., & Ferriani, R. A. (2011). TAGLN expression is deregulated in endometriosis and may be involved in cell invasion, migration, and differentiation. *Fertility and Sterility*, *96*(3), 700-703.

Dreyfuss, G., Matunis, M. J., Pinol-Roma, S., & Burd, C. G. (1993). hnRNP proteins and the biogenesis of mRNA. *Annual Review of Biochemistry*, *62*(1), 289-321.

Dutta, B., Ren, Y., Hao, P., Sim, K. H., Cheow, E., Adav, S., ... & Sze, S. K. (2014). Profiling of the chromatin-associated proteome identifies HP1BP3 as a novel regulator of cell cycle progression. *Molecular & Cellular Proteomics*, *13*(9), 2183-2197.

Fackelmayer, F. O., & Richter, A. (1994). Purification of two isoforms of hnRNP-U and characterization of their nucleic acid binding activity. *Biochemistry*, *33*(34), 10416-10422.

Fahien, L. A., Kmiotek, E. H., MacDonald, M. J., Fibich, B., & Mandic, M. (1988). Regulation of malate dehydrogenase activity by glutamate, citrate, alpha-ketoglutarate, and multienzyme interaction. *Journal of Biological Chemistry*, *263*(22), 10687-10697.

Fatimah, Z., Mahmood, A. A., Hapipah, M. A., Suzita, M. N., & Salmah, I. (2009). Anti-ulcerogenic activity of aqueous extract of *Ficus deltoidea* against ethanol-induced gastric mucosal injury in rats. *Research Journal of Medical Sciences*, *3*(2), 42-46.

Farhana, M. H., Fauzi, P. A., & Lim, H. F. (2007). Market potential for Mas Cotek (*Ficus deltoidea*) products in selected states in peninsular Malaysia. *Forest Research Institute Malaysia (FRIM)*, 132-135.

Foley, K. S., & Young, P. W. (2013). An analysis of splicing, actin-binding properties, heterodimerization and molecular interactions of the non-muscle α-actinins. *Biochemical Journal*, *452*(3), 477-488.

Franceschini, A., Szklarczyk, D., Frankild, S., Kuhn, M., Simonovic, M., Roth, A., ... & Jensen, L. J. (2012). STRING v9. 1: Protein-protein interaction networks, with increased coverage and integration. *Nucleic Acids Research*, *41*(D1), D808-D815.

Francis, G. A., Fayard, E., Picard, F., & Auwerx, J. (2003). Nuclear receptors and the control of metabolism. *Annual Review of Physiology*, *65*(1), 261-311.

Fu, H., Subramanian, R. R., & Masters, S. C. (2000). 14-3-3 proteins: Structure, function, and regulation. *Annual Review of Pharmacology and Toxicology*, *40*(1), 617-647.

Garfinkel, B. P., Melamed-Book, N., Anuka, E., Bustin, M., & Orly, J. (2015). HP1BP3 is a novel histone H1 related protein with essential roles in viability and growth. *Nucleic Acids Research*, *43*(4), 2074-2090.

Gelpi, J. L., Dordal, A., Montserrat, J., Mazo, A., & Cortes, A. (1992). Kinetic studies of the regulation of mitochondrial malate dehydrogenase by citrate. *Biochemical Journal*, *283*(1), 289-297.

Gelperin, D. M., White, M. A., Wilkinson, M. L., Kon, Y., Kung, L. A., Wise, K. J., ... & Gerstein, M. (2005). Biochemical and genetic analysis of the yeast proteome with a movable ORF collection. *Genes & Development*, *19*(23), 2816-2826.

Gibson, D. A., & Saunders, P. T. (2013). Endocrine disruption of oestrogen action and female reproductive tract cancers. *Endocrine-related Cancer*, *21*(2), 13-31.

Göhring, F., & Fackelmayer, F. O. (1997). The scaffold/matrix attachment region binding protein hnRNP-U (SAF-A) is directly bound to chromosomal DNA *in vivo*: A chemical cross-linking study. *Biochemistry*, *36*(27), 8276-8283.

Han, S. P., Tang, Y. H., & Smith, R. (2010). Functional diversity of the hnRNPs: Past, present and perspectives. *Biochemical Journal*, *430*(3), 379-392.

Hasham, R., Choi, H. K., Sarmidi, M. R., & Park, C. S. (2013). Protective effects of a *Ficus deltoidea* (Mas cotek) extract against UVB-induced photoageing in skin cells. *Biotechnology and Bioprocess Engineering*, *18*(1), 185-193.

Hassan, W. W., & Mahmood, M. (2006). *Healing Herbs of Malaysia*. Biotropics Malaysia Berhad.

He, Y., & Smith, R. (2009). Nuclear functions of heterogeneous nuclear ribonucleoproteins A/B. *Cellular and Molecular Life Sciences*, *66*(7), 1239-1256.

Heran, B. S., Wong, M. M., Heran, I. K., & Wright, J. M. (2008). Blood pressure lowering efficacy of angiotensin converting enzyme (ACE) inhibitors for primary hypertension. *Cochrane Database of Systematic Reviews*, (4).

Hillenkamp, F., Karas, M., Beavis, R. C., & Chait, B. T. (1991). Matrix-assisted laser desorption/ionization mass spectrometry of biopolymers. *Analytical Chemistry*, *63*(24), 1193A-1203A.

Hergeth, S. P., & Schneider, R. (2015). The H1 linker histones: Multifunctional proteins beyond the nucleosomal core particle. *EMBO Reports*, *16*(11), 1439-1453.

Hochstrasser, D. F. (1997). Clinical and biomedical applications of proteomics. In *Proteome research: New frontiers in functional genomics* (pp. 187-219), Berlin, Heidelberg: Springer.

Horowitz, A., Menice, C. B., Laporte, R., & Morgan, K. G. (1996). Mechanisms of smooth muscle contraction. *Physiological Reviews*, *76*(4), 967-1003.

Huang, P. R., Tsai, S. T., Hsieh, K. H., & Wang, T. C. V. (2008). Heterogeneous nuclear ribonucleoprotein A3 binds single-stranded telomeric DNA and inhibits telomerase extension *in vitro*. *Biochimica et Biophysica Acta (BBA)-Molecular Cell Research*, *1783*(2), 193-202.

Huang, Y., Lin, L., Yu, X., Wen, G., Pu, X., Zhao, H., ... & Xiao, Q. (2013). Functional involvements of heterogeneous nuclear ribonucleoprotein A1 in smooth muscle differentiation from stem cells *in vitro* and *in vivo*. *Stem Cells*, *31*(5), 906-917.

IJsselstijn, L., Stoop, M. P., Stingl, C., Sillevis Smitt, P. A., Luider, T. M., & Dekker, L. J. (2013). Comparative study of targeted and label-free mass spectrometry methods for protein quantification. *Journal of Proteome Research*, *12*(4), 2005-2011.

Ikeda, S., Cunningham, L. A., Boggess, D., Hobson, C. D., Sundberg, J. P., Naggert, J. K., ... & Nishina, P. M. (2003). Aberrant actin cytoskeleton leads to accelerated proliferation of corneal epithelial cells in mice deficient for destrin (actin depolymerizing factor). *Human Molecular Genetics*, *12*(9), 1029-1036.

Izzo, A., & Schneider, R. (2016). The role of linker histone H1 modifications in the regulation of gene expression and chromatin dynamics. *Biochimica et Biophysica Acta (BBA)-Gene Regulatory Mechanisms*, *1859*(3), 486-495.

Jaffe, A. B., & Hall, A. (2005). Rho GTPases: biochemistry and biology. *Annual Review of Cell and Development Biology*, *21*, 247-269.

Jain, V., Saade, G. R., & Garfield, R. E. (2000). Structure and function of the myometrium. *Advances in Organ Biology*, *8*, 215-246.

Janeway, C. A., Travers, P., Walport, M., & Shlomchik, M. (1996). *Immunobiology: The immune system in health and disease*. London: Current Biology.

Jensen, E. V. (1990). Molecular mechanisms of steroid hormone action in the uterus. In *Uterine Function* (pp. 315-359). Springer, Boston, MA.

Johnson, M. H. (2018). *Essential reproduction*. United States: John Wiley & Sons Ltd.

Kaingu, C. K., Oduma, J. A., & Kanui, T. (2012). Preliminary investigation of contractile activity of *Ricinus communis* and *Euclea divinorum* extracts on isolated rabbit uterine strips. *Journal of Ethnopharmacology*, *142*(2), 496-502.

Kamatenesi-Mugisha, M., & Oryem-Origa, H. (2007). Medicinal plants used to induce labour during childbirth in western Uganda. *Journal of Ethnopharmacology*, *109*(1), 1-9.

Kamishima, T., Davies, N. W., & Standen, N. B. (2000). Mechanisms that regulate $[Ca^{2+}]i$ following depolarization in rat systemic arterial smooth muscle cells. *The Journal of Physiology*, *522*(2), 285-295.

Karas, M., & Krüger, R. (2003). Ion formation in MALDI: The cluster ionization mechanism. *Chemical Reviews*, *103*(2), 427-440.

Kawarabayashi, T. (1994). Electrophysiology of the human myometrium. *The uterus*, 148-172.

Khurana, S., Chakraborty, S., Cheng, X., Su, Y. T., & Kao, H. Y. (2011). The actin-binding protein, actinin alpha 4 (ACTN4), is a nuclear receptor coactivator that promotes proliferation of MCF-7 breast cancer cells. *Journal of Biological Chemistry*, *286*(3), 1850-1859.

Khurana, S., Chakraborty, S., Zhao, X., Liu, Y., Guan, D., Lam, M., ... & Kao, H. Y. (2012). Identification of a novel LXXLL motif in alpha actinin 4 (ACTN4) spliced isoform that is critical for its interaction with estrogen receptor alpha and co-activators. *Journal of Biological Chemistry*, *287*(42), 35418-35429.

Kimura, T., Ogita, K., Kusui, C., Ohashi, K., Azuma, C., & Murata, Y. (1999). What knockout mice can tell us about parturition. *Reviews of Reproduction*, *4*(2), 73-80.

Klose, J. (1975). Protein mapping by combined isoelectric focusing and electrophoresis of mouse tissues. *Humangenetik*, *26*(3), 231-243.

Kolarich, D., Turecek, P. L., Weber, A., Mitterer, A., Graninger, M., Matthiessen, P., ... & Schwarz, H. P. (2006). Biochemical, molecular characterization and glycoproteomic analyses of α1-proteinase inhibitor products used for replacement therapy. *Transfusion*, *46*(11), 1959-1977.

Kruse, A. C., Ring, A. M., Manglik, A., Hu, J., Hu, K., Eitel, K., ... & Christopoulos, A. (2013). Activation and allosteric modulation of a muscarinic acetylcholine receptor. *Nature*, *504*(7478), 101.

Kugler, W., & Lakomek, M. (2000). Glucose-6-phosphate isomerase deficiency. *Best Practice & Research Clinical Haematology*, *13*(1), 89-101.

Kumar, C. C., Mohan, S. R., Zavodny, P. J., Narula, S. K., & Leibowitz, P. J. (1989). Characterization and differential expression of human vascular smooth muscle myosin light chain 2 isoform in nonmuscle cells. *Biochemistry*, *28*(9), 4027-4035.

Kumeta, M., Yoshimura, S. H., Harata, M., & Takeyasu, K. (2010). Molecular mechanisms underlying nucleocytoplasmic shuttling of actinin-4. *Journal of Cell Science*, *123*(7), 1020-1030.

Kuure, S., Cebrian, C., Machingo, Q., Lu, B. C., Chi, X., Hyink, D., ... & Costantini, F. (2010). Actin depolymerizing factors cofilin1 and destrin are required for ureteric bud branching morphogenesis. *PLoS Genetics*, *6*(10), Article #e1001176.

Laemmli, U. K. (1970). Cleavage of structural proteins during the assembly of the head of bacteriophage T4. *Nature*, *227*(5259), 680-685.

Lanzafame, A. A., Christopoulos, A., & Mitchelson, F. (2003). Cellular signaling mechanisms for muscarinic acetylcholine receptors. *Receptors and Channels*, *9*(4), 241-260.

Larsen, B. H., Soelberg, J., Kristiansen, U., & Jäger, A. K. (2016). Uterine contraction induced by Ghanaian plants used to induce abortion. *South African Journal of Botany*, *106*, 137-139.

Lawson, D., Harrison, M., & Shapland, C. (1997). Fibroblast transgelin and smooth muscle SM22α are the same protein, the expression of which is down-regulated in many cell lines. *Cell Motility and the Cytoskeleton*, *38*(3), 250-257.

Lazar, V., & Garcia, J. G. (1999). A single human myosin light chain kinase gene (MLCK; MYLK) transcribes multiple nonmuscle isoforms. *Genomics*, *57*(2), 256-267.

Lénárt, P., Bacher, C. P., Daigle, N., Hand, A. R., Eils, R., Terasaki, M., & Ellenberg, J. (2005). A contractile nuclear actin network drives chromosome congression in oocytes. *Nature*, *436*(7052), 812-818.

Li, J. Y., Patterson, M., Mikkola, H. K., Lowry, W. E., & Kurdistani, S. K. (2012). Dynamic distribution of linker histone H1.5 in cellular differentiation. *PLoS Genetics*, *8*(8), Article #e1002879.

Lutz, C. S., Cooke, C., O'Connor, J. P., Kobayashi, R., & Alwine, J. C. (1998). The snRNP-free U1A (SF-A) complex(es): Identification of the largest subunit as PSF, the polypyrimidine-tract binding protein-associated splicing factor. *RNA*, *4*(12), 1493-1499.

MacGillivray, R. T., Moore, S. A., Chen, J., Anderson, B. F., Baker, H., Luo, Y., ... & Mason, A. B. (1998). Two high-resolution crystal structures of the recombinant N-lobe of human transferrin reveal a structural change implicated in iron release. *Biochemistry*, *37*(22), 7919-7928.

Mangelsdorf, D. J., & Evans, R. M. (1995). The RXR heterodimers and orphan receptors. *Cell*, *83*(6), 841-850.

Mangelsdorf, D. J., Thummel, C., Beato, M., Herrlich, P., Schütz, G., Umesono, K., ... & Evans, R. M. (1995). The nuclear receptor superfamily: The second decade. *Cell*, *83*(6), 835-839.

Martinez-Contreras, R., Cloutier, P., Shkreta, L., Fisette, J. F., Revil, T., & Chabot, B. (2008). 8 hnRNP proteins and splicing control. *Advances in Experimental Medicine & Biology*, *623*, 123.

Mat, N., Rosni, N. A., Ab Rashid, N. Z., Haron, N., Nor, Z. M., Nudin, N. F. H., ... & Ali, A. M. (2012). Leaf morphological variations and heterophylly in *Ficus deltoidea* Jack (Moraceae). *Sains Malaysiana*, *41*(5), 527-538.

Mat-Salleh, K., & Latif, A. (2002). Dikotiledon: Subkelas Hamamelidae. *Ficus deltoidea* jack. *Tumbuhan Ubatan Malaysia*, (pp. 184-185).

Matthew, A., Shmygol, A., & Wray, S. (2004). Ca^{2+} entry, efflux and release in smooth muscle. *Biological Research*, *37*(4), 617-624.

Maverakis, E., Kim, K., Shimoda, M., Gershwin, M. E., Patel, F., Wilken, R., ... & Lebrilla, C. B. (2015). Glycans in the immune system and the altered glycan theory of autoimmunity: A critical review. *Journal of Autoimmunity*, *57*, 1-13.

Megger, D. A., Bracht, T., Meyer, H. E., & Sitek, B. (2013). Label-free quantification in clinical proteomics. *Biochimica et Biophysica Acta (BBA)-Proteins and Proteomics*, *1834*(8), 1581-1590.

Meirzon, D., Jaffa, A. J., Gordon, Z., & Elad, D. (2011). A new method for analysis of non-pregnant uterine peristalsis using transvaginal ultrasound. *Ultrasound in Obstetrics & Gynecology*, *38*(2), 217-224.

Miean, K. H., & Mohamed, S. (2001). Flavonoid (myricetin, quercetin, kaempferol, luteolin, and apigenin) content of edible tropical plants. *Journal of Agricultural and Food Chemistry*, *49*(6), 3106-3112.

Minarik, P., Tomaskova, N., Kollarova, M., & Antalik, M. (2002). Malate dehydrogenases-structure and function. *General Physiology and Biophysics*, *21*(3), 257-266.

Misbah, H., Aziz, A. A., & Aminudin, N. (2013). Antidiabetic and antioxidant properties of *Ficus deltoidea* fruit extracts and fractions. *BMC Complementary and Alternative Medicine*, *13*(1), 118.

Moretti, A. I. S., & Laurindo, F. R. M. (2017). Protein disulfide isomerases: Redox connections in and out of the endoplasmic reticulum. *Archives of Biochemistry and Biophysics*, *617*, 106-119.

Mueller, A., Siemer, J., Schreiner, S., Koesztner, H., Hoffmann, I., Binder, H., ... & Dittrich, R. (2006). Role of estrogen and progesterone in the regulation of uterine peristalsis: Results from perfused non-pregnant swine uteri. *Human Reproduction*, *21*(7), 1863-1868.

Munns, M., & Pennefather, J. N. (1998). Pharmacological characterization of muscarinic receptors in the uterus of oestrogen-primed and pregnant rats. *British Journal of Pharmacology*, *123*(8), 1639-1644.

Musa, Y. (2005). Kepelbagaian morfologi dan agronomi beberapa aksesi emas cotek yang terdapat di Kelantan dan Terengganu. *Buletin Teknologi Tanaman*, *2*, 35-48.

Nakatsuji, H., Nishimura, N., Yamamura, R., Kanayama, H. O., & Sasaki, T. (2008). Involvement of actinin-4 in the recruitment of JRAB/MICAL-L2 to cell-cell junctions and the formation of functional tight junctions. *Molecular and Cellular Biology*, *28*(10), 3324-3335.

Nargis, J., Melati, K., Lai, C. S., Hasnah, O., Wong, K. C., Vikneswaran, M., & Khaw, K. Y. (2013). Antioxidant, anti-cholinesterase and antibacterial activities of the bark extracts of *Garcinia hombroniana*. *African Journal of Pharmacy and Pharmacology*, *7*(8), 454-459.

Nikolajsen, T., Nielsen, F., Rasch, V., Sørensen, P. H., Ismail, F., Kristiansen, U., & Jäger, A. K. (2011). Uterine contraction induced by Tanzanian plants used to induce abortion. *Journal of Ethnopharmacology*, *137*(1), 921-925.

O'Brien, W. F. (1995). The role of prostaglandins in labor and delivery. *Clinics in Perinatology*, *22*(4), 973-984.

OECD (1992), *Test No. 203: Fish, Acute Toxicity Test*, OECD Guidelines for the Testing of Chemicals, Section 2. Paris: OECD Publishing.

OECD (1995), *Test No. 407: Repeated Dose 28-day Oral Toxicity,* OECD Guidelines for the Testing of Chemicals. Paris: OECD Publishing.

O'Farrell, P. H. (1975). High resolution two-dimensional electrophoresis of proteins. *Journal of Biological Chemistry*, *250*(10), 4007-4021.

Oh-Ishi, M., & Maeda, T. (2007). Disease proteomics of high-molecular-mass proteins by two-dimensional gel electrophoresis with agarose gels in the first dimension (Agarose 2-DE). *Journal of Chromatography B*, *849*(1-2), 211-222.

Ong, S. L., Ling, A. P. K., Poospooragi, R., & Moosa, S. (2011). Production of Flavonoid compounds in cell cultures of *Ficus deltoidea* as influenced by medium composition. *International Journal of Medicinal and Aromatic Plants*, *1*(2), 62-74.

Pamplona-Roger, G. D. (2005). Encyclopedia of medicinal plants. Republic of Kenya: Editorial Safeliz.

Patton, J. G., Porro, E. B., Galceran, J., Tempst, P., & Nadal-Ginard, B. (1993). Cloning and characterization of PSF, a novel pre-mRNA splicing factor. *Genes & Development*, *7*(3), 393-406.

Pennefather, J. N., Gillman, T. A., & Mitchelson, F. (1994). Muscarinic receptors in rat uterus. *European Journal of Pharmacology*, *262*(3), 297-300.

Phinney, B. S., & Thelen, J. J. (2005). Proteomic characterization of a triton-insoluble fraction from chloroplasts defines a novel group of proteins associated with macromolecular structures. *Journal of Proteome Research*, *4*(2), 497-506.

Ramamurthy, S., Kumarappan, C., Dharmalingam, S. R., & Sangeh, J. K. (2014). Phytochemical, pharmacological and toxicological properties of *Ficus deltoidea*: A review of a recent research. *Annual Research and Review in Biology*, *4*(14), 2357-2371.

Reynolds, M. (2013). A toxicological study using Zebrafish (*Danio rerio*) as a model. *The Journal of Toxicological Education, 1*, 10-20.

Riffle, R. L. (1998). *The tropical look: An encyclopedia of dramatic landscape plants*. Portland, US: Timber Press.

Rosenquist, M., Sehnke, P., Ferl, R. J., Sommarin, M., & Larsson, C. (2000). Evolution of the 14-3-3 protein family: Does the large number of isoforms in multicellular organisms reflect functional specificity? *Journal of Molecular Evolution*, *51*(5), 446-458.

Ruan, Y. C., Zhou, W., & Chan, H. C. (2011). Regulation of smooth muscle contraction by the epithelium: Role of prostaglandins. *Physiology*, *26*(3), 156-170.

Sakamoto, T., Unno, T., Matsuyama, H., Uchiyama, M., Hattori, M., Nishimura, M., & Komori, S. (2006). Characterization of muscarinic receptor-mediated cationic currents in longitudinal smooth muscle cells of mouse small intestine. *Journal of Pharmacological Sciences*, *100,* 215-226.

Salleh, N., & Ahmad, V. N. (2013). *In-vitro* effect of *Ficus deltoidea* on the contraction of isolated rat's uteri is mediated via multiple receptors binding and is dependent on extracellular calcium. *BMC Complementary and Alternative Medicine*, *13*(1), Article #359.

Samah, O. A., Zaidi, N. T. A., & Sule, A. B. (2012). Antimicrobial activity of *Ficus deltoidea* Jack (Mas Cotek). *Pakistan Journal of Pharmaceutical Sciences*, *25*(3), 675-678.

Sanborn, B. M. (2001). Hormones and calcium: mechanisms controlling uterine smooth muscle contractile activity. *Experimental Physiology*, *86*(2), 223-237.

Shafaei, A., Muslim, N. S., Nassar, Z. D., Aisha, A. F., Majid, A. M. S. A., & Ismail, Z. (2014). Antiangiogenic effect of *Ficus deltoidea* Jack standardised leaf extracts. *Tropical Journal of Pharmaceutical Research*, *13*(5), 761-768.

Sharp, P., & Villano, J. S. (2012). *The laboratory rat*. USA: CRC press.

Shav-Tal, Y., & Zipori, D. (2002). PSF and p54nrb/NonO–multi-functional nuclear proteins. *FEBS Letters*, *531*(2), 109-114.

Şimşek, Y., Parlakpınar, H., Turhan, U., Tağluk, M. E., & Ateş, B. (2014). Dual effects of melatonin on uterine myoelectrical activity of non-pregnant rats. *Journal of the Turkish German Gynecological Association*, *15*(2), 86-91.

Sjöblom, B., Salmazo, A., & Djinović-Carugo, K. (2008). α-Actinin structure and regulation. *Cellular and Molecular Life Sciences*, *65*(17), 2688-2701.

Snel, B., Lehmann, G., Bork, P., & Huynen, M. A. (2000). STRING: A web-server to retrieve and display the repeatedly occurring neighbourhood of a gene. *Nucleic Acids Research*, *28*(18), 3442-3444.

Soepadmo, E., Saw, L. G., & Chung, R. C. K. (2004). Tree flora of Sabah and Sarawak: Volume 5. Malaysia: Forest Research Institute Malaysia (FRIM).

Starr, F., Starr, K., & Loope, L. (2003). *Ficus deltoidea. United States Geological survey-Biology Resources Division, Haleakala Field Station, Maui, Hawai'i*, 120-300.

Steinberg, T. H. (2009). Protein gel staining methods: An introduction and overview. In *Methods in enzymology* (Vol. 463, pp. 541-563). Academic Press.

Suckow, M. A., Weisbroth, S. H., & Franklin, C. L. (Eds.). (2005). *The laboratory rat*. San Diego: Elsevier Academic Press.

Sulaiman, M. R., Hussain, M. K., Zakaria, Z. A., Somchit, M. N., Moin, S., Mohamad, A. S., & Israf, D. A. (2008). Evaluation of the antinociceptive activity of *Ficus deltoidea* aqueous extract. *Fitoterapia*, *79*(7-8), 557-561.

Sylow, L., Nielsen, I. L., Kleinert, M., Møller, L. L., Ploug, T., Schjerling, P., ... & Richter, E. A. (2016). Rac1 governs exercise-stimulated glucose uptake in skeletal muscle through regulation of GLUT4 translocation in mice. *The Journal of Physiology*, *594*(17), 4997-5008.

Szklarczyk, D., Morris, J. H., Cook, H., Kuhn, M., Wyder, S., Simonovic, M., ... & Jensen, L. J. (2016). The STRING database in 2017: Quality-controlled protein–protein association networks, made broadly accessible. *Nucleic Acids Research*, *45*(D1), D362-368.

Taggart, M. J. (2001). Smooth muscle excitation-contraction coupling: A role for caveolae and caveolins? *Physiology*, *16*(2), 61-65.

Tolosano, E., & Altruda, F. (2002). Hemopexin: Structure, function, and regulation. *DNA and Cell Biology*, *21*(4), 297-306.

Tripathi, K. D. (2008). Essential of Medical Pharmacology. New Delhi: Jaypee Brothers Medical Publishers (P) Ltd, (pp. 235-236).

Turgut, A., Goruk, N. Y., Sak, M. E., Deveci, E., Akdemir, F., Nur, A., ... & Gul, T. (2014). Effects of genistein, estrogen and progesterone therapies on bladder morphology and M2, M3 receptor expressions in oophorectomized rats. *Acta Medica*, *30*, 907-916.

Van Gestel, I., Ijland, M. M., Hoogland, H. J., & Evers, J. L. H. (2003). Endometrial wave-like activity in the non-pregnant uterus. *Human Reproduction Update*, *9*(2), 131-138.

van Koppen, C. J., zu Heringdorf, D. M., Alemany, R., & Jakobs, K. H. (2001). Sphingosine kinase-mediated calcium signaling by muscarinic acetylcholine receptors. *Life Sciences*, *68*(22-23), 2535-2540.

Van Troys, M., Huyck, L., Leyman, S., Dhaese, S., Vandekerkhove, J., & Ampe, C. (2008). Ins and outs of ADF/cofilin activity and regulation. *European Journal of Cell Biology*, *87*(8-9), 649-667.

Vane, J. R., & Williams, K. I. (1973). The contribution of prostaglandin production to contractions of the isolated uterus of the rat. *British Journal of Pharmacology*, *48*(4), 629-639.

Varol, F. G., Hadjiconstantinou, M., Zuspan, F. P., & Neff, N. H. (1989). Pharmacological characterization of the muscarinic receptors mediating phosphoinositide hydrolysis in rat myometrium. *Journal of Pharmacology and Experimental Therapeutics*, *249*(1), 11-15.

Wagner, W. L., Herbst, D. R., & Sohmer, S. H. (1999). *Manual of the Flowering Plants of Hawai'i, Vols. 1 and 2.*, (Edn 2).

Wahid, S., Mahmud, T. M. M., Maziah, M., Yahya, A., & Rahim, M. A. (2010). Total phenolics content and antioxidant activity of hot water extracts from dried *Ficus deltoidea* leaves. *Journal of Agriculture and Food Science*, *38*(1), 115-122.

Wang, G., Xiao, Q., Luo, Z., Ye, S., & Xu, Q. (2012). Functional impact of heterogeneous nuclear ribonucleoprotein A2/B1 in smooth muscle differentiation from stem cells and embryonic arteriogenesis. *Journal of Biological Chemistry*, *287*(4), 2896-2906.

Wilson, L., & Kurzrok, R. (1938). Studies on the motility of the human uterus in vivo. *Endocrinology*, *23*(1), 79-86.

Woodcock, C. L., Skoultchi, A. I., & Fan, Y. (2006). Role of linker histone in chromatin structure and function: H1 stoichiometry and nucleosome repeat length. *Chromosome Research*, *14*(1), 17-25.

Woon, S. M., Seng, Y. W., Ling, A. P. K., Chye, S. M., & Koh, R. Y. (2014). Anti-adipogenic effects of extracts of *Ficus deltoidea* var. *deltoidea* and var. *angustifolia* on 3T3-L1 adipocytes. *Journal of Zhejiang University SCIENCE B*, *15*(3), 295-302.

Wray, S. (2007). Insights into the uterus. *Experimental Physiology*, *92*(4), 621-631.

Wrayzx, S., Jones, K., Kupittayanant, S., Li, Y., Matthew, A., Monir-Bishty, E., ... & Shmygol, A. V. (2003). Calcium signaling and uterine contractility. *Journal of the Society for Gynecologic Investigation*, *10*(5), 252-264.

Yang, X., Lee, W. H., Sobott, F., Papagrigoriou, E., Robinson, C. V., Grossmann, J. G., ... & Elkins, J. M. (2006). Structural basis for protein–protein interactions in the 14-3-3 protein family. *Proceedings of the National Academy of Sciences*, *103*(46), 17237-17242.

Yang, Z., Chang, Y. J., Miyamoto, H., Ni, J., Niu, Y., Chen, Z., ... & Chang, C. (2007). Transgelin functions as a suppressor via inhibition of ARA54-enhanced androgen receptor transactivation and prostate cancer cell growth. *Molecular Endocrinology*, *21*(2), 343-358.

Zakaria, Z. A., Hussain, M. K., Mohamad, A. S., Abdullah, F. C., & Sulaiman, M. R. (2012). Anti-inflammatory activity of the aqueous extract of *Ficus deltoidea*. *Biological Research for Nursing*, *14*(1), 90-97.

Zurlo, J., Rudacille, D., & Goldberg, A. M. (1994). *Animals and alternatives in testing: History, science, and ethics* (p. 86). New York: Mary Ann Liebert.

LIST OF PUBLICATIONS AND PAPERS PRESENTED

PRESENTED AT INTERNATIONAL CONFERENCES:

1. Aminudin, N., **Khalil, K.H.**, & Hashim, O.H. Penggunaan Mas Cotek untuk meningkatkan potensi pengecutan uterus. Persidangan Antarabangsa Perubatan Melayu 2017, 15-16 November 2017, Universiti Malaya, Kuala Lumpur, Malaysia. (Oral presentation).

2. **Khalil, K.H.**, Aminudin, N., & Hashim, O.H. Enhancement of uterus contractility potential following administration of *Ficus deltoidea*. International Conference on Natural Products 2015, 24-25 March 2015, Johor Bharu, Johor, Malaysia. (Oral presentation).

3. **Khalil, K.H.**, Aminudin, N., & Hashim, O.H. Differential expression of serum proteome of ICR mice treated with *Ficus deltoidea*. 5th Global Summit on Medicinal and Aromatic Plants (GOSMAP-5), 8 -12 December 2013, Miri, Sarawak, Malaysia. (Oral presentation).